

# NIASRA

NATIONAL INSTITUTE FOR APPLIED  
STATISTICS RESEARCH AUSTRALIA



## 2013 - 2018 Oman Rainfall Enhancement Trials

Final Report

May 2019



NATIONAL INSTITUTE FOR APPLIED  
STATISTICS RESEARCH AUSTRALIA  
University of Wollongong  
NSW 2522  
Australia  
Tel: +61 2 4221 5435  
Fax: +61 2 4221 4845



---

This document is not to be reproduced, modified, adapted, published, translated in any material form in whole or in part nor disclosed to any third party without the prior written permission of ART.

## Copyright, Disclaimer and Acknowledgements

© AUSTRALIAN RAIN TECHNOLOGIES PTY LTD 2019

This work is subject to copyright and is the property of Australian Rain Technologies Pty Ltd (ART).

**Prepared by:**

**Prof. Raymond Chambers**

National Institute For Applied Statistics Research Australia  
University of Wollongong  
NSW 2522  
AUSTRALIA

**Dr. Stephen Beare**

National Institute For Applied Statistics Research Australia  
University of Wollongong  
NSW 2522  
AUSTRALIA

**Mr. Scott Peak**


Australian Rain Technologies  
Pier 8/9, 23 Hickson Rd, Millers Point  
NSW 2000  
AUSTRALIA

## Table of Contents

1	Executive Summary .....	5
2	Introduction .....	8
2.1	Rainfall Enhancement Trials in Oman.....	8
2.2	Ground-Based Ionisation and Atlant Rainfall Enhancement.....	9
3	Hajar Mountains Trial Area and Instrumentation 2013 - 2018.....	10
3.1	Geography and Climate of the Hajar Mountains Trial Area .....	10
3.2	Positioning of the Atlant Sites and Related Instrumentation.....	11
3.3	Deployment of Rain Gauges.....	13
3.4	DGMAN Automatic Weather Stations (AWS) Used in the Trial .....	16
3.5	Radiosonde Data on Meteorological Conditions .....	16
3.6	Atlant Operating Schedules .....	18
3.7	Design of Atlant Operating Schedules .....	19
4	Meteorology Conditions in the Hajar Mountains 2013 - 2018.....	20
4.1	Rainfall .....	20
4.2	Steering Winds .....	21
4.3	Meteorological Indices Derived from Radiosonde Data.....	25
4.4	Meteorological Indices Derived from DGMAN AWS Data .....	31
5	Statistical Analysis 2013 - 2018.....	37
5.1	Methodology .....	37
5.1.1	Meteorological Covariates .....	38
5.1.2	Attribution .....	39
5.1.3	Confidence Levels.....	39
5.2	Comparison of Target and Control Gauge-Day Rainfall, 2013 - 2018 .....	40
5.3	Regression Modelling of Downwind Gauge-Day Rainfall, 2013 - 2018 .....	44
5.4	Estimating Atlant Attribution from Downwind Gauge-Day Rainfall, 2013 - 2018..	48
5.5	Statistical Analysis of Gauge-Day Attribution Estimates.....	51
6	Analysis for 6-Year Gauges .....	56
7	Modelling of Downwind Positive Rainfall Averages .....	59
8	Exploratory Analysis of 2018 Atlant Salah Trial .....	61
8.1	Trial instrumentation and Implementation in the Salah Region.....	61
8.2	Rainfall in the Salah Trial Area 2018.....	64
8.3	Attribution Analysis for Salah 2018 .....	66

---

9	Summary and Conclusions .....	68
10	References.....	70
	Appendix A.1 – Instrumentation .....	72
	A.1 Atlant Installations with Operating Years .....	72
	A.2 DGMAN Automatic Weather Stations (AWS) with Contributing Years .....	73
	A.3 TIE Rain Gauges Locations .....	74
	Appendix B – Operating Schedules 2013 - 2018.....	80
	B.1 2013 Operating Schedule .....	80
	B.2 2014 Operating Schedule .....	85
	B.3 2015 Operating Schedule .....	90
	B.4 2016 Operating Schedule .....	94
	B.5 2017 Operating Schedule .....	99
	B.6 2018 Operating Schedule .....	103



## 1 Executive Summary

This is the final report on the Oman trials of the ATLANT™ (hereafter, Atlant) rainfall enhancement system, carried out jointly by Australian Rain Technologies (ART) and Trading and Investment Establishment (TIE) over 2013 - 2018. These six years have spanned a variety of climatic conditions, with more rainfall observed in the first three years of the trial, and less rainfall in the last three years. Separate reports were prepared by ART for each of the five trials 2013 - 2017. However, because of missing data from the Muscat radiosonde in 2018, no 2018 specific report is presented here. Instead, we combine the available 2018 data with the existing 2013 - 2017 data to present an analysis of all six years of these trials. This allows us to provide a definitive view on what we have learnt over the entire six-year experiment, and avoids the necessity of making the very strong assumptions about missing radiosonde information that would be necessary for a separate analysis of the 2018 data from the Hajar Mountains trial.

The 2018 trial itself was conducted July 1 - Oct 31 in two quite separate areas: The ten Atlant mechanisms (H1 - H10) used in the 2017 trial were again operated in the Hajar Mountains in the north of Oman while two new Atlant mechanisms (H11 - H12) were deployed in the Salalah region in the south of Oman. Atlant is a ground-based ionisation technology well-suited for field trials using a randomised experimental design and based on a fixed network of sites and rainfall gauges. The 2018 experiment in the Hajar Mountains was an independent repetition of the 2017 experiment design, and consisted of 10 sites operated according to a spatially and temporally balanced randomised design across a network of 201 rainfall gauges, while the two sites used in Salalah experiment were independently operated using a randomised cross-over design across a network of 19 rainfall gauges. The meteorological and topographical conditions in the Salalah region are quite different from those in the Hajar Mountains, and so one would expect to see a different rainfall enhancement signal for the Salalah trial. This consideration, together with the small size of this trial, meant that the 2018 results for rainfall enhancement in Salalah presented here are exploratory in nature, and should be used as a guide for any further trials there. They are briefly described later in this summary.

The fundamentals of the statistical methodology used in the analysis of the combined data for the Hajar Mountains trials are unchanged from those used in the initial 2013 trial, and in all subsequent trials. The daily rainfall measurement from a gauge is designated as a target measurement if the gauge is downwind of at least one active Atlant site; more specifically, it lies inside one of the 70km leeward sections of 30km wide by 140km long corridors that are centred on Atlant sites and aligned with the steering wind direction on the day, and the Atlant is also active that day. Because the relative orientation of the Atlant sites with respect to the steering wind changes from day to day, a gauge can be downwind of more than one active Atlant. However, only around 4 per cent of target measurements relate to more than one active Atlant. Downwind gauge readings that are not target measurements are classified as control measurements. By definition, these gauge readings are downwind of inactive Atlants.

The analysis itself focuses on positive gauge level rainfall values for gauges that are located in these (dynamically changing) corridors. In particular rainfall data from upwind gauges, i.e. gauges that are in the upwind corridor of an Atlant on the day, and also not in the downwind corridor of any other Atlant, are used to develop a regression model for expected natural rainfall downwind. This expected rainfall is then used as the main covariate in a model for downwind rainfall that also includes gauge elevation and Atlant indicators for the target measurements. Both the upwind and downwind models are specified on a logarithmic scale, with a random day effect to allow for unexplained day to day meteorological variability, and with the downwind model fit used to calculate a factor reflecting Atlant-related enhancement (if any) in a downwind rainfall reading. The estimated Atlant attribution component of a downwind rainfall reading is computed as the actual rainfall value times one minus the inverse of this factor. The overall Atlant attribution over the six years of the trial is the total of these daily gauge-level attribution estimates, expressed as a percentage of the total estimated natural rain component of the same daily gauge-level readings, with natural rainfall defined as observed rainfall less Atlant attributed rainfall.

The precision or significance of the estimated enhancement effect described in the previous paragraph is estimated using bootstrap techniques that account for the potential correlation or lack of independence of rainfall gauge observations due to geographic proximity and exposure to similar meteorological conditions on the day. In addition, the potential for the estimated attribution to be a chance occurrence due to a propitious arrangement of Atlant operating schedules over the six years of the experiment is assessed via a permutation analysis, which re-estimates attributions on the basis of a large number of alternative feasible Atlant operating schedules and then compares the resulting permutation distribution of estimated attributions with the actual estimated attribution.

**Table 1 Cumulative estimates of Atlant attribution 2013 - 2018.**

<b>Analysis Period</b>	<b>Estimated Enhancement over Period</b>	<b>Standard Error of Estimated Enhancement</b>	<b>Bootstrap Probability of a Positive Enhancement over Period</b>	<b>Permutation Probability that Enhancement is Due to Chance</b>
<b>2013-14</b>	19.7 per cent	6.3 per cent	99.99 per cent	0.17 per cent
<b>2013-15</b>	19.4 per cent	4.5 per cent	100 per cent	0.02 per cent
<b>2013-16</b>	20.8 per cent	3.8 per cent	100 per cent	0 per cent
<b>2013-17</b>	19.1 per cent	3.4 per cent	100 per cent	0 per cent
<b>2013-18</b>	16.3 per cent	2.9 per cent	100 per cent	0 per cent

Table 1 shows the bootstrap analysis-based estimated enhancement (attribution), with associated standard error and probability of being greater than zero as well as the permutation-based probability of the observed enhancement being a chance occurrence. Values are provided for cumulating analysis periods, and are all based on

the same final model specifications developed using the 2013 - 2018 data. They show how accumulating data over the six years of the trial improves the precision of the final analysis. The drop in the estimated enhancement when the 2018 data are added reflects the unbalanced nature of these data due to missing radiosonde information in 2018, as well as the dry conditions that were prevalent in this year.

Although the same model specification was used for each analysis period in Table 1, the actual models fitted were different, due to the different data sets that were used. Another perspective on the overall impact of Atlant operation over the six years of the trials is to therefore look at the enhancement estimates for each year generated using the data from all six years. These are set out in Table 2.

**Table 2 Annual estimates of Atlant attribution 2013 - 2018.**

Year	Estimated Enhancement for Year	Standard Error of Estimated Enhancement	Bootstrap Probability of a Positive Enhancement for Year
<b>2013</b>	18.1 per cent	1.7 per cent	100 per cent
<b>2014</b>	16.4 per cent	2.6 per cent	100 per cent
<b>2015</b>	15.5 per cent	2.7 per cent	100 per cent
<b>2016</b>	15.9 per cent	2.6 per cent	100 per cent
<b>2017/18*</b>	17.7 per cent	9.9 per cent	99.4 per cent

\* The unbalanced 2018 data could not be used alone because of the very high variability of the resulting attribution estimate. They are combined with 2017 data here.

The consistency and level of precision of these results is a direct consequence of the extensive rainfall and meteorological data that were collected over the six Atlant trials in the Hajar Mountains, coupled with a scientifically rigorous experimental design and the use of advanced statistical methodology for analysis of the trial data. The fact that Atlant operation resulted in an annual enhancement of between 15 per cent and 18 per cent for each year of the Hajar Mountains trial is a convincing argument for deployment of Atlant technology as a long-term low-cost addition to Oman's water supply in this area.

Finally, we comment on the exploratory trial carried out in the Salalah area in 2018. Two Atlants (H11 and H12) were deployed in this region in 2018, along with a network of 19 rain gauges. Since the meteorological and topographic characteristics of the Salalah area are quite different from those of the Hajar Mountains, the 2018 Salalah trial was designed and analysed separately from the 2013 - 2018 Hajar Mountains trial. Given the relatively sparse instrumentation of the Salalah trial (19 gauges compared with the 120 gauges initially used to evaluate H1 and H2 in 2013), it was clear that the most that could be achieved using the 2018 Salalah trial data would be an exploratory analysis, perhaps indicating whether Atlant operation in the Salalah area had the potential to lead to rainfall enhancement similar to that experienced in the Hajar Mountains.

Unfortunately, placement of rain gauges relative to H11 and H12 for the 2018 trial was less than optimal, with approximately 73 per cent of rainfall events observed at these

gauges occurring when they were neither downwind nor upwind of H11 and H12. That is, almost three-quarters of the rainfall data obtained in the 2018 Salalah trial could not be used to evaluate a rainfall enhancement effect. As a consequence, the effective sample size for the Salalah trial was quite small, and it was not surprising that no significant results were obtained.

Using all the available data from Salalah, an estimated attribution of 6.3 per cent was calculated, with a standard error of 12.5 percentage points. However, this was influenced significantly by an extreme rainfall event on October 14, which accounted for approximately 75 per cent of all downwind rain observed in the Salalah trial area in 2018. When this event was discarded from the analysis, the estimated attribution jumped to 35.2 per cent. This value is clearly not a realistic estimate of the actual Atlant rainfall enhancement effect in the 2018 Salalah trial, and further trials in this area, with a better placement of rainfall gauges seems advisable.

In summary, the Atlant technology is low cost with minimal environmental impact, and on the basis of the results reported in the Hajar Mountains (15-18 per cent increased rainfall each year with a probability of a positive enhancement greater than 99 per cent) it appears to have the potential to significantly increase the availability of water resources in a region where these resources are under a high level of stress. But the climatic conditions that underpin summer rainfall in the Hajar Mountains of Oman are relatively unique. Ideally further experimentation using Atlant type (ground-based ionisation) methods in different environments is necessary.

## 2 Introduction

### 2.1 Rainfall Enhancement Trials in Oman

Oman is one of most water-stressed countries in the world, with Intergovernmental Panel on Climate Change (IPCC) simulations showing that the northern part of Oman is expected to face decreasing average annual rainfall in the coming decades of up to 40% (Charabi, 2013). Any technology that can increase rainfall or mitigate projected future reduction is therefore of considerable interest.

It was against this background that Trading and Investment Establishment (TIE) contracted Australian Rain Technologies (ART) to train their personnel and assist in the operation of a six-year rainfall enhancement trial using ART's Atlant technology in the Hajar Mountains of northern Oman, starting in 2013. The trial was managed from a local TIE project headquarters in Muscat, Oman, and included the coordination of the operations of the Atlant sites and data instrument arrays across the trial region, as well as sourcing meteorological data for the trial period from the network of DGMAN (Oman Directorate General of Meteorology and Air Navigation) automatic weather stations in the trial area, and also obtaining daily radiosonde data from Seeb airport (now Muscat International Airport) on wind direction and speed, as well as relevant daily meteorological indices. ART monitored the operation of the trial remotely from Australia,



including the provision of randomised Atlant operating schedules for each year of the trial, conducting monitoring visits as required during the trial, and coordinating an independent annual assessment of the effect of the Atlant technology based on rainfall and meteorological measurements recorded during the trial. This assessment was carried out by the National Institute for Applied Statistics Research Australia (NIASRA) at the University of Wollongong, and resulting in the provision of annual reports that used the trial data collected up to that point to summarise the performance of the Atlant systems in place up to and including the previous year.

This report constitutes the final report prepared for the trial, and so provides an analysis of the entire data set collected during the six years of the trial, 2013 - 2018.

## 2.2 Ground-Based Ionisation and Atlant Rainfall Enhancement

Ground-based ionisation as a means of weather modification has a long history of investigation, including numerous field experiments into the electrification of clouds that have sometimes led to positive results. This electrification is typically via the widespread releases of ions into the sub-cloud air using a high-voltage power supply that generates corona discharges from an extensive array of small diameter wires elevated above the ground and exposed to local winds and updrafts (Vonnegut and Moore 1959; Vonnegut et al. 1961, 1962; Moore et al. 1986; Kaufman and Ruiz-Columbié 2005, 2009; Beare et al. 2010; 2011; Chambers et al. 2012). Several mechanisms exist by which ions might influence the microphysical processes of precipitation formation at multiple stages through the process (Harrison and Carslaw 2003; Khain et al. 2004; Tinsley et al. 2000; Tinsley and Zhou 2014). However, while previous studies provide at least semi-plausible “chain of events” mechanisms by which generated ions may influence precipitation, they are yet to be verified observationally.

Each Atlant device consists of a high-voltage generator connected to a network of thin metal wires supported on a frame, generating ions via corona discharges at voltages up to 100KV. Although questions remain to be answered about the underlying processes, a working hypothesis based on current understanding is that negative ions generated from the Atlant high-voltage corona discharge wire array become attached to aerosols or particles in the atmosphere (especially soluble particles), which later act as cloud condensation nuclei. The ionised aerosols are conveyed into the cloud base by wind, atmospheric convection and turbulence, and the electric charges on these particles are transferred to cloud droplets. The resulting increased electrostatic forces on droplet interaction aid the coalescence of droplets, resulting in enhanced raindrop growth rate and increasing rainfall downwind from the Atlant.

The four Atlant sites displayed in Figure 1 illustrate the three Atlant frame designs that have been employed in the Oman trials, and reflect design improvements aimed at greater ion generation efficiency, durability and maintainability. The original design comprised thin wires wrapped around a pyramid frame (top left). The next design comprised thin wires wrapped around a ‘Fish Eye’ frame and elevated further from the ground (top right). The most recent design comprises wire wrapped around a triangle frame (bottom).



**Figure 1 The Atlant designs. Pyramid at H2 (top left). Fish Eye at H4 (Top Right). Triangle at H10 (Bottom left). Triangle at H11 (Bottom right).**

### **3 Hajar Mountains Trial Area and Instrumentation 2013- 2018**

#### **3.1 Geography and Climate of the Hajar Mountains Trial Area**

The climate in the Sultanate of Oman varies from one region to another and from one season to another but there are mainly two seasons, with transition months separating, namely:

- Winter or Northeast Monsoon (December-March)
- Transition Northeast-Southwest Monsoon (April-May)
- Summer or Southwest Monsoon (June-September)
- Transition Southwest-Northeast Monsoon (October-November)

Past climatological studies have identified the winter season (December through March) as accounting for the bulk of rain in flat and coastal areas in northern Oman. Troughs, depressions, and the occasional tail end of cold fronts, move through the region from the west and northwest resulting in large-scale systems that can provide significant rainfall. However, the occurrence and amount of rainfall is highly variable, not occurring at all in some years, and provides few opportunities for regular rainfall enhancement operations. During the summer season (June through September), convective rainfall over the Hajar Mountains is a phenomenon that is known locally and has been recently

studied. The reported high occurrence of convective storms over these mountains with consistently suitable microphysical conditions makes summer the most suitable time for rainfall enhancement operations (Figure 2) since there is the potential of inducing a significant amount of rainfall during these months. These steep mountains have peaks of over 3000 metres, and run parallel to the coast of the Gulf of Oman. Convective clouds forming over them create showers and thunderstorms over a limited area in northern Oman during the summer months. This weather is generally of short duration and intense.

Orographic forcing, the advection of moisture from the south-western parts of the Arabian Sea or via sea breeze from the Gulf of Oman and large-scale lifting are important factors in determining the occurrence of cloud and rainfall. On days with no rain potential, dry north-westerlies converge (over the mountains) with the sea-breeze from the Gulf of Oman. Conversely on days with cloud and/or rain development, the sea-breeze converges with moisture flow advected from the Arabian Sea. Dry desert air will lead to moist convection being suppressed, whereas moist air advected from the Arabian Sea will enhance moist convection. Moisture advection from the Arabian Sea in a column of at least 1 kilometre in depth is required for proper convection (Al-Maskari et al. 2006). The stronger the flow from the Arabian Sea and the deeper the column of the moist air, the heavier the precipitation. Generally, clouds that develop over the peaks of the Hajar Mountains dissipate as they move west.



**Figure 2 Convection clouds along the Hajar Mountains 10 July 2004 (source: Al Brashdl, 2007).**

### **3.2 Positioning of the Atlant Sites and Related Instrumentation**

The trial commenced with the deployment of two Atlant systems in 2013. An extra two systems were then deployed each subsequent year in the Hajar Mountains trial area up

to and including 2017. In 2018 two further systems were deployed, but these were located in the Salalah trial area in the south of Oman. The systems were sequentially labeled, starting with H1 and H2 in 2013, H3 and H4 in 2014, H5 and H6 in 2015, H7 and H8 in 2016 and H9 and H10 in 2017. The two systems set up in the Salalah trial area in 2018 were labeled H11 and H12. Figure 3 shows the Hajar mountains trial area in 2013. This was extended each year with the deployment of additional Atlants and extensions to the rain gauge network (see Section 3.3)



**Figure 3 Trial area for first year (2013) of the trial.**

Initial Atlant placement (H1 and H2) targeted the Batinah/Dakhliyah Region of Oman. This region was chosen considering synoptic and local wind flows, cloud types, widespread uplift, and moisture availability. Such features affect the delivery of charged particles or aerosols to the cloud layer and potential subsequent rainfall enhancement. The aim was that rainfall enhancement operations would then occur in areas with a high frequency of suitable clouds and where there was irrigation flow and ground water recharge. In Oman, groundwater recharge is mainly in the Wadis (dry river beds) that cut through the mountains. Subsequent Atlant sites were then generally positioned either side of Atlants that were already in place, with sites chosen so that they were sufficiently separated from one another so that their areas of influence did not significantly overlap and also so that they effectively covered the main north-west to south-east range of peaks in the Hajar Mountains area. That is, they were effectively placed along a line running at 90° to the main NE wind direction and so located to take advantage of orographic lifting of the ionised aerosols generated from operation of the Atlant mechanism. Table 3 sets out the locations, elevations and years of deployment of all the Atlants used in the trial.

In addition to the actual Atlant mechanisms at each site, SODAR wind profilers were installed at Atlant sites H1 and H2 in 2014 and also at H5 in 2015 in order to develop a better understanding of uplift conditions in the mountains. The SODAR at H1 was damaged by lightning strike in 2015, but data collected from these instruments in 2014 and 2015 were a key input to confirming the 2013 decision that the most likely place to look for a rainfall enhancement effect associated with an operating Atlant was in a 30km wide corridor extending 70km downwind of the Atlant. These profilers were used in

2014 (H1 and H2) and 2015 (H2 and H5). In addition, AWS were installed at all Atlants in order to assess how local meteorological conditions at a site correlated with upper atmosphere behaviour. In the end these local conditions proved too unstable to be useful indicators of any rainfall enhancement impact downwind from the Atlant operation, and so these data were not used in the final trial analysis.

**Table 3 Atlant locations, elevations and years deployed.**

Atlant	Latitude (decimal)	Longitude (decimal)	Elevation (m)	2013	2014	2015	2016	2017	2018
<b>Hajar Mountains trial area</b>									
H1	23.32	57.12	2670	x	x	x	x	x	x
H2	23.18	57.53	2157	x	x	x	x	x	x
H3	23.69	56.80	1621		x	x	x	x	x
H4	23.17	58.04	1395		x	x	x	x	x
H5	23.16	58.61	1876			x	x	x	x
H6	23.55	56.55	1466			x	x	x	x
H7	23.04	58.89	1574				x	x	x
H8	23.52	56.98	1501				x	x	x
H9	24.50	56.28	1200					x	x
H10	23.12	58.34	1675					x	x
<b>Salalah trial area</b>									
H11	16.81	53.64	984						x
H12	16.73	53.11	1289						x

### 3.3 Deployment of Rain Gauges

From the start of trial planning it was known that relying on DGMAN rainfall data would be too limiting since these data are obtained from a relatively small number of rainfall gauges that are co-located with DGMAN automatic weather stations (AWS) sites. Due to the localised and short-lived nature of rainfall throughout the trial area, an extensive array of 120 rain gauges was therefore installed by TIE prior to the start of the 2013 trial. These gauges were installed on an approximate 10 km regular grid throughout the trial and provided rainfall data on an hourly basis. Subsequent extension of the Hajar Mountains trial by the deployment of additional Atlants over 2014-2017 meant that additional rain gauges were required in order to cover the new areas that could be impacted by the operation of the additional Atlants. By 2017 the rain gauge network covering the Hajar Mountains trial area was made up of 201 gauges. No new gauges were installed in the Hajar Mountains trial area in 2018 since no new Atlants were deployed there. A further 19 gauges were installed in the Salalah area in 2018 to provide rainfall data for analysis of the performance of H11 and H12 that year. Table 4 lists the number of operating rain gauges in each year 2013 - 2018.

Figure 4 shows the locations of the 201 gauges that covered the Hajar Mountains trial area in 2017, as well as the locations of the Atlants (H1-H10) in this area and the locations of the DGMAN AWS whose data were used in the analysis, while Figure 5 shows the change in the extent of the gauge network on a year by year basis, providing

some perspective on the increase in the coverage of this network as the trial continued and more Atlants were deployed.

**Table 4 Size of rain gauge network by year, 2013 - 2018.**

Year	2013	2014	2015	2016	2017	2018
No. of gauges	120*	149	179	191	201	201 (Hajar) 19 (Salalah)

\* 12 of these gauges (all located in the Battinah Plain in 2013) were moved to other sites more likely to record rain in 2014, and were also renumbered. This meant that there were effectively 41 "new" gauge locations in 2014.

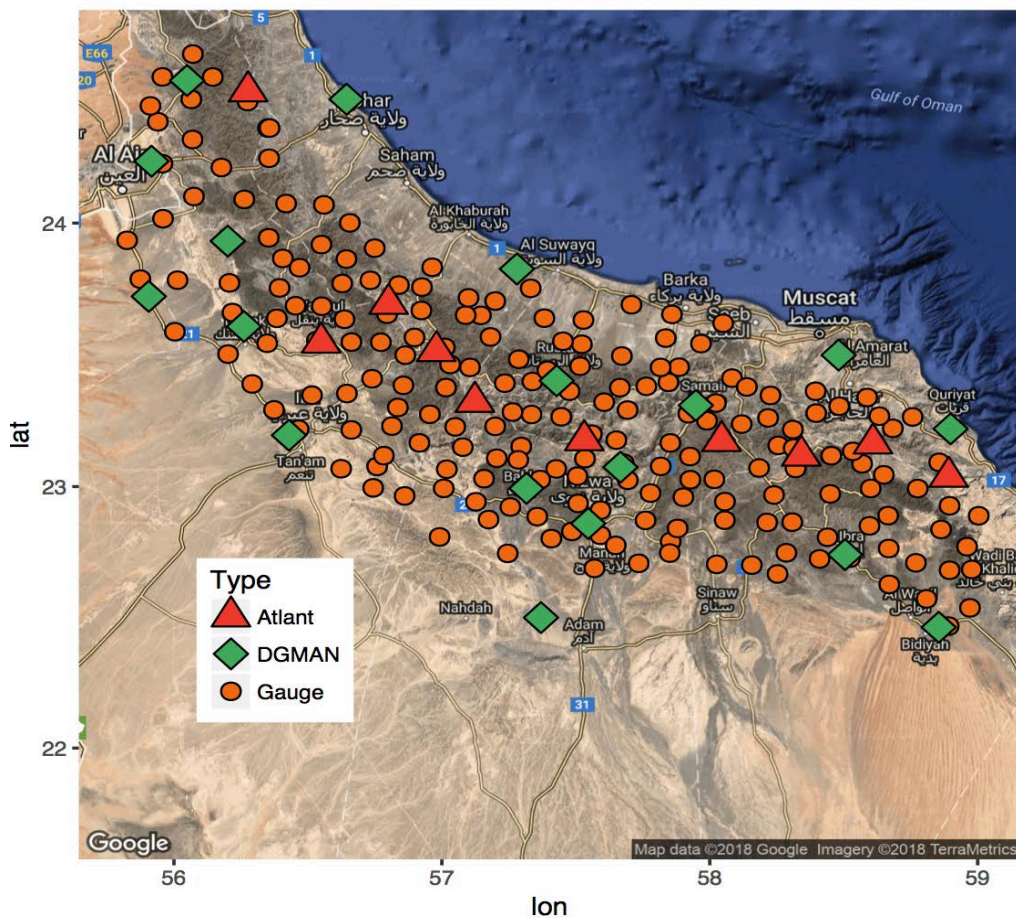


**Figure 4 Instrument locations in the Hajar Mountains trial area 2017.**

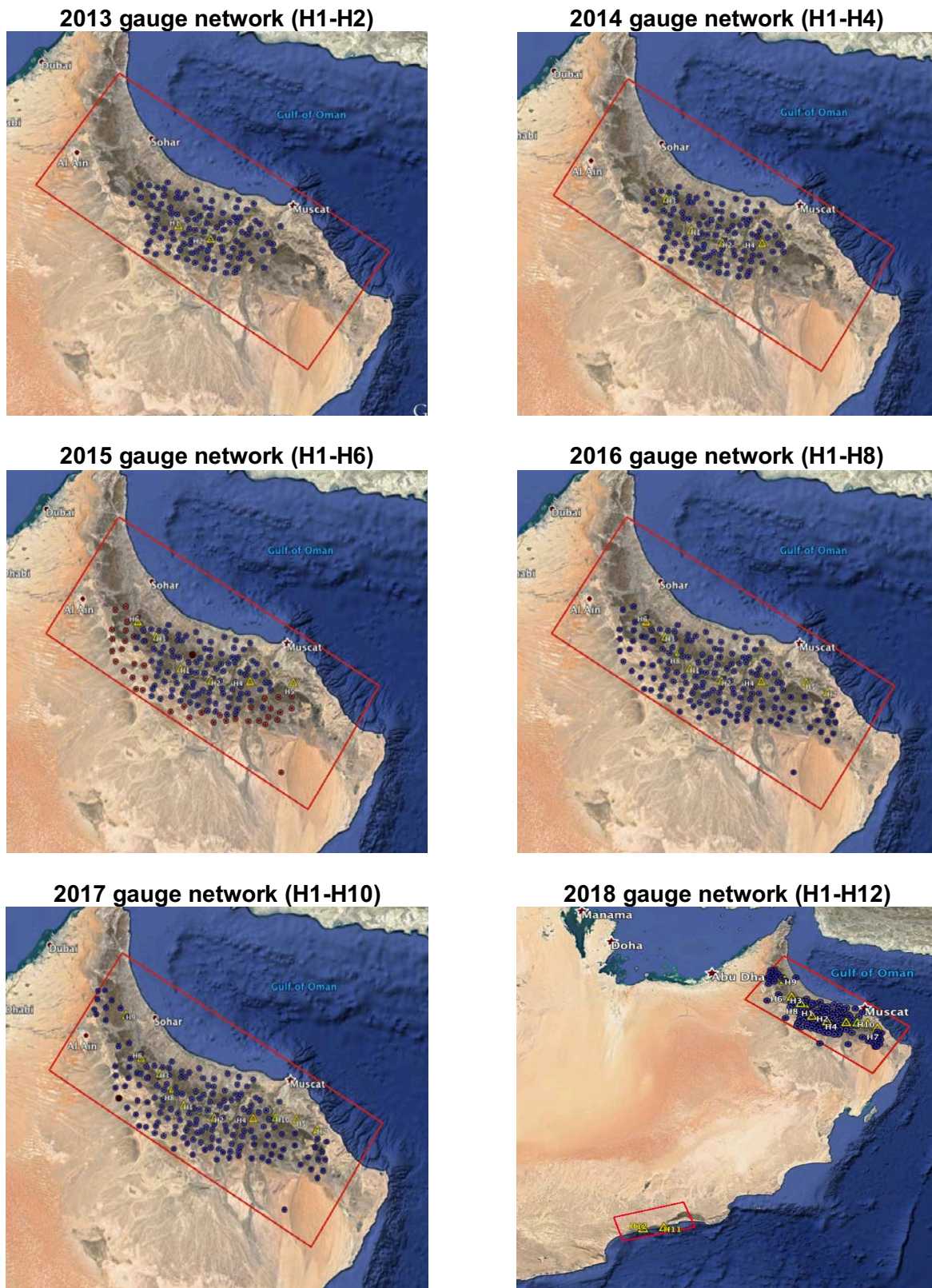


**Figure 5 Growth in the gauge network 2013 - 2018.**

### 3.4 DGMAN Automatic Weather Stations (AWS) Used in the Trial

DGMAN operates a number of AWS in both trial areas (Hajar Mountains and Salalah). Hourly observations were available from these stations and were used to characterise prevailing weather conditions on the day when modelling the rainfall data collected by the rainfall gauge network. Appendix A.2 lists the locations and elevations of DGMAN AWS used by year. Note that not all were used in each year, due to data availability problems. Table shows the number of DGMAN AWS that contributed data to the analysis of the Hajar Mountain trial over 2013 - 2018.

**Table 5 Number of DGMAN AWS contributing data to analysis of the Hajar Mountains trial.**

Year	2013	2014	2015	2016	2017	2018
No. of AWS	10	11	17	17	18	17

The main measurements collected from each AWS, and used in the analysis of the trial data were:

- Wind speed (m/s);
- Dry air temperature (°C);
- Dew point temperature (°C);
- Relative humidity (%);
- QFE air pressure (hPa);
- QNH air pressure (hPa).

All AWS measurements are available on an hourly basis. For the purpose of analysis of daily rainfall in the trial area, daily averages of these measurements were used. Since cloud formation in the Hajar mountains is essentially a late morning and afternoon phenomenon, these averages were computed using readings from 10:00 to 20:00 inclusive.

### 3.5 Radiosonde Data on Meteorological Conditions

DGMAN operates a radiosonde at Muscat International Airport, which is used to collect daily data on vertical wind profiles (direction and speed) as well as the values of key meteorological indices thought to be predictive of rainfall propensity in the Northern Oman area. This radiosonde is nominally supposed to launch at 4am local time (00z) daily, with data from it used to define steering wind speed and direction each day. Given the elevation of some of the Atlant locations in the Hajar Mountains, and particularly H1 and H2, a decision was made prior to analysis of the 2013 trial data to define the steering wind direction and speed on a day as that obtained by averaging the wind directions and speeds measured between the 700hPa and 500hPa pressure levels in the vertical wind profile data obtained by the 4am radiosonde. Another radiosonde is launched at Salalah Airport at the same time, and data from it was used in analysis of the performance of H11 and H12 in 2018. In 2015, 2017 and 2018, TIE also contracted



with DGMAN for an extra radiosonde to be launched at Muscat each day. In 2015 this second radiosonde was supposed to be launched at 4pm, while in 2017 and 2018 it was supposed to be launched around mid-day. In both cases these extra launches were aimed at investigating whether wind directions later in the day were more informative in terms of identifying the actual direction of air transport over the Atlants operating in the Hajar Mountains.

In addition to information on vertical wind profiles, radiosonde data are the basis for calculation of a number of key daily meteorological indices that were then used in analysis of the trial data. These are:

- Total totals index: An indicator for storm development;
- Lifted index: An indicator for thunderstorm development;
- Precipitable water: The amount of rainfall if a column of the atmosphere were to be precipitated;
- Convective Available Potential Energy (CAPE): The amount of energy available for atmospheric convection;
- Lifted Condensation Level (LCL): A measure of cloud base height.

Measurement of steering wind direction and speed is crucial in identification of the area where an operating Atlant is supposed to have a rainfall enhancement effect. As a consequence, access to high quality radiosonde data is essential for the analysis of the data collected in the trial. Over 2013 - 2014 the radiosonde data were generally of good quality, with occasional missing days due to operational issues at Seeb (Muscat International) airport. However, between 2015 and 2018 there were some serious issues with missing radiosonde data due to changes in radiosonde technology at the airport. In these cases, statistical imputation methods were used to fill in the missing values where possible. Two main imputation methods were used:

- When wind speed and direction data were missing from one radiosonde on a day, but these data were available from another later (or earlier) radiosonde, then a bivariate Gaussian distribution was fitted to the u and v components of wind direction and speed for days where both radiosondes provided data, and this distribution was then used to impute the missing u and v values for days when only one radiosonde's data were available, as the expected values of the missing components given the observed components for the same day. These imputed u and v component values were then back transformed to obtain imputed wind direction and speed values for the missing radiosonde on the day;
- When there was just one radiosonde on the day (2013, 2014 and 2016) with missing data, or both radiosondes (2015, 2017 and 2018) had missing data, then each missing radiosonde was imputed separately, using data from the same radiosonde just before and just after the day with the missing data. This was done via twiced nonparametric regression imputation, applied to the known u and v components for those days with data. Separate smooth non-parametric "loess" functions were first extracted from these known u and v values. Residuals from

these fits were then computed and re-smoothed using a loess function with a smaller bandwidth than the original fit. Finally, both large bandwidth and small bandwidth loess functions were summed and used to compute predicted values for the missing u and v components in each series. These predicted values were finally back transformed to obtain imputed wind direction and speed values for the missing radiosonde on the day.

The preceding non-parametric regression imputation method was used provided there were no more than three days of missing radiosonde data at a time, with observed radiosonde data just before and just after. For longer periods of missing radiosonde data, it was decided that imputation would not be appropriate, and so these days were excluded from the trial. Table shows the number of days over each year of the trial when data from the 4am Muscat radiosonde were available or where missing values could be imputed. The sum of these days (740 days) is one measure of the effective size of the Hajar Mountains trial.

**Table 6 Number of radiosondes and number of days with radiosonde data 2013 - 2018.**

Year	2013	2014	2015	2016	2017	2018
<b>Muscat radiosondes (time)</b>	1 (4am)	1 (4am)	2 (4am, 4pm)	1 (4am)	2 (4am, 1pm)	1 (4am, 1pm)
<b>No of days with actual or imputed radiosonde data</b>	170	140	127	125	108	70

### 3.6 Atlant Operating Schedules

Operation of Atlants in the 2013-2018 trial were carried out according to a randomised operating schedule that was defined each year before commencement of operations for that year (usually around May) and was strictly followed, irrespective of weather patterns. The only exceptions were due to mechanical and electrical breakdowns in individual Atlants, or when the Atlant (all of which were remotely controlled from TIE offices in Muscat) had to be switched off because of concerns that their continued operation could exacerbate the risk of flash flooding due to extreme weather in the Hajar Mountains that day. However, this was extremely rare. Provided at least one Atlant continued to be operated on such days, the pre-set operating regime continued as planned when the Atlants that had been shut down returned to operational status. Table 7 lists the effective trial periods over 2013-2018 when Atlants were operated. Note that these periods were impacted both by mechanical failure of Atlants (2016) and by missing radiosonde data (2017 and 2018).

**Table 7 Effective trial periods 2013 - 2018 for the Hajar Mountains trial.**

Year	2013	2014	2015	2016*	2017**	2018***
<b>Trial Period</b>	15/5 - 31/10	1/6 - 18/10	14/6 - 18/10	H1-H6 1/6 - 31/10 H7 6/8- 31/10 H8 29/7 - 31/10	<b>16/7 - 31/10</b>	<b>1/7 - 23/8 1/10 - 16/10</b>

\* The Atlants H7 and H8 introduced in 2016 were a new design that was supposed to commence operation on July 1. However, design deficiencies meant that they both suffered weather-related damage after installation. The times set out here are the actual operating periods for these Atlants after they were repaired and reinstalled.

\*\* All Atlants were operational July 1 - Oct 31. However, missing radiosonde data July 1 - July 15 meant that these days had to be excluded from the trial.

\*\*\* All Atlants were operational July 1 - Oct 31. However, missing radiosonde data Aug 24 - Sep 30 and Oct 17 - Oct 31 meant that these days had to be excluded from the trial.

### 3.7 Design of Atlant Operating Schedules

Appendix B lists the complete set of operating schedules that were specified for the six years of the trial. The design of the operating schedule in any given year depended on the number of Atlants that needed to be randomised. In 2013 the two sites (H1 and H2) were operated on a randomised crossover schedule defined by randomly permuting the equal number of days over the summer when one Atlant was off and the other on, and vice versa. This ensured that each Atlant was operated the same number of days. In 2014, the same scheme was used with four Atlants (H1 - H4) by now operating two out of the four each day, with the two operating Atlants always chosen so that they were always "separated" by one non-operating Atlant and with the permutations blocked by month. Finally, from 2015 onwards (i.e. with six or more Atlants involved in the trial) the operating schedule used by H1 - H10 each day was randomly chosen to simultaneously meet three constraints. The first was that there were an equal number of operational and non-operational Atlants each day, with the second requiring that no more than two "adjacent" Atlants operate together on the same day, and the third requiring that any particular Atlant not be allowed to operate more than twice in succession. Selection of the actual operating schedule with this more complicated design was carried out by simulation-based optimisation subject to these constraints with the optimality criterion defined to be minimisation of the number of times individual Atlants were operated on successive days. For 2018 the operating scheme used by H11 and H12 in the Salalah area was a randomised crossover schedule defined by randomly selecting one half of the days involved in the 2018 trial as H11 operating days (with H12 then being off) and the remaining as H12 operating days (with H11 then being off).

The advice provided by DGMAN was that convective cloud development in the Hajar mountains generally begins earliest at 10am local and dissipates at approximately 8pm

local. Consequently, Atlants were switched on and off in accordance with a nominal switching time at 7am (local Oman time) on their designated operating days. This was to ensure that enough time elapsed before the onset of convective cloud development, allowing Atlant generated ions to be transported across the target areas. A 30-minute "temporal buffer" was also added to the switch time, so that the ions from the off-going Atlant had time to clear the area before switching on the ongoing Atlant. With a nominal switch time at 7am, the operating Atlant was therefore turned off at 6.30am and the ongoing Atlant was then turned on at 7am.

## 4 Meteorological Conditions in the Hajar Mountains 2013 - 2018

### 4.1 Rainfall

The rain gauge network installed across the Hajar Mountains 2013-2018 provided hourly rainfall readings at each gauge, for each day of the trial. These readings were added together to produce 122,259 gauge-day values for rainfall over the six years of the trial, where a gauge-day rainfall value is the total amount of rainfall recorded at a gauge on a specified day. Given the arid conditions that are prevalent across the Hajar Mountains trial area, it is not surprising that over the 740 days of rainfall data recorded during the trial, approximately 92.5 per cent were zero values, with an overall average gauge-day rainfall of 0.35mm. From a rainfall enhancement viewpoint, however, it is the amount of rain that actually falls to the ground that is of interest, since the claim is that one can increase this amount. For the Hajar Mountains trial area the average gauge-day positive rainfall value over the six years of the trial was 4.74mm. That is, an average of 4.74mm of rain was recorded by gauges that reported rainfall 2013 - 2018.

As with most averages, this value conceals a lot of gauge to gauge and day to day variability. To illustrate this, in Figure 6 we show bubble plots of the gauge day values of positive rainfall separately for each year of the trial and for the different gauge locations defining the gauge network that year. The vertical axis in each plot is gauge latitude, while the horizontal axis is gauge longitude. The larger the circle, the larger the corresponding rainfall measurement at the gauge relative to other rainfall measurements that year. That is, the circles show relative, rather than absolute size. Note that in any given year there will be multiple rainfall measurements at a gauge, of differing magnitudes, leading to the portrayal of concentric circles with a gauge at their centre. Note that yearly average values of gauge-day positive rainfall are shown in parentheses next to the year identifier. The plots in Figure 6 graphically illustrate the drying out of the trial area from 2016 (echoed by the decreasing values of average gauge-day positive rainfall shown in parentheses above each plot), as well as the expansion of the gauge network each year. Unsurprisingly, the largest positive rainfall tends to occur along the NW to SE "spine" of the Hajar mountains.

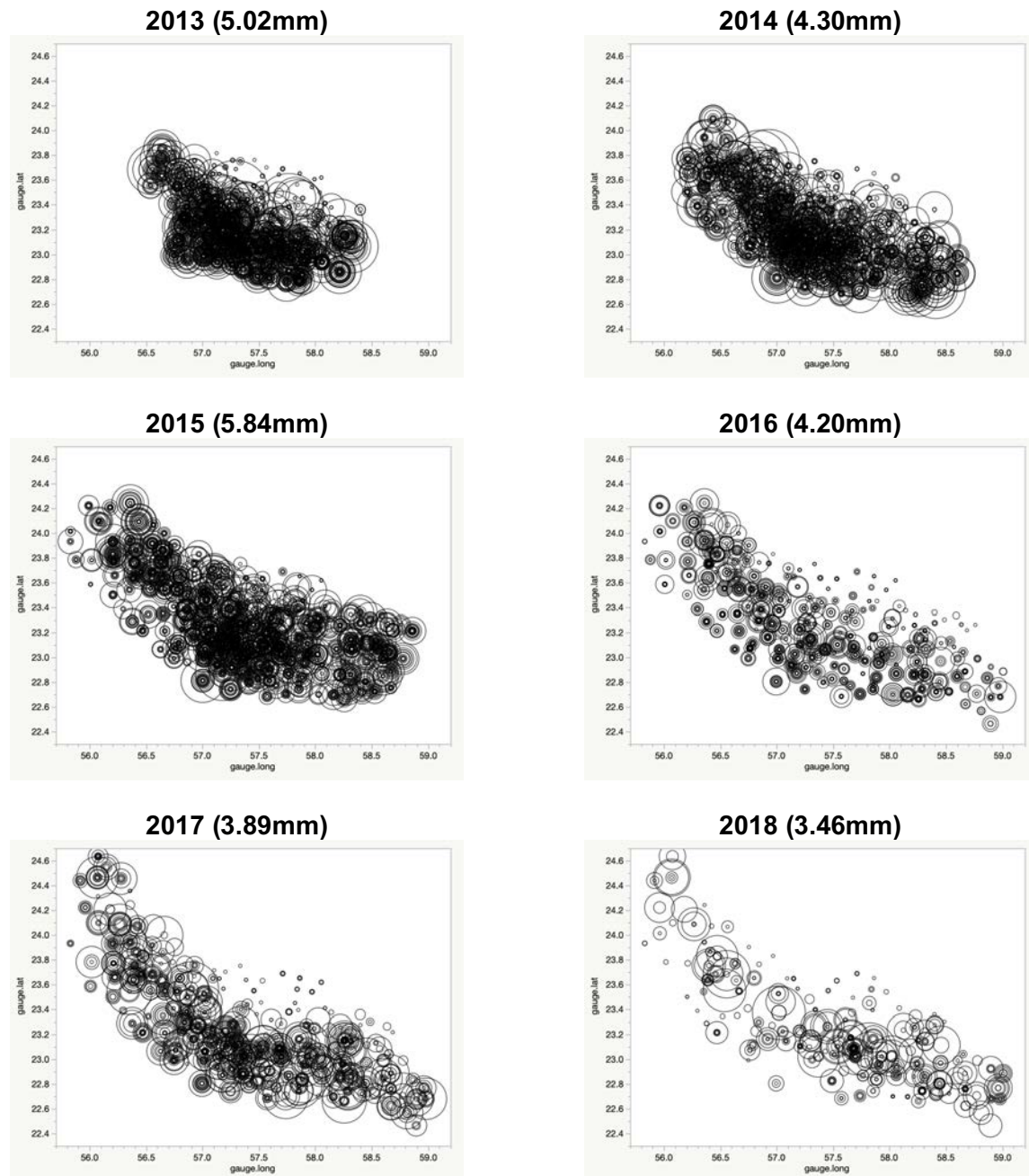


**Figure 6 Bubble plots of gauge locations showing 2013 - 2018 spatial distributions of gauge-day values of positive rainfall. Average positive rainfall for contributing gauge-days in parentheses.**

## 4.2 Steering Winds

As noted in Section 2.2, the underlying hypothesis for the Atlant rainfall enhancement mechanism is updraft transportation of charged aerosols into the cloud layer, followed by dispersal and rain drop formation in the direction of the steering wind. In effect, any rainfall enhancement due to operation of Atlant can only occur "downwind" of the Atlant

mechanism itself. Determination of the direction of the steering wind is a therefore prerequisite to identification of the Atlant "footprint", and consequent evaluation of an Atlant-induced rainfall enhancement effect, if it exists.

Prior to analysis of the 2013 trial data, it was decided that the speed-weighted average of the wind directions detected by a radiosonde between 700hPa and 500hPa would be a reasonable approximation to this steering wind direction, with the 4am Muscat radiosonde then used to determine a daily steering wind direction for the Hajar Mountains trial area. In Figure 7 we show the distribution of trial gauge-days (i.e. the 122,259 gauge-days contributing to the analysis of the trial data) when this steering wind direction is categorised according to one of eight principal directions. Here NNE corresponds to a wind direction between 0° and 45°, ENE is 45° to 90°, and so on, until NNW which is 315° to 360°. It is clear that the main wind directions experienced in the trial were NNE and ENE, i.e. the prevailing steering winds were from the NE. Interestingly, the plot of the distribution of positive rainfall value by wind direction in Figure 7 also shows that the main rainfall tended to occur when the steering winds were SSE, indicating occasional very strong monsoonal downpours.

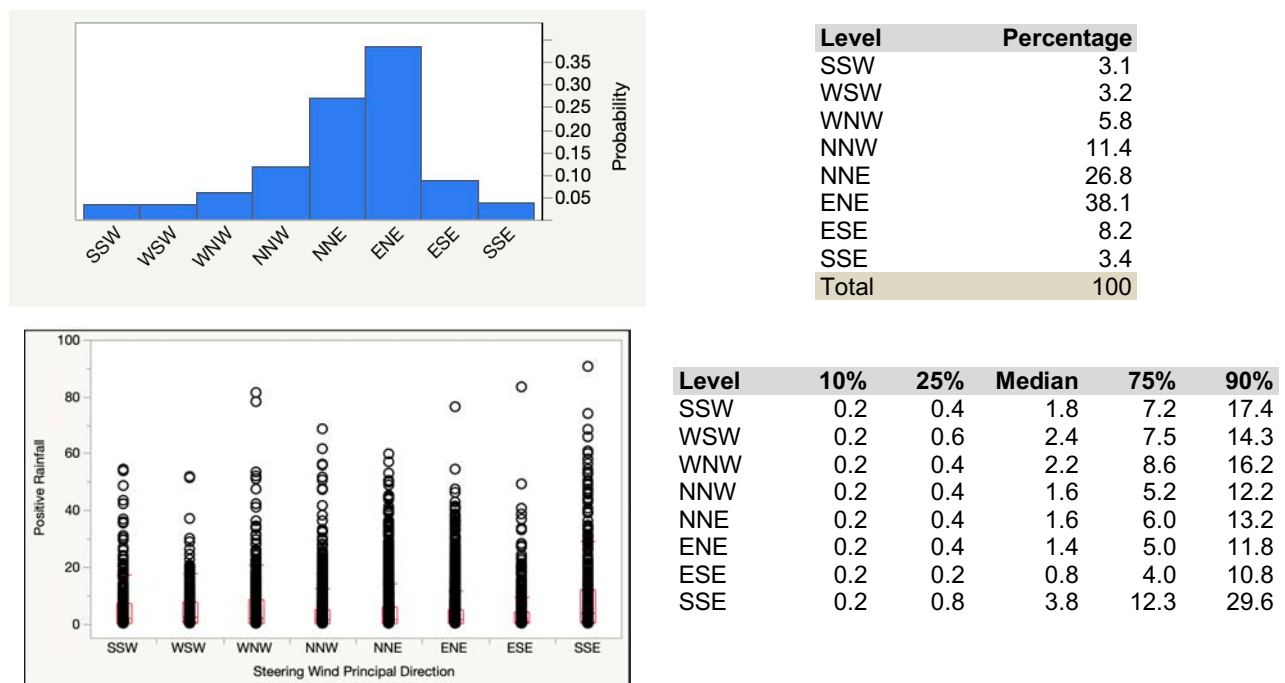


**Figure 7 Distribution of gauge-days by principal steering wind directions 2013 - 2018 with corresponding distributions of gauge-day positive rainfall values.**

Figure 8 shows the distribution of gauge-days by principal steering wind direction for each year of the trial. Here we see that the main NE direction for the steering winds persists each year, with some year to year variation. In particular it appears that over 2014 and 2014 there are more northerly winds, while in 2018 there appears to have been a slight increase in winds that have a more southerly aspect. However, this last

result needs to be discounted somewhat, given the large number of potential trial days in 2018 for which there was no radiosonde data (and hence no wind direction data).

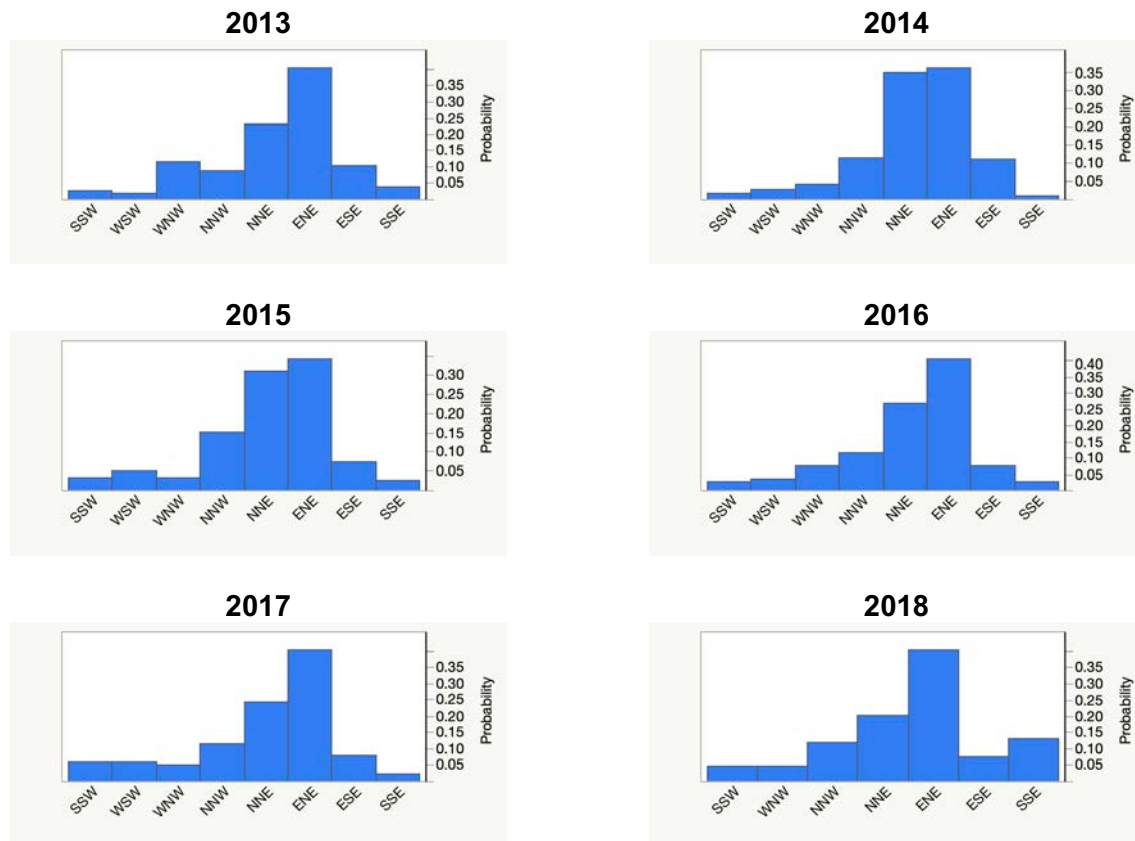


**Figure 8 Distributions of trial gauge-days by principal steering wind directions by year 2013 - 2018.**

From Figure 9 we see that increased rainfall with more southerly winds was evident in 2013, 2015, 2016 and 2017. As one might expect, since most trial gauge-days were under the influence of NE winds, average positive rainfall values when NE winds are prevalent are close to the overall trial average for gauge-day positive rainfall.

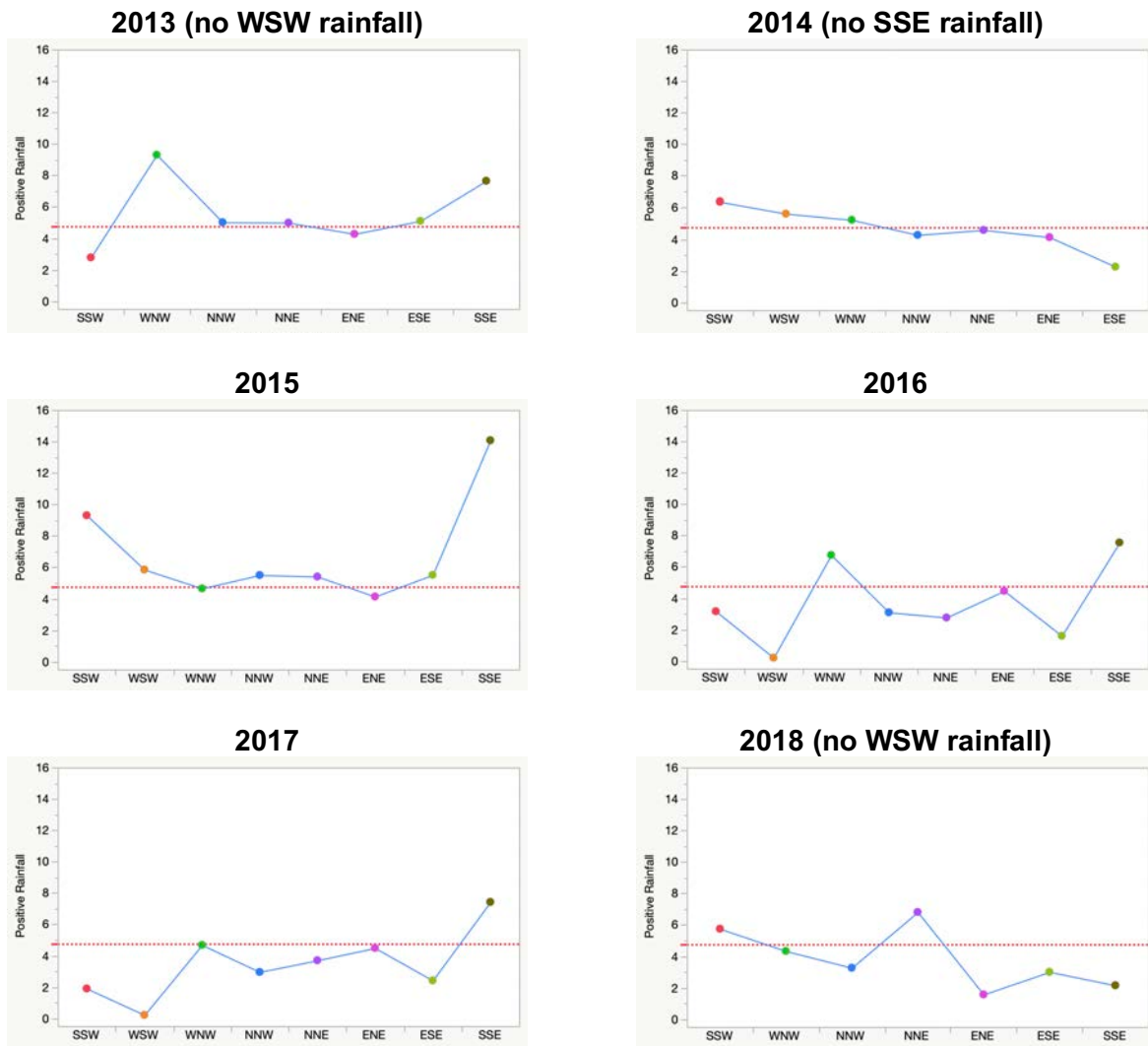


**Figure 9 Average values of gauge-day positive rainfall by principal steering wind direction, by year 2013 - 2018. Horizontal line is six-year average.**

Figure 10 displays the steering wind speeds (m/s) that were observed on trial days each year, with a non-parametric smooth trend superimposed. There is little here to comment on beyond a tendency for wind speeds to decrease towards the end of October in later years.



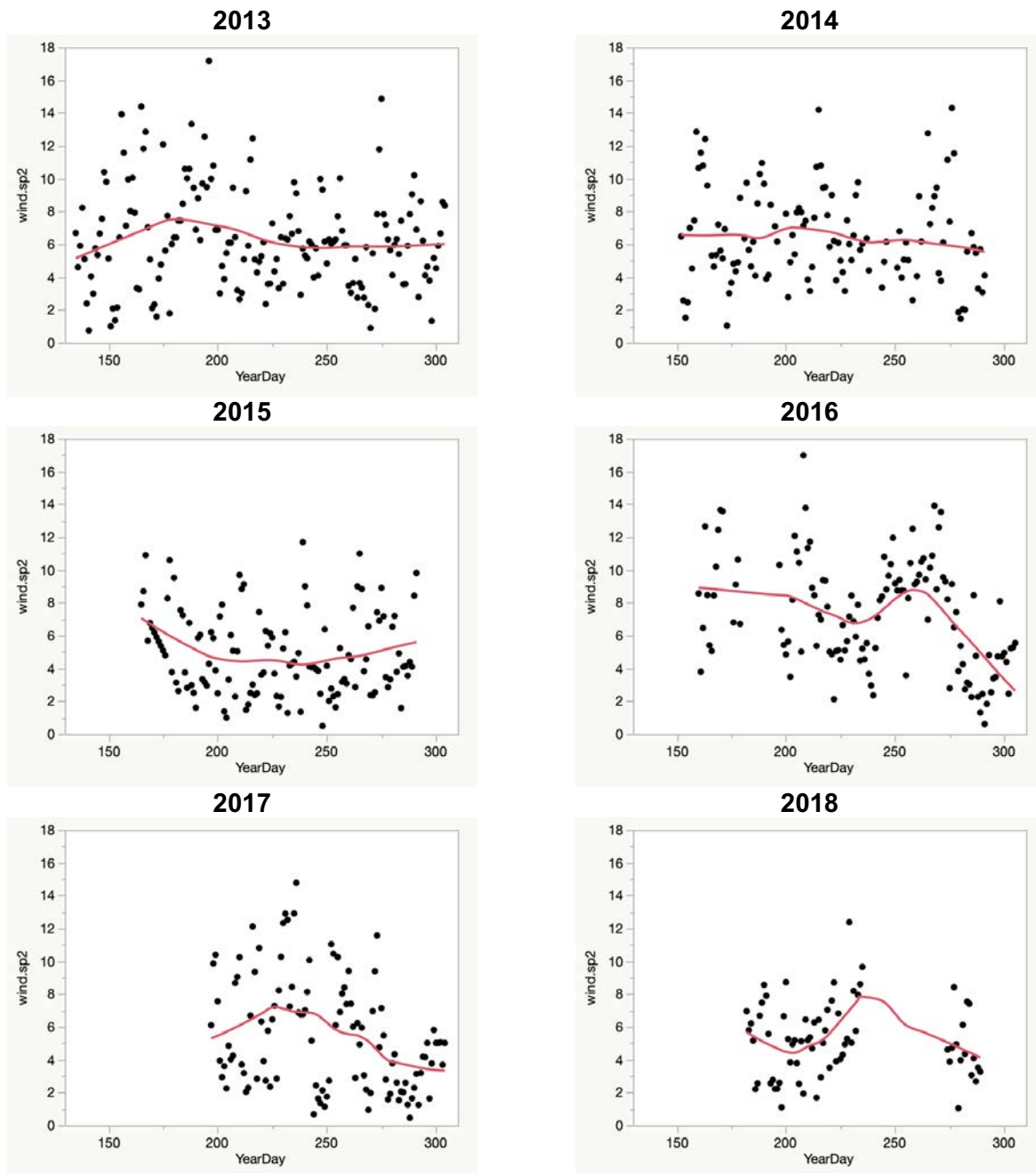


**Figure 10 Daily trends in steering wind speeds 2013 - 2018. YearDay is day of year.**

### 4.3 Meteorological Indices Derived from Radiosonde Data

There were four main daily meteorological indices for which there was data for all 740 days of the 2013 - 2018 Hajar Mountains trial. These were:

- Lifted index (lifted.index); a measure of atmospheric stability and a predictor of storm severity;

- Total totals (total.totals); another measure of atmospheric stability and also a predictor of storm severity;
- LCL Pressure (hPa) (lcl.pres); lifted condensation level, the elevation at which relative humidity reaches 100 per cent; and
- Precipitable Water (mm) (prec.water); a measure of the maximum potential for precipitation.

Table 8 shows the correlations between these indices and with average gauge-day positive rainfall for the 549 (out of 740) days when there was rainfall reported in the trial area.

**Table 8 Correlation matrix defined by daily values of meteorological indices, proportion of gauges reporting rainfall (Rainfall Event) and average gauge-day positive rainfall (Positive Rainfall) on days when there was rainfall.**

	lifted.index	total.totals	lcl.pres	prec.water	Rainfall Event	Positive Rainfall
lifted.index	1.000	-0.745	-0.671	-0.697	-0.394	-0.414
total.totals	-0.745	1.000	0.267	0.655	0.416	0.395
lcl.pres	-0.671	0.267	1.000	0.615	0.202	0.335
prec.water	-0.697	0.655	0.615	1.000	0.388	0.485
Rainfall Event	-0.394	0.416	0.202	0.388	1.000	0.573
Positive Rainfall	-0.414	0.395	0.335	0.485	0.573	1.000

We see that all four indices correlate with both the occurrence and the amount of actual rainfall. However, the correlation is not strong, averaging between 30 to 40 per cent in absolute value. Unsurprisingly, the highest correlation (0.485) is between Precipitable Water and Positive Rainfall. This implies that these indices may be useful as indicators of the potential for rain, and can be used as control variables in any analysis of actual observed rainfall.

Figures 11 to 14 show how the four meteorological indices change each year, with a non-parametric smooth trend superimposed on each plot to provide a better understanding of within year change. Again, it is clear that there is no great difference in year to year behaviour of these indices. This implies that it should be reasonable to combine data on meteorological indices across years when modelling rainfall.

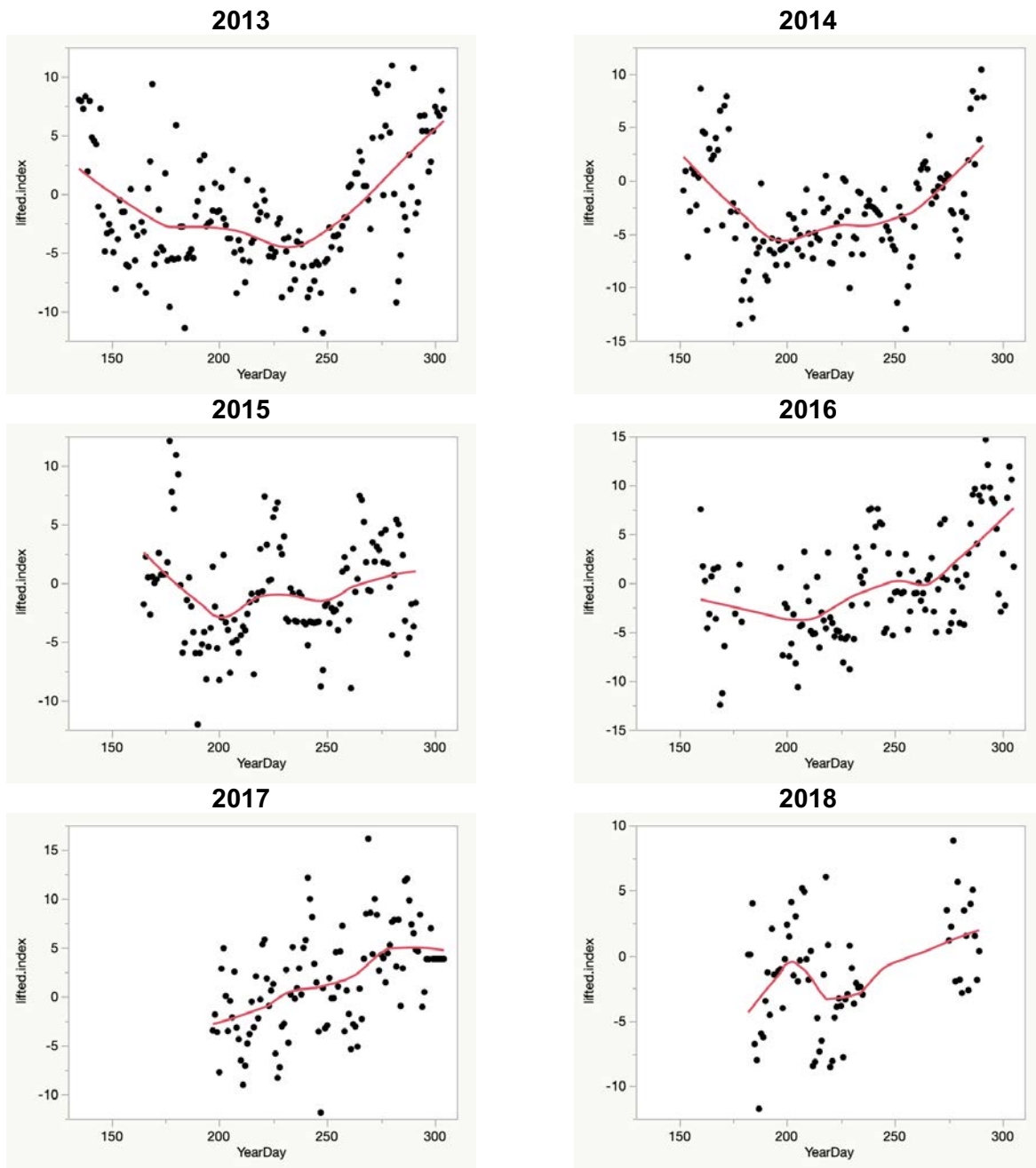


**Figure 11 Daily trends in Lifted Index values 2013-2018. YearDay is day of year.**

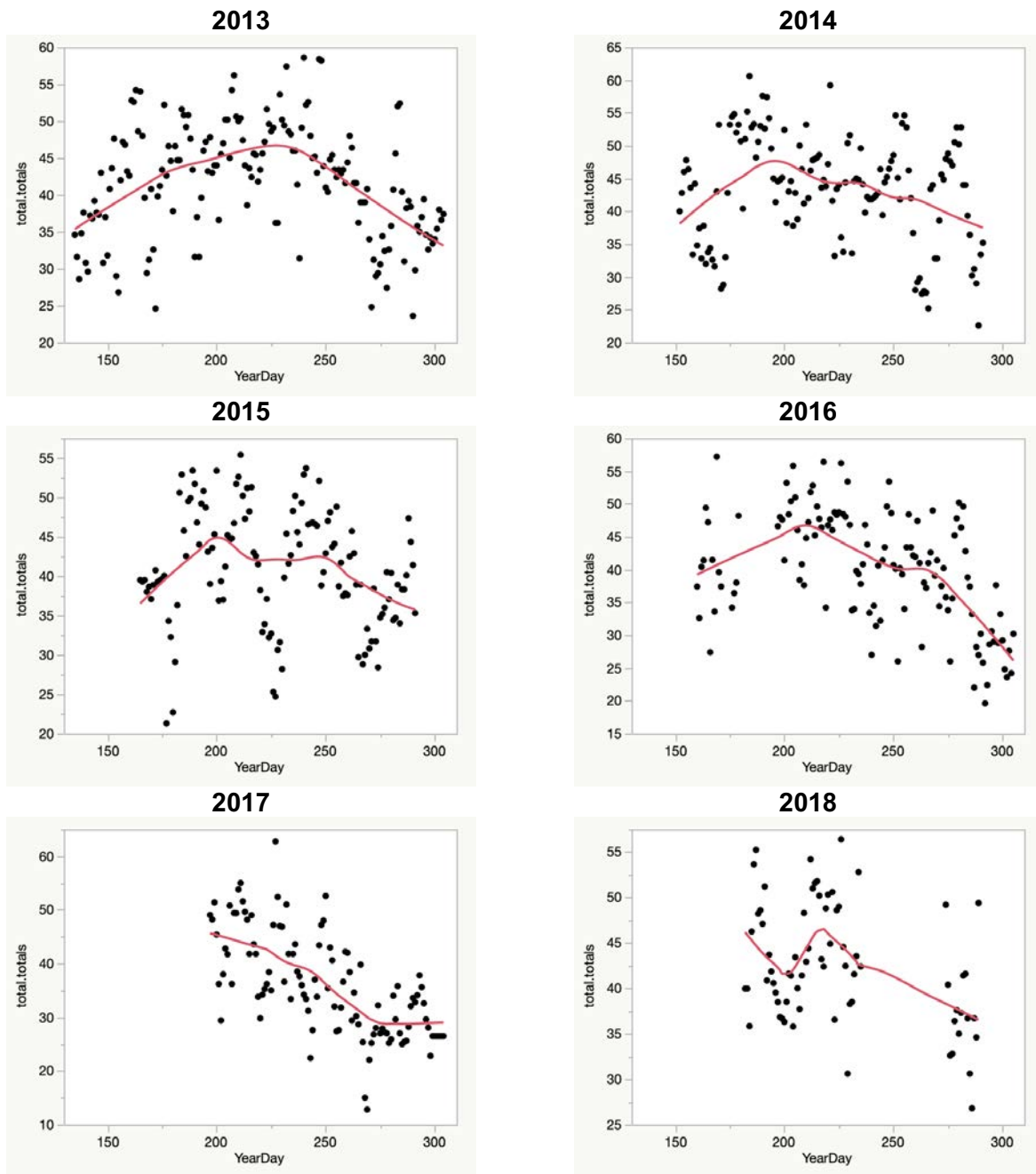
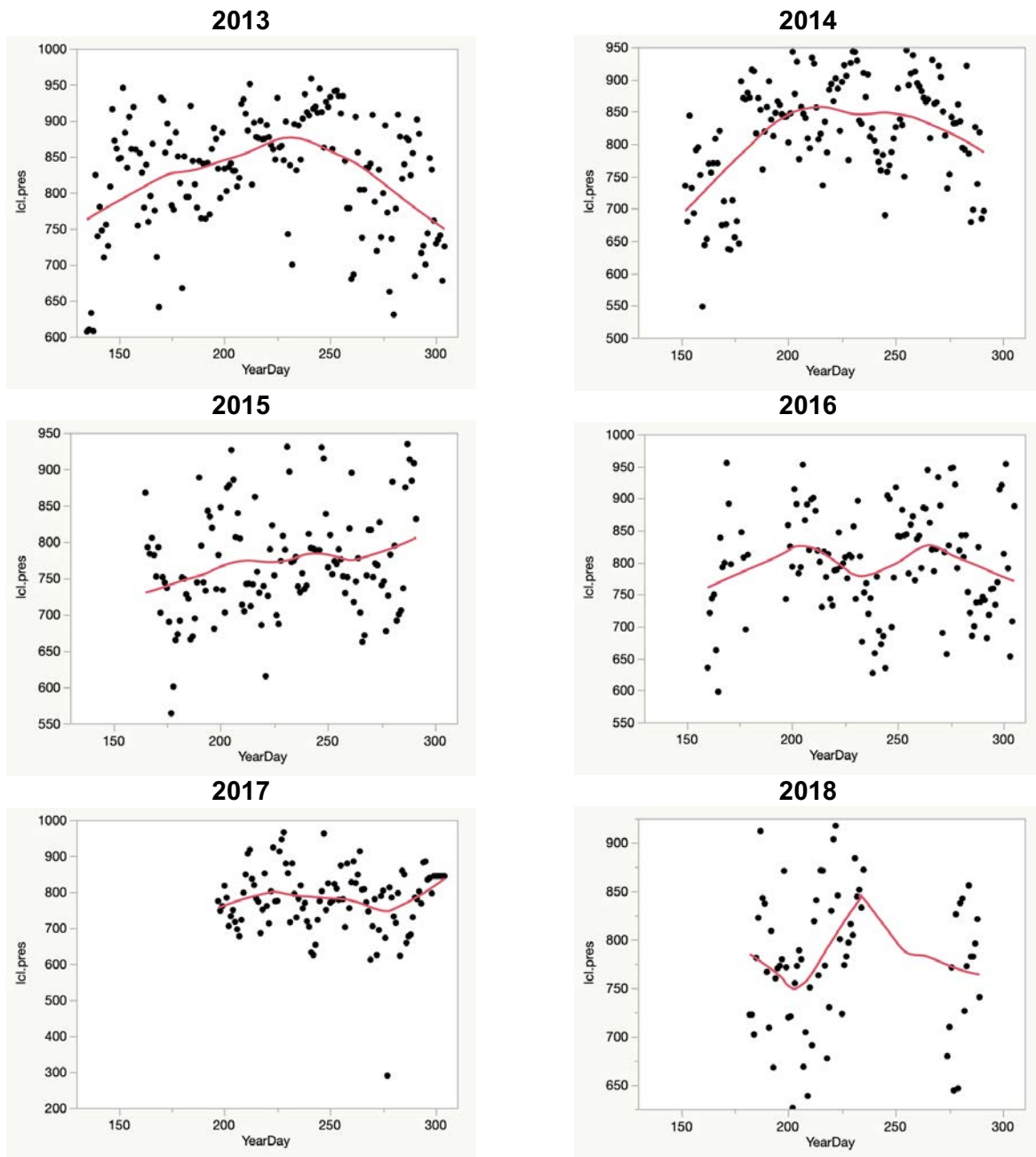
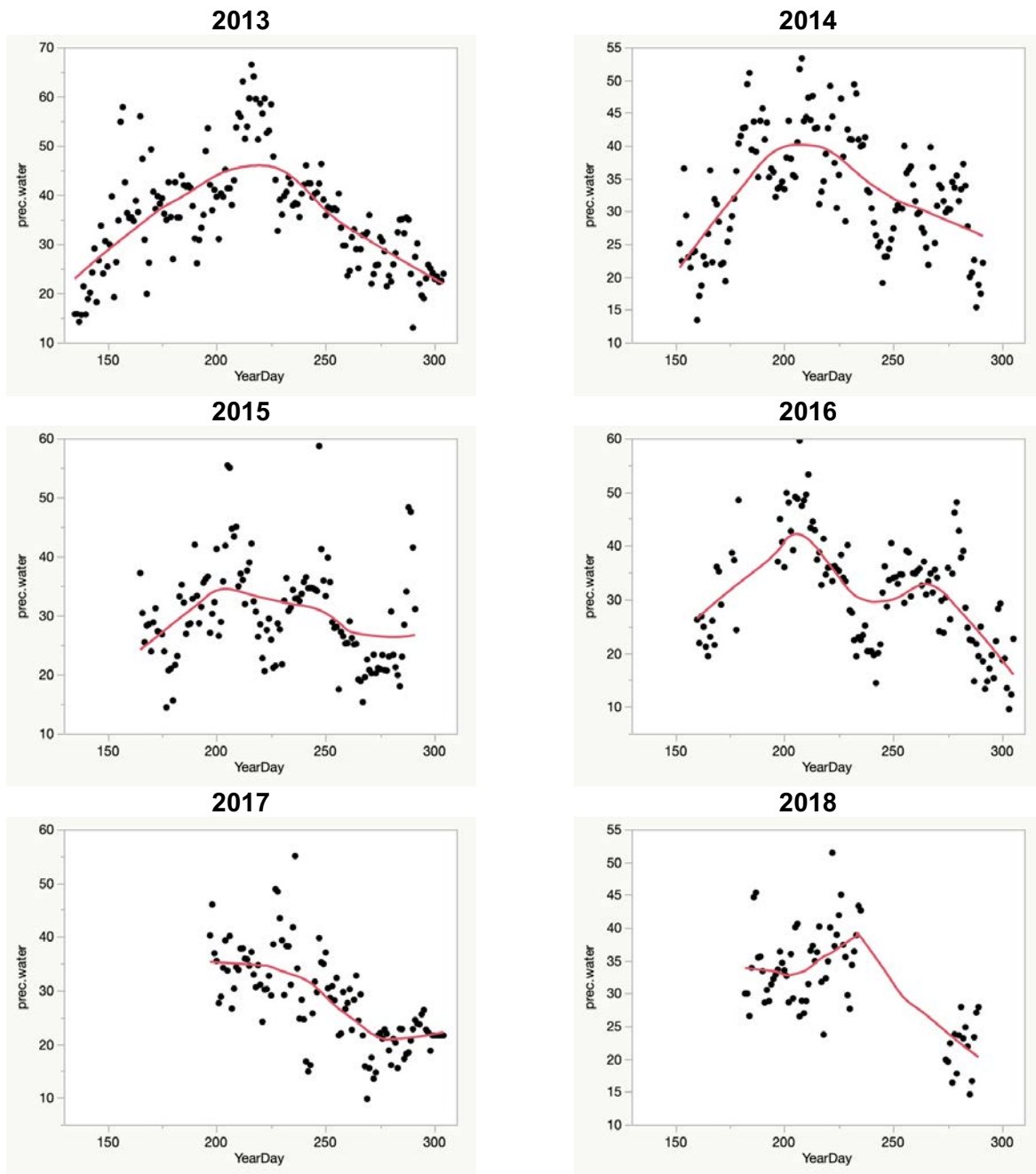


Figure 12 Daily trends in Total totals values 2013-2018. YearDay is day of year.



**Figure 13 Daily trends in LCL Pressure (hPa) values 2013-2018. YearDay is day of year.**



**Figure 14 Daily trends in Precipitable Water (mm) values 2013-2018. YearDay is day of year.**

#### 4.4 Meteorological Indices Derived from DGMAN AWS Data

As noted in Section 3.4, daily data on a number of key meteorological variables are available from the DGMAN AWS network in northern Oman. These data can be used to provide indicators of background rainfall propensity across the trial area on the day, making them potentially useful as control variables in an analysis. In order to capture an overall picture of the daily patterns of meteorological conditions across the trial area on a day, we summarise the individual AWS measurements by their first and second principal components. Table 9 shows the correlations between these principal components and proportion of gauges reporting rain on the day and the average rainfall for gauges that report rain. Note that we do not present results for the other variables measured by the DGMAN AWS network because there were gaps in their data that rendered them unsuitable for analysis.

**Table 9 Correlation matrix defined by daily values of the first and second principal components of dry air temperature (temp.dry.1, temp.dry.2), relative humidity (relh.1, relh.2) and the first principal component of QFE air pressure (pres.1), proportion of gauges reporting rainfall (Rainfall Event) and average gauge-day positive rainfall (Positive Rainfall) on days when there was rainfall.**

	temp.dry.1	temp.dry.2	relh.1	relh.2	pres.1	Rainfall Event	Positive Rainfall
temp.dry.1	1.000	-0.042	-0.519	0.078	-0.849	-0.141	-0.115
temp.dry.2	-0.042	1.000	-0.271	-0.724	0.190	0.118	-0.068
relh.1	-0.519	-0.271	1.000	0.002	0.144	0.465	0.519
relh.2	0.078	-0.724	0.002	1.000	-0.119	-0.186	-0.034
pres.1	-0.849	0.190	0.144	-0.119	1.000	-0.029	-0.098
Rainfall Event	-0.141	0.118	0.465	-0.186	-0.029	1.000	0.584
Positive Rainfall	-0.115	-0.068	0.519	-0.034	-0.098	0.584	1.000

With the exception of the first principal component of relative humidity (relh.1), these variables generally appear to correlate less with both rainfall propensity (Rainfall Event) and amount of rain (Positive Rainfall) than the meteorological indices examined in Section 4.3 above. This is somewhat surprising since the DGMAN data are based on actual AWS measurements on the day. In contrast, the comparatively strong correlation with relative humidity is to be expected, and indicates that this variable has the potential to be an important control.

Figures 15 to 19 show how the principal components change each year, with a non-parametric smooth trend again superimposed on each plot to provide a better understanding of within year change. Once more we note that there is no great difference in year to year behaviour of these indices, making it reasonable to combine data on these components across years when modelling rainfall.

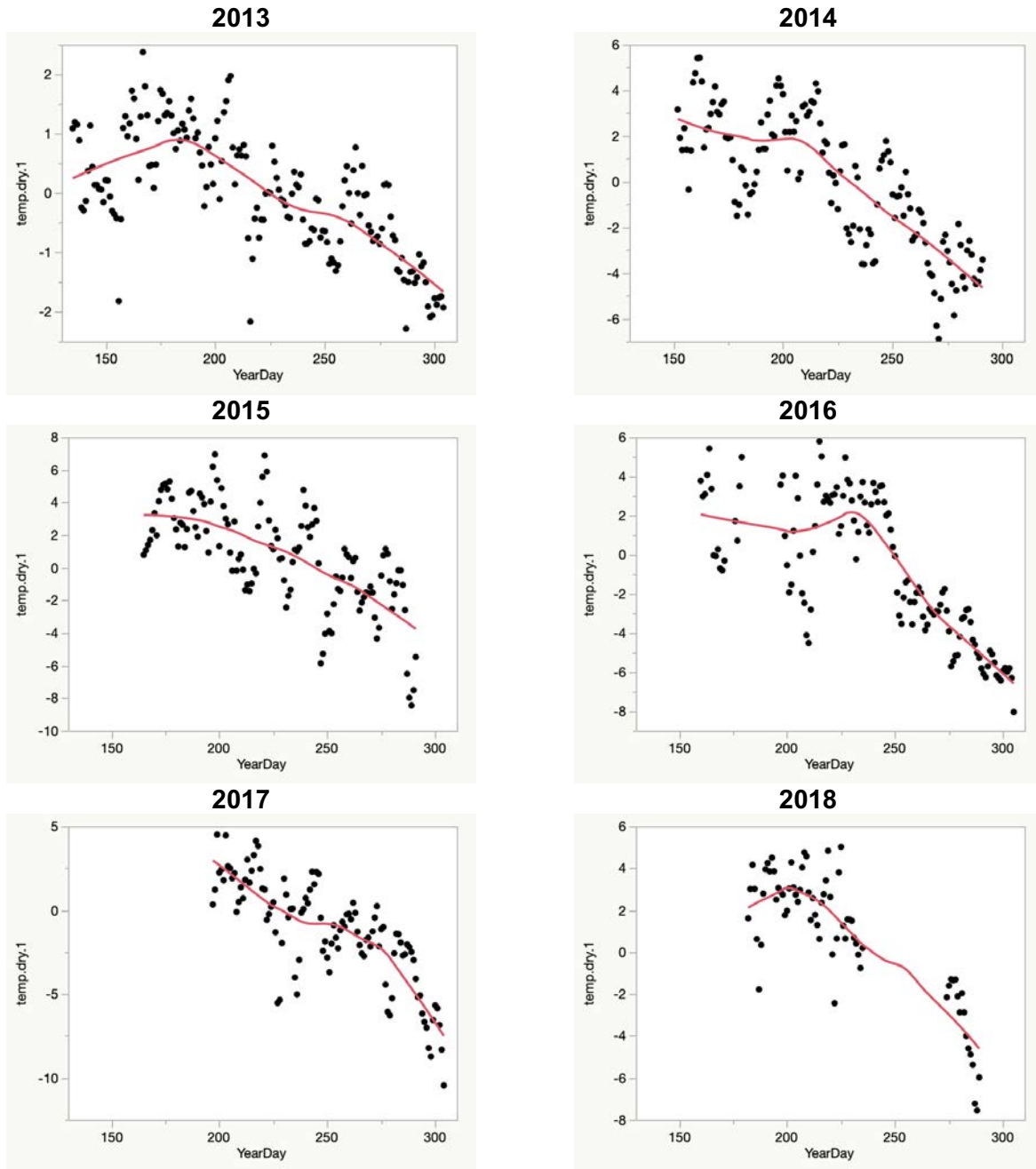


**Figure 15 Daily trends in first principal component (Prin1) of DGMAN Dry Temperature values 2013 - 2018. YearDay is day of year.**



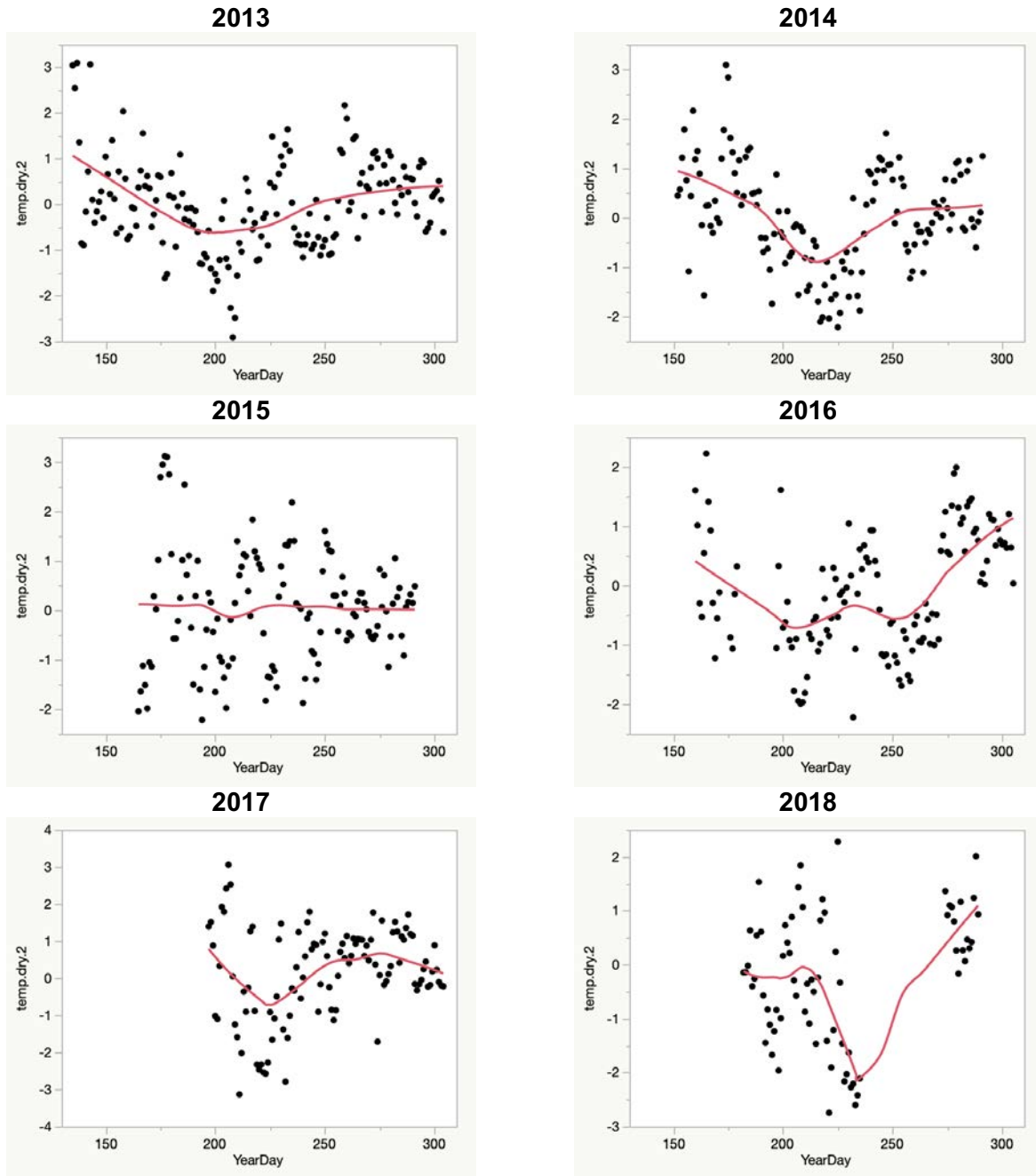


**Figure 16 Daily trends in second principal component (Prin2) of DGMAN Dry Temperature values 2013 - 2018. YearDay is day of year.**

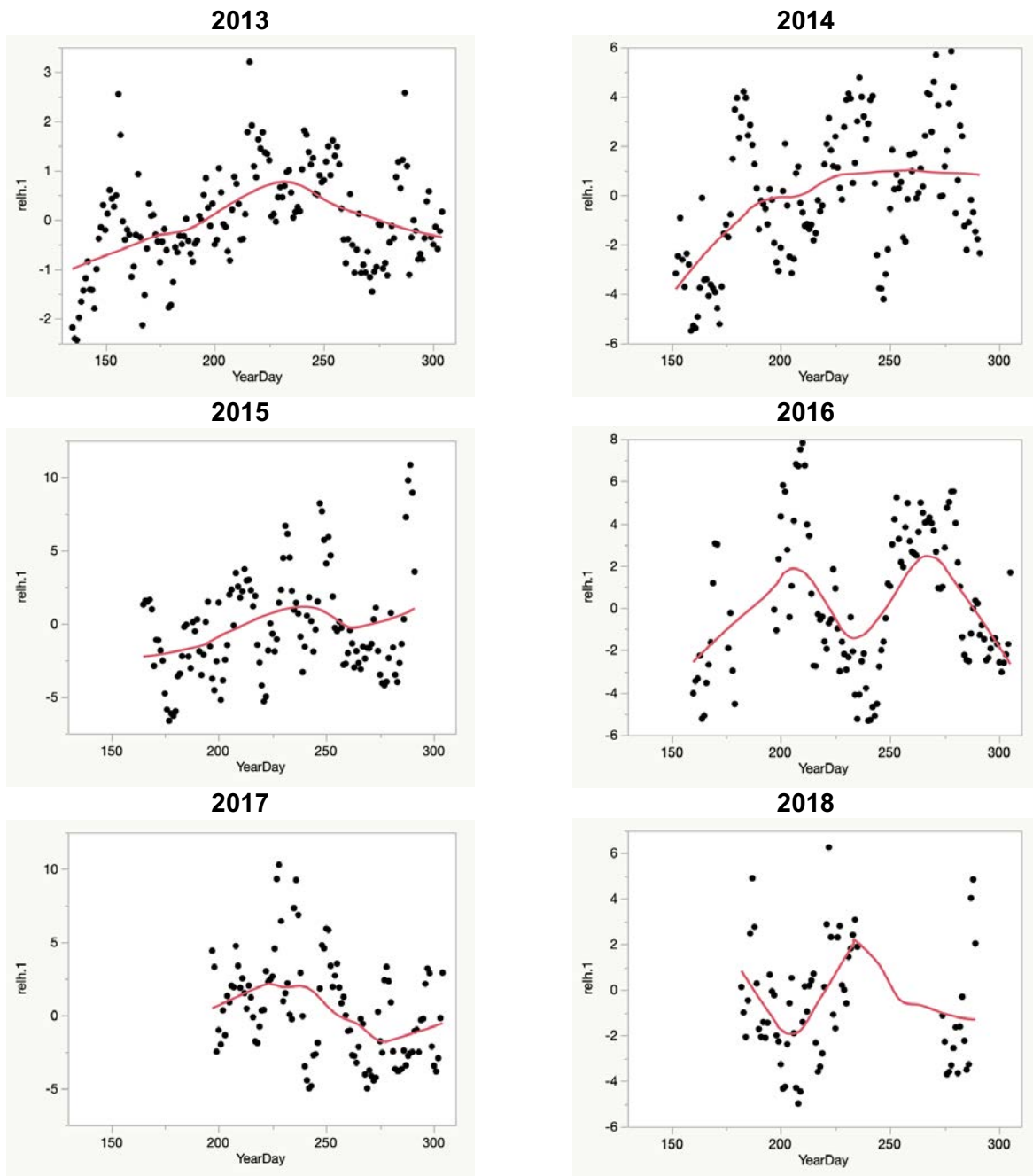


**Figure 17 Daily trends in first principal component (Prin1) of DGMAN Relative Humidity values 2013 - 2018. YearDay is day of year.**

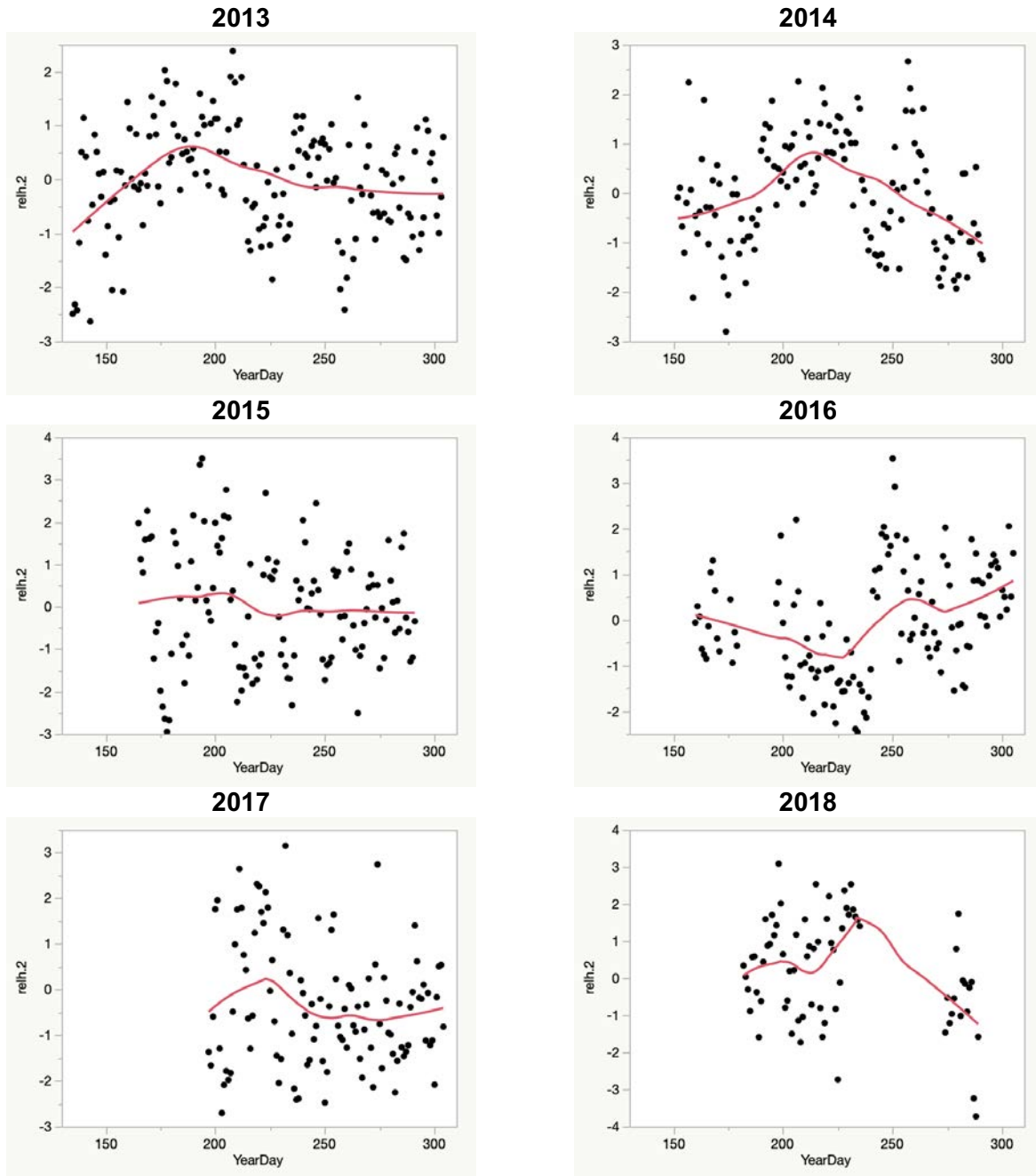


**Figure 18 Daily trends in second principal component (Prin2) of DGMAN Relative Humidity values 2013 - 2018. YearDay is day of year.**

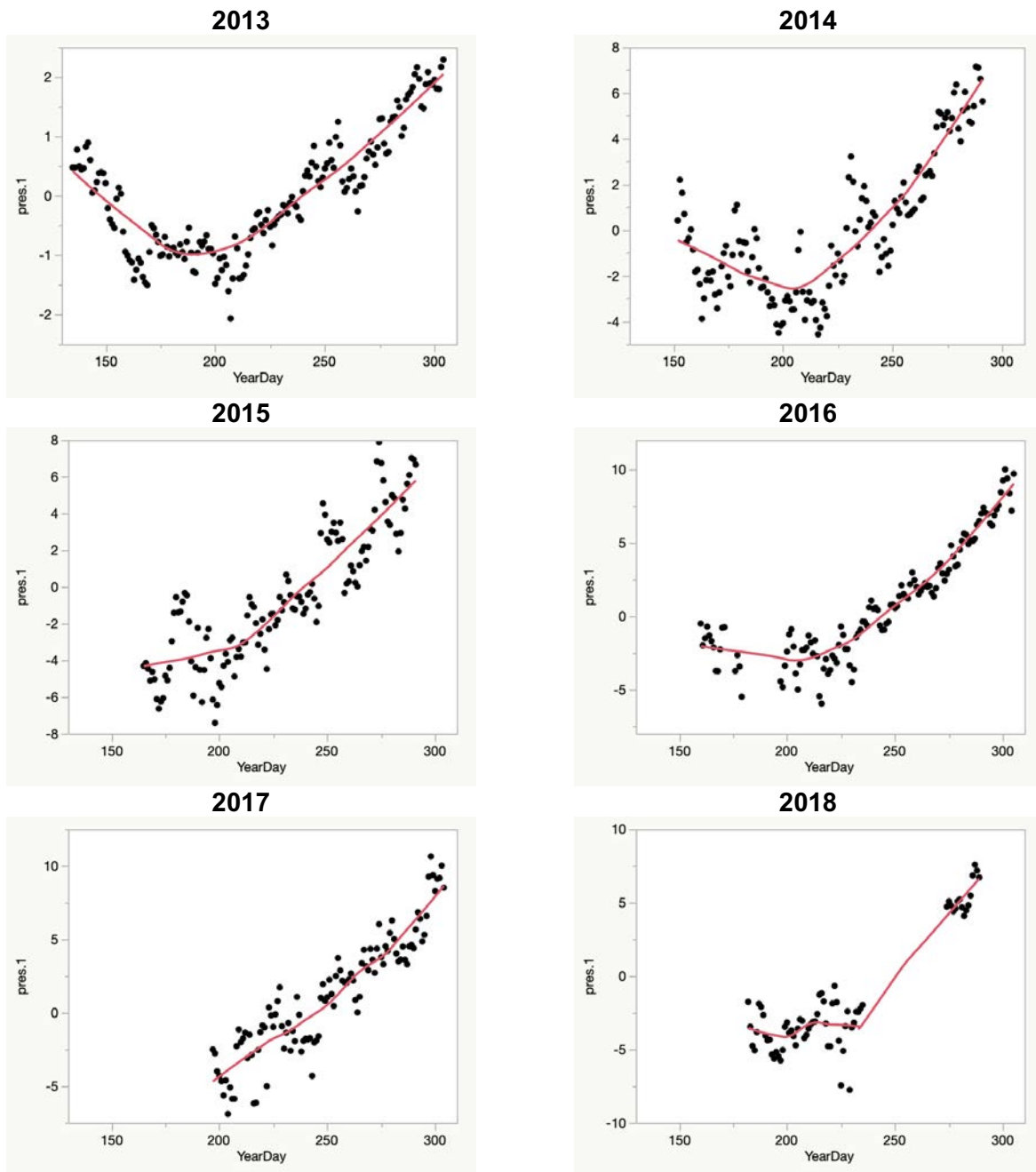


**Figure 19 Daily trends in first principal component (Prin1) of DGMAN Pressure QFE (hPa) values 2013-2018. YearDay is day of year.**

## 5 Statistical Analysis 2013 - 2018

### 5.1 Methodology

The statistical analysis presented in this section is a combined analysis of the gauge-day data from the complete Hajar Mountains trial, i.e. from the six years of field trials, 2013 - 2018. A similar, but more exploratory, analysis of the data from the 2018 Salalah trial is set out in Section 8.

The statistical methodology used in our analysis is described below. It is the same as that specified at the start of the trial, and corresponds to methodology that has been used basically unchanged in all annual reports since then. Essentially, the idea is to define the "footprint" of an Atlant site on a day as a rectangular corridor extending downwind from the site. If rainfall enhancement occurs when this site is operational, then gauges in the footprint should, on average, expect to receive more rainfall than gauges in the footprint of a neighbouring non-operational Atlant. Regression modelling is applied to the observed rainfall from gauges located in all the footprints defined by the direction of the steering wind on a day, and used to estimate enhancement effects due to operation of the different Atlants over the period of interest. Note that these estimates can be negative. Finally, this regression model is used to estimate the total amount of rainfall in the different footprints attributable to the operation of the Atlants over the period of interest. This estimate is expressed as a percentage of the corresponding estimate of the "natural rain" in these footprints over the same period, i.e. the total gauge-day rainfall that would have been expected if the Atlants has not been operating. This ratio is referred to as the Atlant attribution, and is the primary goal of the analysis.

To start, each gauge-day observation is classified as:

- Downwind of a specific Atlant site: that is, in a 30km wide and 75km long leeward corridor starting at the Atlant site and perpendicular to the steering wind direction on the day;
  - Downwind gauge-day values are designated as target values if they are from a gauge downwind of an active site on the day. Note that gauges can be simultaneously downwind of multiple active sites;
  - Downwind gauge measurements are designated as control values if they are from a gauge downwind of an inactive site on the day and also not downwind of any active sites;
- Upwind of a specific Atlant site: that is, from a gauge located in a 30km wide and 75km long windward corridor as specified above, while not being simultaneously downwind of any other site; and
- Out of scope: neither upwind nor downwind of an Atlant site on the day.

Gauge-day rainfall observations are modelled as the result of two events being observed, corresponding to the occurrence of rainfall at the gauge on the day (a yes/no or binary 1/0 value), and a positive rainfall reading if in fact there is rainfall. It is assumed, and past field trials have shown, that rainfall occurrence events are

essentially independent of the operating status of the Atlants. Consequently, estimation of the potential rainfall enhancement effect is confined to positive rainfall observations, some proportion of which is attributed to natural rainfall, i.e. rain that would have occurred in any case. These positive rainfall observations are converted to a logarithmic scale to reduce the level of skewness in the data and to reduce the influence of very large rainfall measurements, which occur irregularly and are also assumed to be independent of the operating status of the Atlant systems. All modelling is therefore carried out on the logarithmic scale, and relates to gauge-day values.

The modelling of these positive rainfall values is done sequentially:

- Gauge-data data from the 75km corridors that are upwind of the Atlant sites each day are used to model natural rainfall as a function of meteorological conditions and gauge elevation. Since the data used to fit this model are not downwind of any Atlant site on the day, the model fit can be considered to be unaffected by Atlant operation;
- This model is used to predict gauge-day natural rainfall downwind of the Atlant site; and
- Observed downwind gauge-day rainfall values are then modelled as a function of this predicted downwind rainfall, gauge elevation and an indicator variable for each Atlant which, for each gauge-day value, is equal to one if the gauge-day value is a target value for that Atlant, i.e., it is in the Atlant's footprint and the Atlant is operational that day. Otherwise the indicator variable takes the value zero. By construction these indicators are all zero for gauge-day values that are controls. In what follows, we refer to these indicators as target status indicators. There is one target status indicator for each Atlant.

### 5.1.1 Meteorological Covariates

Potential meteorological covariates, which can control for the variation in natural rainfall, are identified in the specification of the upwind model. These covariates include gauge elevation, year of measurement, daily steering wind speed, daily meteorological indices and principal components of daily DGMAN AWS measurements. Since the results of this specification search can be unstable for smaller sample sizes, it was carried out using the entire set of upwind gauge-day positive rainfall values over 2013 - 2018. There were 1545 upwind gauge-day values over this period, and the specification search identified the following covariates for inclusion in the log-scale upwind model for positive rainfall:

- Gauge elevation (gauge.elev)
- Steering wind speed (wind.sp)
- Total totals index (total.totals)
- Second principal component of average dry air temperature 10:00-20:00 (temp.dry.2)
- First principal component of average relative humidity 10:00-20:00 (relh.1)
- First principal component of QFE air pressure 10:00-20:00 (pres.1)

It is noteworthy that this model does not include effects for the different years of the trial, all of which were tried and were found to be insignificant, reinforcing the observation made earlier that there does not appear to be any large differences in the behaviour of many of the meteorological covariates from one year to the next.

### 5.1.2 Attribution

As noted above, estimation of the Atlant attribution over the six years of the trial is a key outcome. This is calculated in a number of steps. Initially, the contribution to the logarithm of observed rainfall at a gauge due to the estimated coefficients of the target status indicators for the different Atlant sites in the downwind rainfall model is computed. This contribution is then transformed to a ratio (which can be larger or smaller than one) that reflects the estimated level of attribution at the gauge on the day. Natural rainfall is estimated as observed rainfall divided by this attribution ratio. The estimated Atlant attribution is then observed rainfall minus estimated natural rainfall. Finally, the reported attribution for the trial is the total of these estimated Atlant attribution values from all downwind gauges divided by the corresponding estimate of total natural rainfall in the same downwind gauges.

### 5.1.3 Confidence Levels

Determining the significance or confidence level of the estimated Atlant attribution for the trial is the most complex aspect of the modelling. The calculation of the standard error of a coefficient in a statistical model is usually carried out on the basis that observations on the variable of interest are independent of one another. In our case, the variable of interest is daily gauge rainfall, and observations at nearby locations may be similar or positively correlated. This can be a consequence of exposure to similar meteorological conditions as storm cells move over a region, particularly in the direction of the steering winds. These conditions will only be imperfectly accounted for by the model covariates. Furthermore, if storm systems move in on consecutive days then gauge observations may be correlated temporally as well as spatially. This lack of independence will reduce the number of effective measurements, for example the data from 10 correlated downwind gauges might only have the information content of the data from five independent gauges. With fewer effective measurements the precision of the estimates derived from the model will be overstated, as will the associated confidence levels.

Three approaches have been adopted to deal with the potential issue of overstating confidence levels:

- A random day effect is added to both the downwind and upwind models in order to allow for imperfect model specification;
- A two-stage block bootstrap resampling strategy (Chambers and Chandra, 2013) that accounts for zero as well as positive rainfall observations that are spatially correlated in space and time is used to assess the significance of the estimated attribution given the actual operating schedule; and

- A non-parametric test in which the actual operating schedule is compared to a large number of random permutations of that schedule is used to further assess the significance of the estimated attribution in the context of the observed rainfall.

In the bootstrap, observations are repeatedly resampled with replacement. The sampling is done by randomly selecting days and then whole downwind areas within those days in order to create potential gauge level rainfall patterns, including zero rainfall values, that retain the spatial correlations in the original data. The rainfall values created in this way are then used to re-estimate the downwind model and a new attribution calculated. This process is repeated 10,000 times and the resulting empirical distribution of attribution values is used to directly measure the standard error of the estimated attribution and to calculate an associated confidence level.

The permutation test is based on the idea that if the actual operation of an Atlant is important for rainfall enhancement then the attribution defined by the operating schedule actually used should stand out relative to attributions associated with all the possible schedules that could have been implemented, but were not. In particular, the actual schedule used is permuted by randomly swapping the operating statuses of the different Atlants within a day (subject to there being equal numbers of operating and non-operating Atlants each day), and whole day operating sequences between days. These new schedules are used to calculate attribution values based on the rainfall data actually observed, and hence build an empirical distribution of attributions derived from the same model and observations but with target and control areas randomly switched. The position of the attribution associated with the actual schedule is then located within this distribution. The confidence level associated with there being a significant Atlant enhancement effect would be greater than 95 per cent if the attribution estimated from the actual schedule lies within the top five per cent of this distribution. It is 100 per cent if there are no permuted attribution values greater than or equal to the observed value. Such permutation confidence intervals tend to be conservative, inasmuch as they are usually not sensitive to extreme observations associated with very heavy rainfalls.

The bootstrap and permutation tests are both based on 10,000 random simulations. As noted above, the permutations of the operating schedule retained the requirement of an equal number of operating Atlant sites on a day. However, the constraint on the same Atlant not operating more than two days in a row was removed to reduce the level of overlap and duplication of schedules in the permuted set.

## **5.2 Comparison of Target and Control Gauge-Day Rainfall, 2013 - 2018**

All gauge-day observations over 2013 - 2018 were classified by whether they were downwind, upwind or out of scope on the day. The downwind observations were then further classified as being either target or control observations, where a target observation was defined as one with at least one target status indicator equal to one. This classification is referred to as Gauge-Day Type in what follows, and Table sets out the distribution of gauge-day rainfall incidence and average positive rainfall by Gauge-Day Type for each year of the trial.



**Table 10 Average daily positive rainfall values by gauge-day type by individual years, 2013 - 2018.**

Gauge-Day Type	Proportion* of rainfall events (rainfall incidence)						Average daily positive rainfall (mm)					
	2013	2014	2015	2016	2017	2018	2013	2014	2015	2016	2017	2018
<b>Out of Scope</b>	0.07	0.10	0.09	0.05	0.05	0.03	5.04	4.14	5.52	4.01	3.82	3.62
<b>Upwind</b>	0.05	0.04	0.10	0.04	0.03	0.02	4.85	3.64	6.71	3.36	3.12	3.43
<b>Control</b>	0.14	0.13	0.15	0.08	0.07	0.04	5.42	4.15	5.47	4.68	3.80	2.68
<b>Target</b>	0.14	0.12	0.13	0.08	0.08	0.04	4.76	5.11	5.74	4.46	4.32	3.95

\* Proportion of all gauge measurements (including zeros) for each cell of the table.

Figure 20 is a graphical representation of the average daily positive rainfall results in Table 10, and gives the impression that target gauge-day rainfall values are somewhat higher than control values. However, there is no clear difference, indicating that simple averages based on individual year data lack the power to identify a rainfall enhancement signal from Atlant operation.

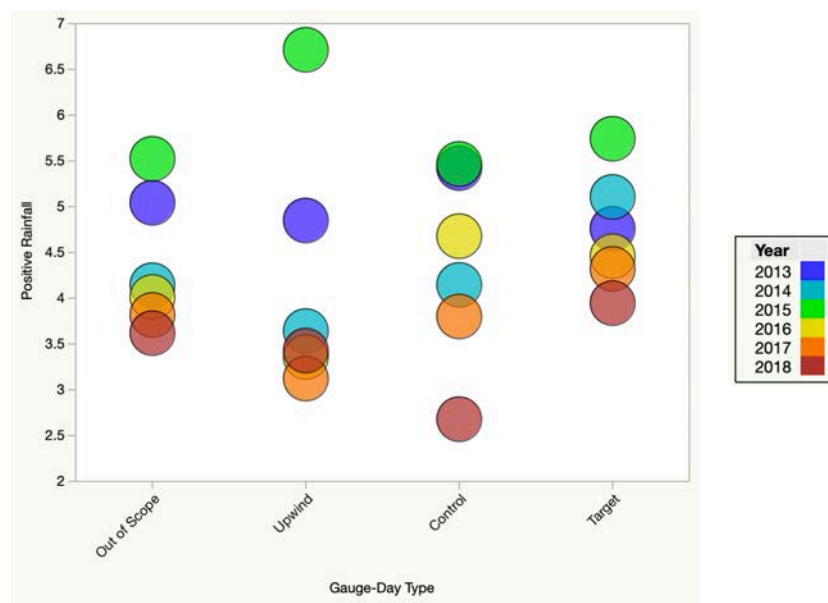


**Figure 20 Comparison of annual values of average positive rainfall by type of gauge-day observation.**

Figure 21 is a spatial comparison of different types of gauge-day observations, showing the values of gauge-day positive rainfall at gauge locations according to the type of observation. This serves to reinforce the perception that target gauge-day observations of positive rainfall were larger than those of control observations when one looks at the six years of the trial as a whole. However, there is clearly a very large amount of variation in these observations, which makes more precise statements impossible without a more sophisticated analysis. Figure 22 and Table 11 serve to emphasise this

point, showing boxplots of the distributions of positive rainfall value for each gauge-day type and also showing the key values in these distributions. As one can see, the average positive rainfall for target gauge-days (4.86mm) is larger than that for control gauge-days (4.66mm), but standard errors of 0.16mm and 0.18mm respectively mean that the usual 95 per cent confidence intervals generated by these average values overlap and so it is difficult to make a strong case for extra rain on average when the Atlants are operating.

A lot of the variability that is evident in gauge-day positive rainfall in Figure 21 is attenuated when one takes a logarithmic transform of this variable. In both Figure 22 and in Table 11 we therefore also show the same information for the variable LogRain, which is the logarithm of positive rainfall. Now we see a much better-behaved set of distributions across the gauge-day types (box plot on right in Figure 22) and average values that are much better separated (0.56 log mm vs. 0.49 log mm with a common standard error of 0.03 log mm). However, even with this transformation it is clear that there is insufficient power available to clearly identify a rainfall enhancement effect when one just uses average target and control values for rainfall. Consequently, in the following sub-section we turn our attention to a more sophisticated regression modelling exercise that controls for both spatial and temporal variability in LogRain in order to identify Atlant effects in the 2013 - 2018 trial data.

**Table 11 Key values in the distributions of gauge-day values of both positive rainfall and LogRain (logarithm of Positive Rainfall) 2013 - 2018.**

Level	Number	Mean	SE	10%	25%	Median	75%	90%
Gauge-day positive rainfall								
Out of Scope	3406	4.65	0.13	0.20	0.40	1.40	5.40	13.40
Upwind	1545	4.90	0.22	0.20	0.20	1.20	5.60	13.80
<b>Control</b>	<b>1992</b>	<b>4.66</b>	<b>0.18</b>	<b>0.20</b>	<b>0.40</b>	<b>1.60</b>	<b>5.80</b>	<b>13.00</b>
<b>Target</b>	<b>2176</b>	<b>4.86</b>	<b>0.16</b>	<b>0.20</b>	<b>0.40</b>	<b>1.80</b>	<b>6.35</b>	<b>13.00</b>
Gauge-day LogRain								
Out of Scope	3406	0.42	0.03	-1.61	-0.92	0.34	1.69	2.60
Upwind	1545	0.33	0.04	-1.61	-1.61	0.18	1.72	2.62
<b>Control</b>	<b>1992</b>	<b>0.49</b>	<b>0.03</b>	<b>-1.61</b>	<b>-0.92</b>	<b>0.47</b>	<b>1.76</b>	<b>2.56</b>
<b>Target</b>	<b>2176</b>	<b>0.56</b>	<b>0.03</b>	<b>-1.61</b>	<b>-0.92</b>	<b>0.59</b>	<b>1.85</b>	<b>2.56</b>

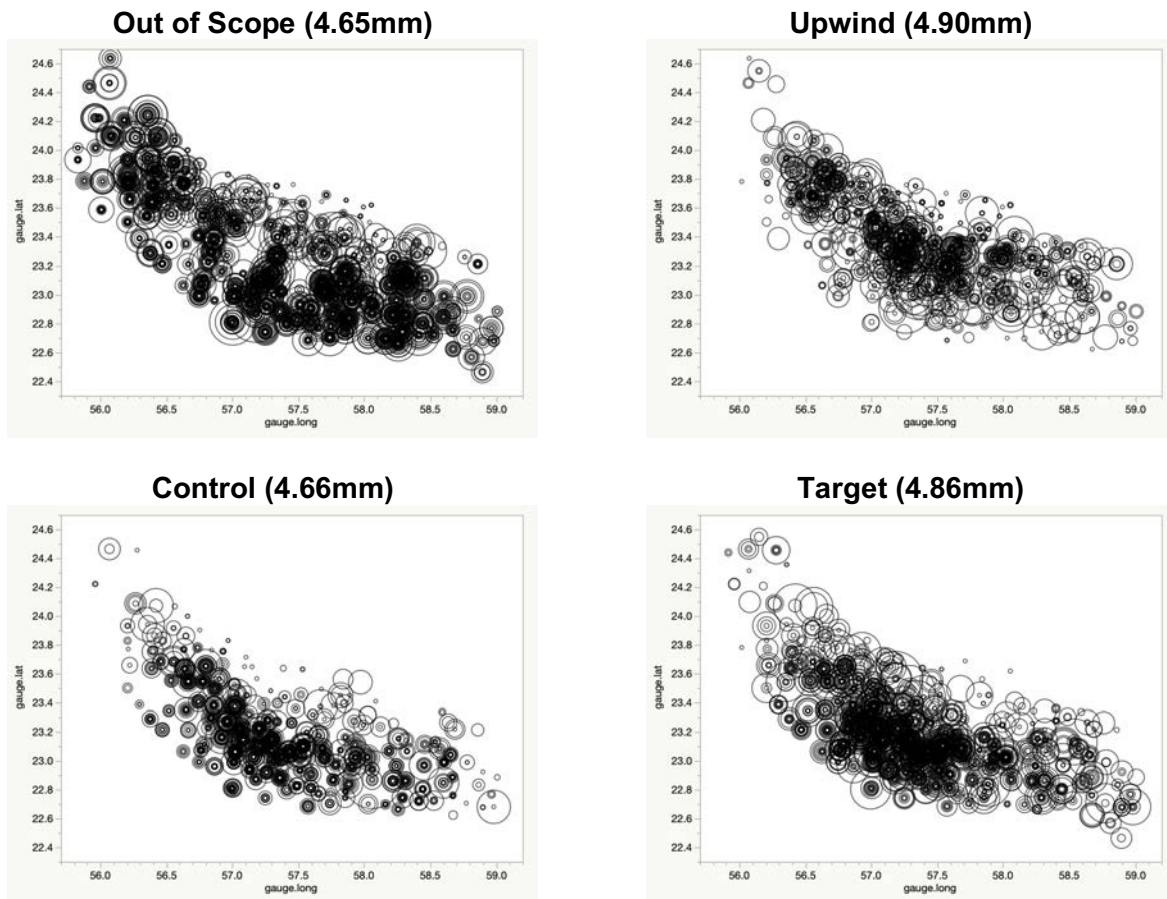


**Figure 21** Bubble plots of gauge locations showing the 2013 - 2018 spatial distributions of gauge-day values of positive rainfall for different gauge-day types. The larger the bubble, the larger the rainfall measurement at the gauge. Average positive rainfall in parentheses.

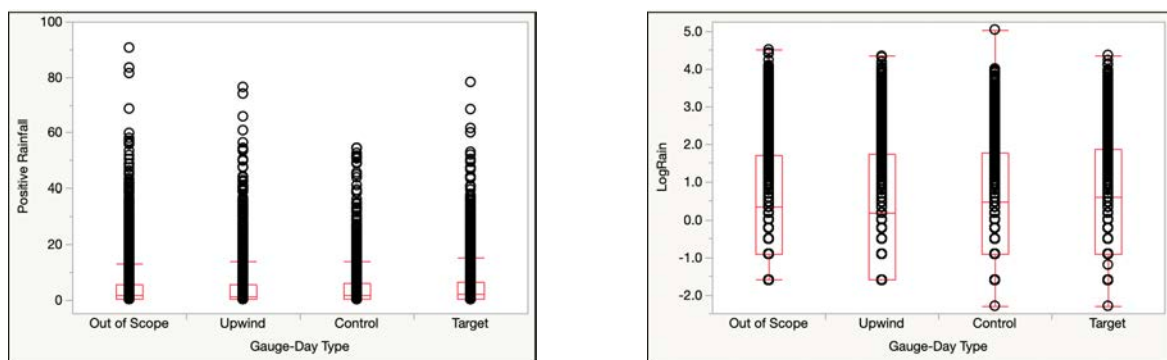


**Figure 22** Box-plots of the 2013 - 2018 distributions of positive rainfall values and LogRain values by gauge-day type.

### 5.3 Regression Modelling of Downwind Gauge-Day Rainfall, 2013 - 2018

The two-step statistical methodology outlined in Section 5.1 requires a regression model first be fitted to the upwind gauge-day values of LogRain. This fitted model is then combined with the downwind gauge-day data to obtain values for a key predictor of the downwind gauge-day values of "natural" LogRain. That is, this predictor explains most of the systematic variability of the logarithm of the natural rainfall downwind. The second step is to then fit another regression model, but this time to the downwind gauge-day values of LogRain. This second model has a very simple specification, with just the upwind predictor, gauge elevation and the Atlant target status indicators as covariates. The estimated values of the model parameters associated with these target status indicators provide measures of the influence of the different Atlants on downwind rainfall. In particular, large positive values indicate that operation of the relevant Atlant tended to lead to increased rainfall downwind, while large negative values indicate the opposite. In order to provide a measure of whether these parameter estimates are reliable, we also compute the values of the so-called t-statistics (t-val) associated with them. An absolute value of 2 or more for t-val is usually taken as indicating that the corresponding estimate can be treated as significantly larger than zero.

An important consideration when analysing the complete 2013 - 2018 trial data is that the trial design deployed pairs of additional Atlants every year in the Hajar Mountains until 2017. This means that Atlants deployed at the start of the trial (H1, H2) had a much longer time to have an impact on downwind gauges compared with Atlants deployed later in the trial. This in turn means that the amount of statistical information available for detecting a rainfall enhancement signal is much greater for early deployment Atlants compared with later deployment Atlants. This is of course complicated by where the Atlants are actually located in the Hajar Mountains, the natural rainfall conditions that prevail in the region and local orographic conditions, which may, or may not, be amenable to rainfall enhancement via updraft-based delivery of ionised aerosols into the cloud layer. Table 12 displays simple counts of the number of target events for each Atlant each year (i.e. the sum of the target status indicators for that Atlant that year). This shows that these counts are much larger for early deployment Atlants, and so if there is a rainfall enhancement signal associated with Atlant operation, then it is much more likely to be detected at these earlier Atlants.

An associated issue is whether there is sufficient information in any individual year's data to reliably detect an enhancement signal that year. If one takes as a rule of thumb that reliable detection of a signal requires at least 50 observations that contain that signal (somewhat optimistic given the variability in gauge-day positive rainfall in the Hajar Mountains) then the counts set out in Table 12 indicate that detection of a consistent signal at H5, H6, H7, H9 and H10 may be problematic using the trial data 2013 - 2017. Note that we exclude 2018 from this assessment since the combination of a dry season and extensive missing data due to radiosonde issues at Muscat make this year completely unsuited to any type of individual year analysis.

**Table 12 Counts of target events (positive rainfall at gauge downwind of operating Atlant) by individual year 2013 - 2018. Note the small numbers of target events for H6, H8 and H9 in 2018.**

No. of target events for	2013	2014	2015	2016	2017	2018	2013-2018
H1	174	91	104	66	86	13	534
H2	127	141	159	73	67	25	592
H3		87	72	67	51	7	284
H4		85	90	61	43	34	313
H5			42	53	18	21	134
H6			44	31	26	1	102
H7				19	23	20	62
H8				61	81	7	149
H9					22	2	24
H10					44	36	80

Table 13 confirms this assessment. This shows, for each year of the trial, estimates of both upwind and downwind model parameters, along with their t-val measures. Estimates that are viewed as significantly different from zero are in red. For the upwind model we see considerably instability in parameter estimates, with only relh.1 (first principal component of DGMAN AWS average relative humidity) providing some consistency of effect. The same issue arises with the downwind model estimates. Here we see that aside from the expected rain variable (which should correlate reasonably with downwind rain), all other effects are transient.

The main advantage of an extended trial like that conducted in the Hajar Mountains 2013 - 2018 is that, for a highly variable phenomenon such as positive rainfall, and a potential rainfall enhancement signal that is easily lost in the consequent noise, collecting and combining data over many years represents the best strategy for identifying the signal. This can be easily seen in the estimates set out in Table 14, where we show the fit of both the upwind and downwind models as data are aggregated across years. To start we see that the fit of the upwind model quickly settles down, with all explanatory variables becoming highly significant after 4 years of data are combined. Next, we see that there is much more stability in the downwind model parameter estimates, with the H1, H2, H3 and H5 target estimates all significantly larger than zero in every set of combined years data. Other target estimates are more unreliable, and are both positive and negative. The consistent negative estimates observed for H4 and H6 are noteworthy, and indicate that these Atlants may not be positioned for optimal rainfall enhancement effect. However, further years of data are required before one could be definitive in this regard. Finally, we also note the relative stability of the negative interaction of operation of H2 with elevation. Reasons for this are unclear at present, and may just reflect the location of higher altitude rain gauges near H2 and the potential "damping" of a rainfall enhancement signal at higher altitudes where natural rainfall is larger anyway.

**Table 13 Individual year modelling for LogRain. Estimates with absolute t-values of 2 or more are shown in red. Note that 2017 and 2018 are combined since there were insufficient data available for 2018 to carry out a year-specific modelling exercise. H1 and H2 interaction terms with gauge elevation are included in the downwind model since without them model fit degrades.**

Control Variable	2013		2014		2015		2016		2017/8		
	Est	t val	Est	t val	Est	t val	Est	t val	Est	t val	
<b>Upwind model estimates (expected rain for downwind model)</b>											
(Intercept)	1.382	1.557	-0.309	-0.268	<b>-2.637</b>	-2.601	-1.922	-1.455	<b>-2.234</b>	-3.435	
gauge.elev	<b>0.493</b>	3.634	<b>0.627</b>	2.415	<b>0.476</b>	3.412	0.233	1.039	0.207	1.135	
wind.sp	<b>-0.219</b>	-5.010	-0.114	-1.545	-0.038	-0.900	-0.015	-0.238	-0.056	-1.657	
total.totals	-0.020	-1.024	0.005	0.201	<b>0.054</b>	2.396	0.034	1.327	<b>0.048</b>	3.446	
temp.dry.2	0.214	1.445	<b>0.380</b>	2.104	0.040	0.397	0.332	1.706	0.055	0.764	
relh.1	<b>0.523</b>	3.706	<b>0.250</b>	3.426	<b>0.221</b>	5.593	0.092	1.538	<b>0.115</b>	2.819	
pres.1	-0.188	-1.320	-0.072	-1.296	-0.070	-1.643	-0.054	-0.889	-0.045	-1.479	
No. gauge-days	229		213		599		244		260		
No. days	55		49		49		45		73		
<b>Downwind model estimates</b>											
(Intercept)	<b>0.414</b>	2.150	<b>0.457</b>	3.239	0.109	0.877	0.082	0.473	0.193	1.638	
gauge.elev	0.187	1.058	-0.293	-1.860	-0.137	-1.000	0.269	1.629	-0.164	-1.476	
expected rain	<b>0.614</b>	4.477	<b>0.811</b>	8.677	<b>0.860</b>	8.827	<b>0.947</b>	4.580	<b>0.913</b>	8.916	
H1 target	0.511	1.887	0.552	1.390	0.121	0.400	-0.087	-0.200	-0.054	-0.178	
H2 target	0.319	1.054	<b>0.732</b>	2.769	0.228	1.014	0.417	1.170	-0.299	-1.028	
H3 target			<b>0.586</b>	3.390	<b>0.416</b>	2.255	0.256	1.308	-0.183	-0.950	
H4 target			-0.192	-1.105	-0.136	-0.813	0.048	0.237	-0.153	-0.889	
H5 target					<b>0.661</b>	2.821	<b>0.489</b>	2.146	0.366	1.572	
H6 target					-0.334	-1.466	-0.104	-0.364	0.158	0.563	
H7 target							0.078	0.230	0.373	1.654	
H8 target							0.007	0.031	0.248	1.508	
H9 target									<b>0.649</b>	2.143	
H10 target									0.175	1.040	
elev*H1 target	<b>-0.569</b>	-2.239	-0.336	-0.711	-0.157	-0.472	0.590	1.029	0.365	1.188	
elev*H2 target	-0.598	-1.968	-0.481	-1.927	-0.066	-0.278	-0.529	-1.484	0.272	1.092	
No. gauge-days	563		807		1077		772		949		
No. days	55		102		92		83		119		

**Table 14 Cumulative years modelling for LogRain. Estimates with absolute t-values of 2 or more are shown in red.**

Control Variable	2013-2014		2013-2015		2013-2016		2013-2017		2013-2018	
	Est	t val	Est	t val	Est	t val	Est	t val	Est	t val
<b>Upwind model estimates (expected rain for downwind model)</b>										
(Intercept)	0.498	0.765	-0.689	-1.257	-0.988	-1.968	-1.535	-3.646	-1.447	-3.593
gauge.elev	0.535	4.734	0.516	5.921	0.488	6.015	0.464	6.077	0.446	6.011
wind.sp	-0.176	-4.608	-0.115	-3.983	-0.111	-4.521	-0.086	-4.005	-0.092	-4.487
total.totals	-0.004	-0.288	0.017	1.451	0.024	2.273	0.033	3.798	0.032	3.814
temp.dry.2	0.304	2.921	0.158	2.132	0.180	2.652	0.151	2.718	0.144	2.722
relh.1	0.300	5.028	0.245	7.906	0.206	7.679	0.176	7.420	0.179	7.966
pres.1	-0.113	-2.433	-0.097	-3.206	-0.080	-3.060	-0.054	-2.421	-0.053	-2.614
No. gauge-days	442		1041		1285		1454		1545	
No. days	104		174		219		259		292	
<b>Downwind model estimates</b>										
(Intercept)	0.367	3.148	0.270	3.166	0.238	3.154	0.279	4.162	0.280	4.368
gauge.elev	-0.009	-0.078	-0.067	-0.748	-0.033	-0.415	-0.127	-1.811	-0.140	-2.120
expected rain	0.709	8.393	0.777	10.954	0.829	12.298	0.878	14.306	0.883	15.035
H1 target	0.566	2.769	0.434	2.595	0.423	2.758	0.307	2.208	0.298	2.189
H2 target	0.517	2.605	0.403	2.711	0.424	3.104	0.300	2.369	0.254	2.074
H3 target	0.425	2.479	0.396	3.155	0.360	3.422	0.264	2.806	0.236	2.551
H4 target	-0.255	-1.454	-0.213	-1.765	-0.130	-1.256	-0.205	-2.177	-0.153	-1.721
H5 target			0.615	2.673	0.490	3.085	0.465	3.236	0.437	3.318
H6 target			-0.449	-2.001	-0.303	-1.731	-0.218	-1.453	-0.197	-1.320
H7 target					0.025	0.075	0.371	1.660	0.228	1.216
H8 target					-0.038	-0.192	0.081	0.620	0.063	0.494
H9 target							0.556	1.737	0.499	1.633
H10 target							0.304	1.376	0.039	0.234
elev*H1 target	-0.441	-2.133	-0.327	-1.884	-0.285	-1.739	-0.119	-0.807	-0.096	-0.669
elev*H2 target	-0.540	-2.804	-0.347	-2.326	-0.394	-2.873	-0.271	-2.182	-0.211	-1.772
No. gauge-days	1370		2447		3219		3905		4168	
No. days	194		286		369		435		488	

#### 5.4 Estimating Atlant Attribution from Downwind Gauge-Day Rainfall, 2013 - 2018

A key objective of the 2013-2018 trial is estimation of the attributed rainfall due to operation of the Atlant mechanisms during the trial. This attribution is computed as the ratio of the total attributed downwind rainfall to total estimated downwind natural rainfall, and is expressed in percentage terms. The reliability of this attribution also needs to be rigorously assessed, since there is considerable interest in being able to compute an objective estimate of the probability that the attribution is actually positive, and more generally the probability that it is greater than any specified value. In this context, we define this probability relative to comparable attributions under alternative rainfall patterns that are judged similar to those actually observed.

Sub-section 5.1 contains a description of the method used to estimate the attribution given the rainfall data actually collected over the trial. In effect, for every gauge-day observation that qualifies as a target we use the fitted downwind model to compute a gauge-day specific factor that represents the proportional increase (or decrease) in rainfall measured at that gauge on that day due to operation of Atlant. The estimated natural rainfall for that gauge-day is the observed positive rainfall divided by this factor. The estimated gauge-day attribution is obtained by subtracting this estimated natural rainfall from the observed rainfall. These values are summed over all downwind gauge-days in scope to obtain the overall attribution estimate. Finally, a distribution of potential attribution values is created using the above approach, by simulating alternative downwind rainfall patterns using a semi-parametric block bootstrap procedure. See sub-section 5.1 for more detail.

**Table 15 Bootstrap estimates of aggregated attribution for downwind corridors defined by daily steering winds (bootstrap standard errors in parentheses).**

Data period	2013-2014	2013-2015	2013-2016	2013-2017	2016-2018	2013-2018
Total rainfall (mm)	16249	30961	36951	41572	12294	43254
Average positive rainfall (mm)	4.65	5.15	4.96	4.82	3.96	4.74
Total downwind rainfall (mm)	6587	12615	16136	18954	7232	19846
Average positive downwind rainfall (mm)	4.81	5.16	5.01	4.85	4.20	4.76
<b>Bootstrap estimates</b>						
Total natural downwind rainfall	5516 (829)	10583 (1550)	13379 (1723)	15930 (2080)	6182 (1260)	17089 (2116)
Attributed downwind rainfall	1071 (344)	2031 (487)	2757 (510)	3024 (546)	1050 (183)	2757 (506)
%attribution	<b>19.67</b> (6.31)	<b>19.39</b> (4.53)	<b>20.76</b> (3.76)	<b>19.13</b> (3.35)	<b>17.19</b> (1.77)	<b>16.25</b> (2.91)
% positive attributions	99.99	100.00	100.00	100.00	100.00	100.00

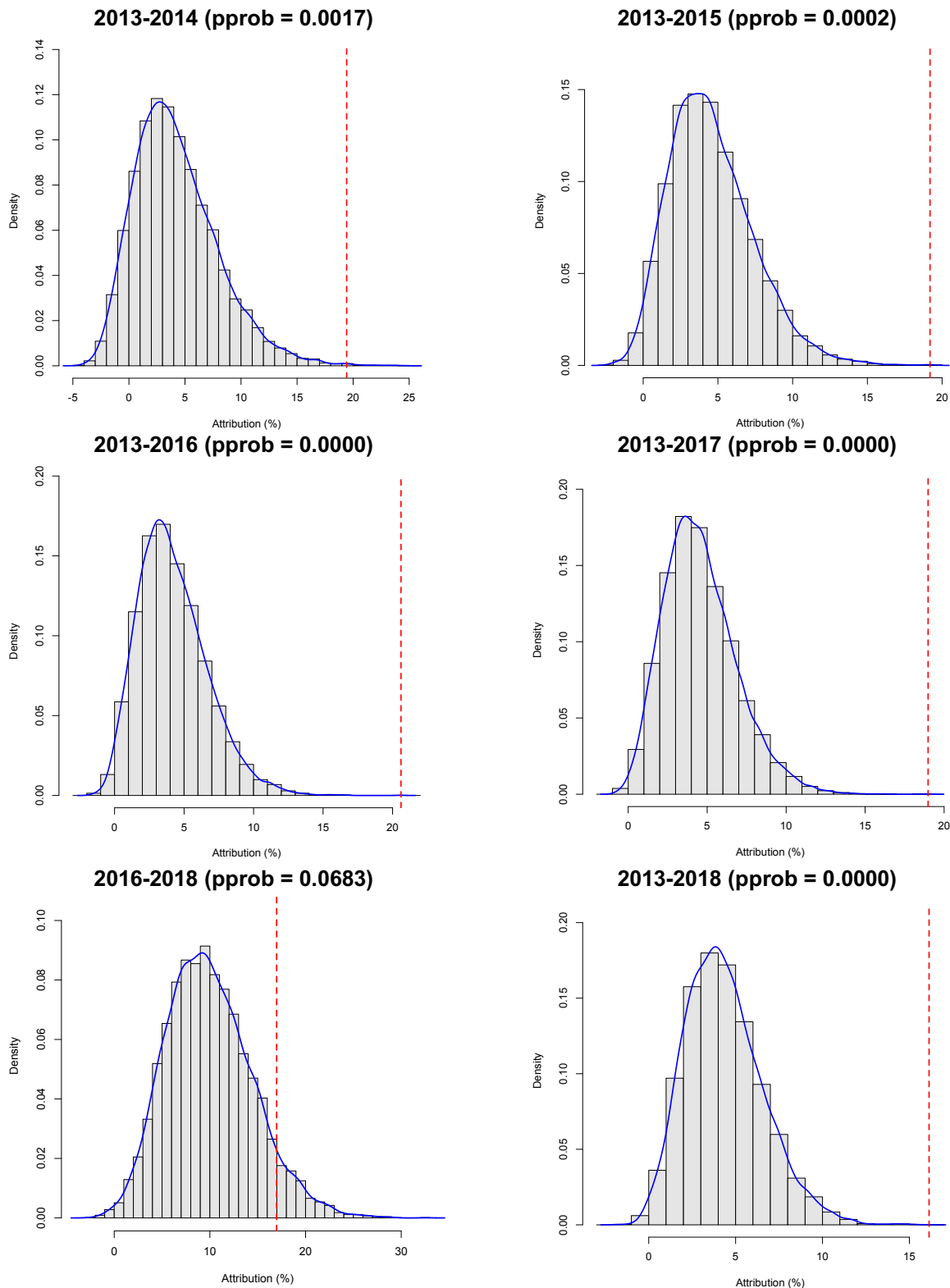


Table 15 shows attribution estimates derived from the bootstrap procedure for trial data aggregated over years, starting with 2013 - 2014 and finishing with all six years, 2013 - 2018. Additionally, since rainfall was more prevalent over 2013-2015 compared with 2016-2018, attribution estimates for the latter comparatively "dry" period are also shown. These attribution estimates are very stable at between 19 and 20 per cent until data from 2018 are included, at which point they drop slightly to just over 17 per cent (2016-2018) and to just over 16 per cent (2013-2018). It is interesting to note that going from 2013-2015 (a comparatively wet period) to 2016-2018 (a comparatively dry period), the attribution changes little, dropping from 19.39 per cent to 17.19 per cent.

The influence of increasing sample size as more years are added is also clear from the steady decrease in the bootstrap estimate of the standard error of the attribution estimate. This reflects the fact that with additional data the bootstrap attribution distribution becomes more and more concentrated around its average value, and is the reason that we see 100 per cent positive attribution values for all bootstrap attribution distributions from 2013 - 2015 onwards. That is, there is effectively zero probability that there has been no rainfall enhancement over the six years of the trial.

A further check on whether operation of the Atlant mechanisms actually result in rainfall enhancement is via a permutation test of the Atlant operating schedules used in the trial. Recollect that these schedules were randomised to ensure validity of the statistical analysis of the rainfall data, since then there is no opportunity to "tailor" Atlant operation to the actual occurrence of rainfall in the trial area. However, it is still possible that by sheer chance Atlants were operated when rain was recorded in the area. The permutation test (also described in subsection 5.1) is based on the premise that if Atlant operation does nothing to enhance rainfall, then the actual Atlant operating sequence has no impact on attribution, and so the observed attribution is not likely to be very different from the attribution one would obtain if one replaced this operating sequence by a permuted version. This permutation process is carried out a large number of times (10,000), and the resulting distribution of permuted attribution estimates is then compared with the actual attribution estimate.

Figure 23 shows these distributions of permuted attribution estimates for different aggregations of the trial data. It also shows where the actual attribution estimate lies in each case. The value of pprob shown for each plot is the proportion of the 10,000 permuted attribution estimates defining each distribution that are larger than the realised estimate of the attribution. It is quite clear that there is virtually zero chance that the achieved attribution could have been attained by any operating schedule over the six years 2013-2018 other than the one that was actually used. Furthermore, it is clear that, with the exception of the dry years 2016-2018, the estimated attribution in preceding periods was either the largest or very close to largest that could have been achieved by permuting the operating schedule. This probability increases to under 7 per cent when one restricts the analysis to 2016-2018, reflecting increased rainfall variability during this period and the unbalanced 2018 data collection effort. Overall, however, it does appear that it did matter during the trial whether one operated an Atlant or not. The observed attribution was not a chance occurrence. And it was linked to operation of the Atlants.



**Figure 23 Cumulative years permutation distributions for attribution. Blue curve is a smooth approximation to the distribution. Red vertical dashed line shows actual attribution estimate based on data from those years.**

## 5.5 Statistical Analysis of Gauge-Day Attribution Estimates

Since attribution estimates are available at gauge-day level, they can be tabulated in order to see how they vary both temporally and spatially. In Table 16 we show how 2013 - 2018 attribution varies by year, going from a low of 15.5 per cent in 2015 (a wet year) to a high of 18.1 per cent in 2013, when the Atlant network consisted of just H1 and H2, both at high elevations. Note that we show a combined result for 2017 and 2018, since the unbalanced nature of the 2018 design (due to missing radiosonde data) leads to results for this year that are too variable to present on their own. The year to year stability in the median bootstrap values of attribution is noticeable, implying a consistent Atlant rainfall enhancement effect of approximately 16 per cent across all six years of the Hajar Mountains trial.

**Table 16 Estimated downwind attribution statistics, by year. Gauge-day estimated attributions are based on 2013 - 2018 modelling.**

Year	gauge-day classification	No. of Rainfall Events	Average Positive Rainfall (mm)	Bootstrap Average Attributed Rain (mm)	Bootstrap Average Percent Attribution (Std Error)	Bootstrap Median Percent Attribution
2013	Out of Scope	883	5.04			
	Upwind	229	4.85			
	Downwind	563	5.07	0.77	18.1 (1.7)	18.0
2014	Out of Scope	802	4.14			
	Upwind	213	3.64			
	Downwind	807	4.63	0.65	16.4 (2.6)	16.3
2015	Out of Scope	844	5.52			
	Upwind	599	6.71			
	Downwind	1077	5.60	0.75	15.5 (2.7)	15.4
2016	Out of Scope	411	4.01			
	Upwind	244	3.36			
	Downwind	772	4.56	0.62	15.9 (2.6)	15.8
2017 - 2018	Out of Scope	466	3.76			
	Upwind	260	3.23			
	Downwind	949	3.91	0.54	17.7 (9.9)*	16.6
2013 - 2018	Out of Scope	3406	4.65			
	Upwind	1545	4.90			
	Downwind	4168	4.76	0.66	16.3 (2.9)	16.1

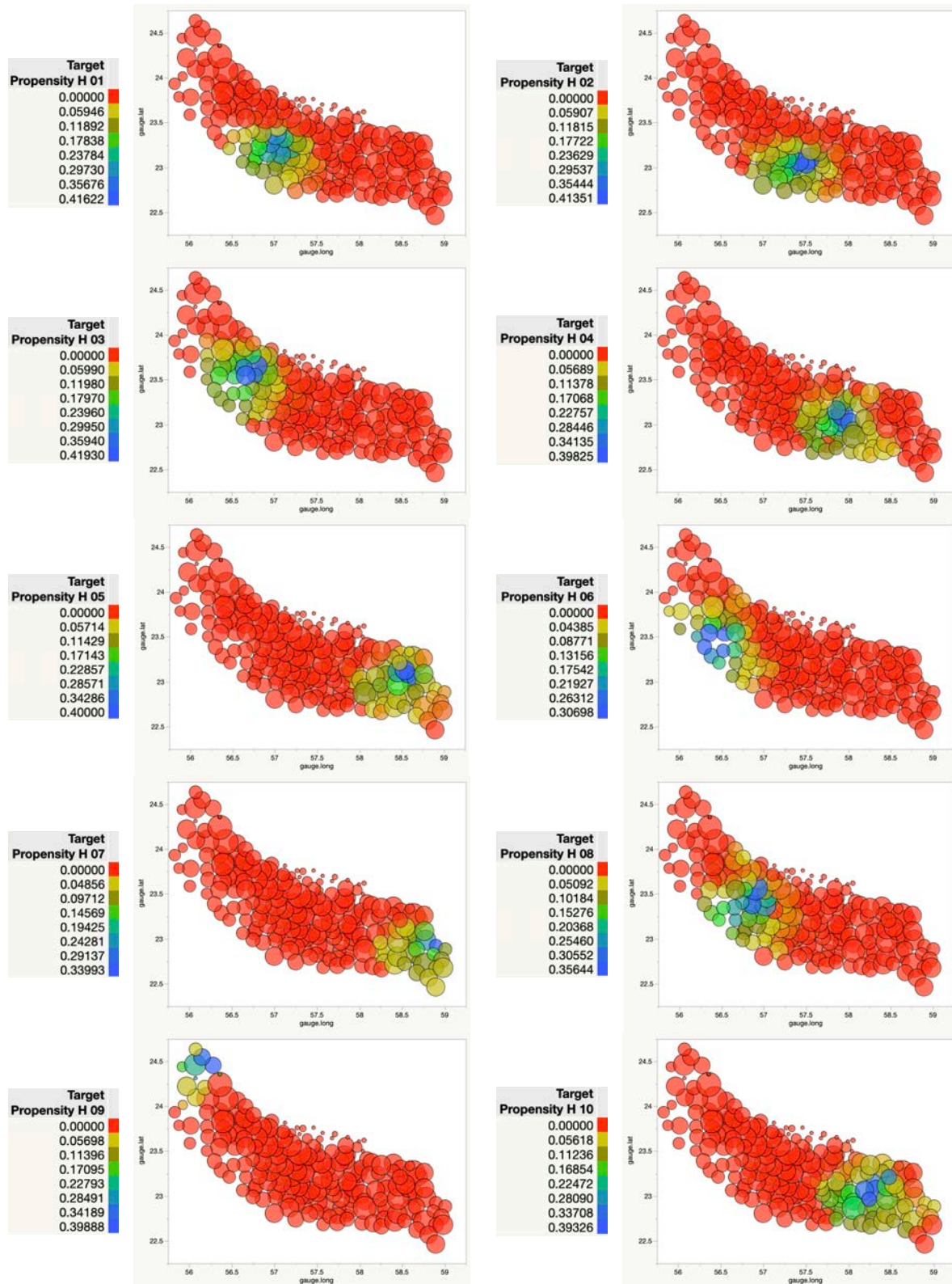
\*After removal of 5 (out of 10,000) extreme values from the bootstrap distribution of attribution. The median is unaffected.

The bubble plots displayed in Figure 24 show the spatial distributions of gauge propensities to be targets for the different Atlants (i.e. to be downwind of them when they are active). The bubble sizes in all the plots are indicative of gauge average positive rainfall over 2013 - 2018 (the bigger the bubble the more rainfall recorded at the gauge). Red bubbles correspond to gauges that were never targets for that Atlant, while blue indicates gauges that have the highest propensity to be a target for the Atlant. Note that the distribution of propensities varies considerably between Atlants, reflecting their location, and also the length of time that they have been operational. The overall N to NE orientation of steering winds over 2013 - 2018 is clear from the spatial orientation of these target propensities.

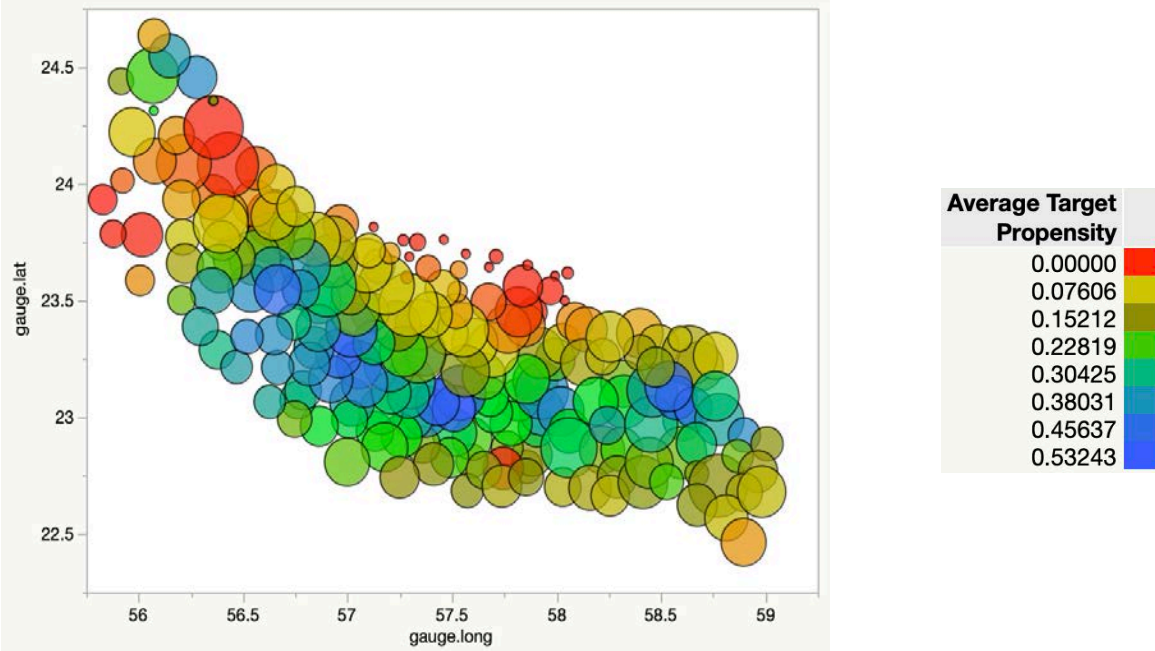
Figure 25 summarises the Atlant-specific information in Figure 24, displaying the same type of bubble plot as in Figure 24, but with colour now indicating the average propensity of each gauge to be a target, with red indicating a gauge that has never been a target. Here we see that there are gauges in the NW of the trial area that have experienced significant rainfall, but have never been targets. There would be scope for deployment of a further Atlant in this area to enhance rainfall if Atlant operation were to continue after the trial. There are also gauges on the NE edges of the ranges that have never been targets, but, given the N - NE general direction of the steering winds, these gauges will have usually been upwind.

Figure 26 is a similar bubble plot of gauge locations, with bubble sizes indicating gauge average positive rainfall over 2013 - 2018 and with bubble colour indicating level of downwind positive rainfall at a gauge. Black bubbles are gauges that did not record any gauge level positive rainfall over 2013 - 2018. We see that high values of average downwind positive rainfall tended to occur in the northern part of the Hajar Mountains and also more towards the central (and higher) parts of this range.

Finally, in Figure 27 we show the same bubble plot as displayed in Figure 25 and Figure 26, but this time colouring the bubbles according to the average attribution estimated for each gauge. Note that large estimated attributions are mainly along the NW and SE sides of the Hajar Mountains. Note also the negative attributions (red bubbles) shown in the plot. At the SW end of the ranges these appear to be gauges that were mainly downwind of H4, while in the NW they appear to be gauges that were mainly downwind of H6.



**Figure 24 Bubble plot of gauge locations. Size indicates gauge average positive rainfall, and colour indicates gauge propensity to be a target for a particular Atlant.**



**Figure 25** Bubble plot of gauge locations. Size indicates gauge average positive rainfall and colour indicates gauge average propensity to be an Atlant target. Red bubbles correspond to gauges that were never targets, while blue indicates gauges that have the highest Atlant target propensity.

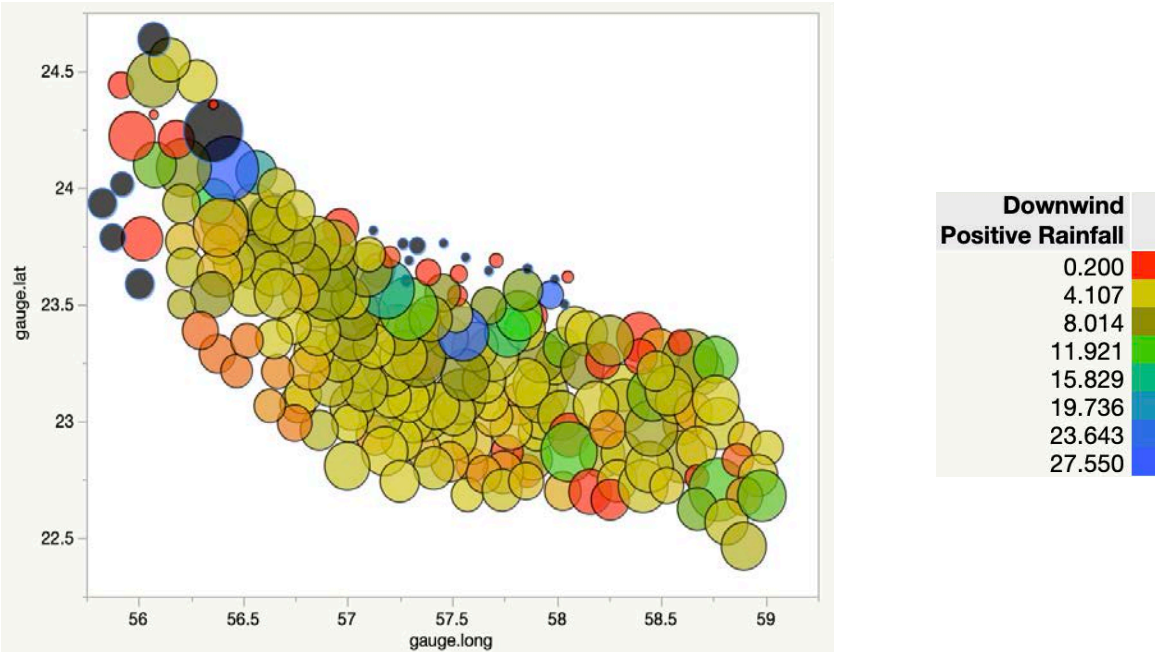


**Figure 26** Bubble plot of gauge locations. Size indicates gauge average positive rainfall and colour indicates level of downwind positive rainfall recorded at the gauge. Black bubbles are gauges that have never recorded downwind positive rainfall.

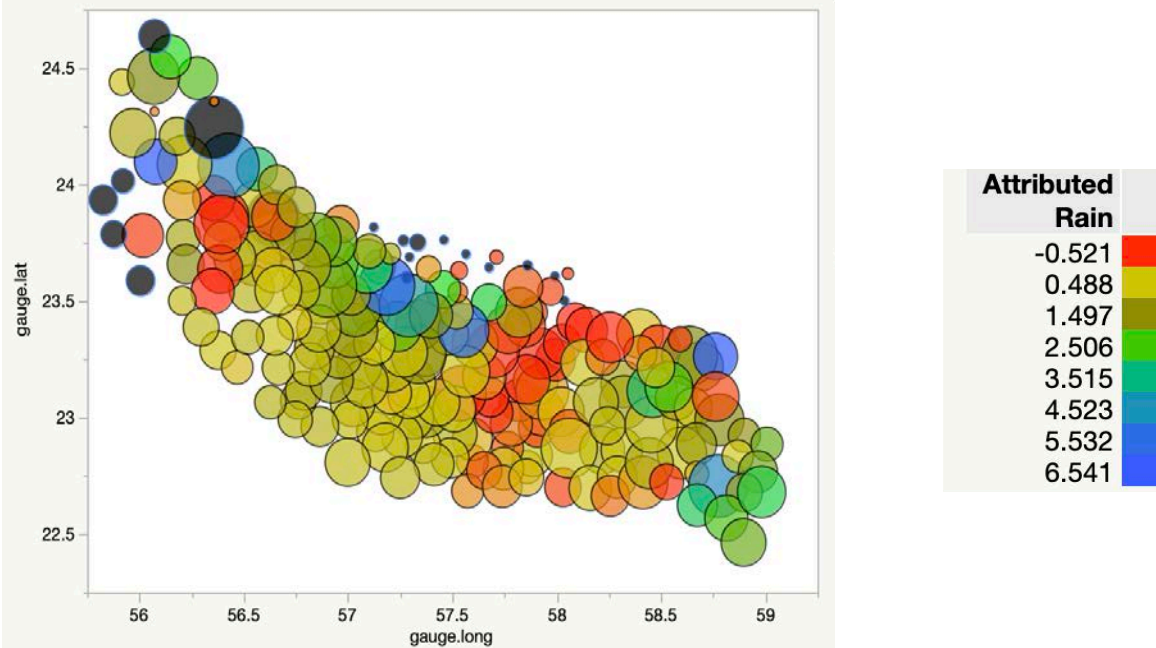


**Figure 27 Bubble plot of gauge locations. Size indicates gauge average positive rainfall and colour indicates gauge average estimated attribution. Dark bubbles are gauges that did not record downwind positive rainfall, and so have no estimated attribution. Large red bubbles correspond to gauges that recorded large average positive rainfall but not large average estimated attribution.**

We now refine our analysis of attribution to focus on the impact of individual Atlant installations. In particular, we look purely at the upwind and downwind corridors defined by individual Atlants, ignoring any rainfall enhancement effect associated with simultaneous operation of other Atlants. In this situation the switching procedures used to control operation of each Atlant allows us to view gauge-days located downwind of the Atlant as targets when it is switched on, and as controls when it is switched off. Table 17 shows the attribution estimates derived from these Atlant-specific analyses when the data are aggregated over time. Note that these values should be treated with some caution since no allowance has been made for other Atlants operating at the same time, and so control gauge-day data used for any particular Atlant may in fact include rainfall enhancement from these other sources. We comment below on the results for H1 - H6 set out in Table 17 since there is a reasonable amount of data covering operation of these Atlants 2013 - 2018. The more limited data available for H7 - H10 preclude further discussion of their results.

The Atlant-specific attribution estimates shown in Table 17 provide further evidence that gauge-day rainfall downwind of H1, H3 and H5 appears to have been considerably increased when these Atlants were operated while corresponding results for H4 and H6 seem to indicate a more negative outcome for these particular installations. The results for H2 point to little or no enhancement effect associated with this site when considered on its own.

At this stage it is not clear why H4 and H6 lead to negative attribution estimates, but it is consistent with the joint modelling of LogRain underpinning the results set out in Table 14 and Table 15. One possibility is that the consistent negative effects found at H4 and H6 (see the H4 target and H6 target parameter estimates set out in Table 14) reflect incorrect identification of the orientation of the Atlant footprints at these sites, perhaps due to localised orographic features. However, without further investigation, this can only be viewed as conjecture.

**Table 17 Corridor-specific cumulative attributions. Note that the Atlant specific figures are direct estimates, and not based on bootstrap simulation as in Table 15. NA indicates no attribution could be calculated due to insufficient data.**

Downwind of	2013-2014	2013-2015	2013-2016	2013-2017	2013-2018
H1	11.7	8.0	12.8	8.7	8.7
H2	11.4	7.2	5.6	0.3	-0.3
H3	73.8	40.2	41.4	35.0	29.6
H4	-5.9	-3.5	-4.5	-3.9	-4.1
H5		65.2	73.9	61.0	62.8
H6		8.9	-4.3	-5.8	-3.9
H7			NA	3.6	24.1
H8			-1.4	8.5	3.1
H9				NA	-2.4
H10				33.5	9.4
H1-H10	19.4	19.2	20.6	19.0	16.1

## 6 Analysis for 6-Year Gauges

Out of the 120 gauges that were installed in 2013, 12 were moved (and renumbered) in 2014 and 7 had incomplete data at some time over 2013-2018. There were 101 gauges that provided complete data (740 gauge-day values) for the entire six-year trial period. These gauges are on average at a higher elevation than the other gauges that were used in the trial (average elevation of 592m compared with average elevation of 531m for all gauges). They are all also more tightly clustered in the central part of the Hajar Mountains trial area. Given these differences, it is of interest to see whether analysis of the rainfall data obtained from these 101 "6-year" gauges is in line with the analysis of the 2013 - 2018 data obtained from the complete set of 201 gauges in the Hajar Mountain trial area.

In this section we provide an analysis of the 74,740 gauge-day records for these 101 "6-year" gauges, starting with Table 28, which compares their distribution according to type (as determined using the 2013 - 2018 classification) with the corresponding distribution for all gauge-days. Not unexpectedly, the main difference from all gauge-days is lower propensity to be out of scope (i.e. not downwind or upwind of an Atlant).



**Table 18 Frequency distribution of gauge-day values by type of gauge-day, 2013 - 2018 (% positive is percentage for gauge-days with positive rainfall).**

Type	All gauge-days			6-year gauge-days		
	Count	%	% positive	Count	%	% positive
No Rainfall	113140	92.5		68617	91.8	
Out of Scope	3394	2.8	37.2	1888	2.5	30.8
Upwind	1552	1.3	17.0	1167	1.6	19.1
Control	2000	1.6	21.9	1453	1.9	23.7
Target	2173	1.8	23.8	1615	2.2	26.4
<b>Total</b>	<b>122259</b>			<b>74740</b>		

There were 92 (out of 101) 6-year gauges that recorded both target and control readings over 2013 - 2018. Figure 28 shows the distribution of the gauge-specific differences (target-control) in average downwind positive rainfall (mm) for these 92 gauges. The distribution is skewed to the right and the average difference is positive, with a t-value of 1.738. This is not usually viewed as significant, but is indicative of higher average positive rainfall being recorded when these gauges were target gauges.

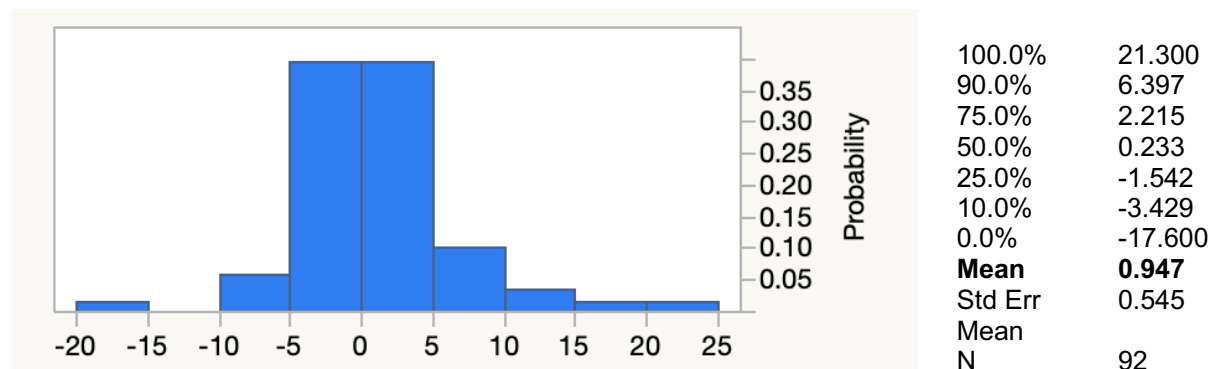


**Figure 28 Histogram and associated key points in the distribution of gauge-specific differences (target-control) in average downwind positive rainfall (mm) for 6-year gauges with both target and control values.**

In Table 11 we compared the key points in the distributions of average positive rainfall and average LogRain for gauge-day observations classified by type. In Table 19 we recreate this analysis, but now restricting coverage to 6-year gauge-day data. We see that the results are in line with our previous analysis, after we make an allowance for the fact that the 6-year gauge-days, being at higher elevations, tended to provide larger rainfall measurements

**Table 19 Summary statistics for positive rainfall gauge-day values and LogRain gauge-day values by gauge-day type for 6-year gauges, 2013 - 2018.**

Level	Count	Mean	SE	10%	25%	Median	75%	90%
Gauge-Day Positive Rainfall								
Out of Scope	1888	4.70	0.19	0.20	0.40	1.60	5.60	13.02
Upwind	1167	4.86	0.26	0.20	0.20	1.00	5.60	14.08
<b>Control</b>	<b>1453</b>	<b>4.73</b>	<b>0.19</b>	<b>0.20</b>	<b>0.40</b>	<b>1.60</b>	<b>6.00</b>	<b>13.60</b>
<b>Target</b>	<b>1615</b>	<b>4.94</b>	<b>0.19</b>	<b>0.20</b>	<b>0.40</b>	<b>2.00</b>	<b>6.40</b>	<b>13.08</b>
Gauge-Day LogRain								
Out of Scope	1888	0.41	0.04	-1.61	-0.92	0.47	1.72	2.57
Upwind	1167	0.25	0.05	-1.61	-1.61	0.00	1.72	2.64
<b>Control</b>	<b>1453</b>	<b>0.52</b>	<b>0.04</b>	<b>-1.61</b>	<b>-0.92</b>	<b>0.47</b>	<b>1.79</b>	<b>2.61</b>
<b>Target</b>	<b>1615</b>	<b>0.57</b>	<b>0.04</b>	<b>-1.61</b>	<b>-0.92</b>	<b>0.69</b>	<b>1.86</b>	<b>2.57</b>

Because 6-year gauges are more clustered around the central part of the Hajar Mountains trial area, one would expect that they would have minimal impact from Atlant sites deployed later in the trial, which were spread further along the ranges. This is confirmed by the counts of target rainfall events (i.e. gauge-days when there was rainfall and the gauge was downwind of an operating Atlant) for 6-year gauge-days shown in Table 20.

**Table 20 Number of target rainfall events by Atlant site for 6-year gauges, 2013 - 2018. Note virtually no target rainfall events associated with H7 and none with H9.**

H1	H2	H3	H4	H5	H6	H7	H8	H9	H10
486	534	174	248	33	38	5	125	0	51

From Table 20 it is clear that modelling downwind rainfall enhancement due to operation of H5 - H10 using 6-year gauge-day data is not recommended. In Table 21 we therefore show the cumulative fits over 2013 - 2018 generated using 6-year gauge data for the same downwind model for LogRain as in Table 14, but with effects for H5 - H10 set to zero. Because of overlapping downwind corridors associated with H5 - H10 from 2015 onwards we expect to see some attenuation in the estimated effect associated with being a target gauge-day for H1 - H4 given this restriction. Nevertheless, the results set out in Table 19 are broadly in line with the more extensive analysis reported in Table 14. In particular, the enhancement signal at H3 is very clear, as is the negative impact of drier conditions combined with extensive missing data in 2018.

**Table 21 LogRain model fit 2013 - 2018 using 6-year gauge data for downwind rain events (3068 gauge-day values). Expected rain calculated using LogRain model fitted to all upwind gauge-day rainfall events 2013 - 2018. Parameter estimates with absolute t-values of 2 or more are shown in red.**

Covariate	2013-2014		2013-2015		2013-2016		2013-2017		2013-2018	
	Est	t val	Est	t val	Est	t val	Est	t val	Est	t val
(Intercept)	0.450	3.360	0.382	3.969	0.300	3.53	0.308	4.04	0.320	4.351
gauge.elev	-0.091	-0.667	-0.128	-1.286	-0.060	-0.68	-0.120	-1.56	-0.173	-2.364
expected rain	1.000	7.707	0.943	10.412	0.933	11.80	0.872	12.88	0.887	13.409
H1 target	0.529	2.218	0.341	1.794	0.336	1.93	0.234	1.49	0.218	1.413
H2 target	0.529	2.531	0.403	2.515	0.442	3.01	0.312	2.28	0.258	1.944
H3 target	0.605	2.606	0.401	2.532	0.375	2.80	0.272	2.27	0.255	2.154
H4 target	-0.253	-1.340	-0.217	-1.632	-0.159	-1.37	-0.238	-2.24	-0.181	-1.784
elev*H1 target	-0.362	-1.400	-0.235	-1.148	-0.185	-0.97	-0.055	-0.33	-0.021	-0.127
elev*H2 target	-0.518	-2.567	-0.326	-2.089	-0.393	-2.75	-0.278	-2.15	-0.206	-1.665
No. gauge-days	1202		1993		2469		2924		3068	
No. days	187		268		342		404		448	

## 7 Modelling of Downwind Positive Rainfall Averages

Modelling rainfall enhancement at the gauge-day level, as in this report, is not the traditional approach to evaluating enhancement, which in many cases relies on differences in (or ratios of) average rainfall to identify an effect. In many cases, these averages are taken over reasonably long periods, and can include rainfall unaffected by any enhancement process. Furthermore, the averages themselves are often based on wildly varying numbers of rainfall events, and so cannot be considered comparable. However, if we put these issues to one side, then there is value in seeing whether average rainfall data obtained in the 2013 - 2018 Hajar Mountains trial also points to the same analytic conclusions obtained using gauge-day data. In particular, in this section we show results from an "average rainfall based" evaluation of the 2013 - 2018 data based on comparing averages of target and control values of daily gauge-level positive rainfall for gauges with the same "profile" in each operating daily downwind corridor in each year. That is, these gauges were all downwind of the same Atlant sites that day and at least one gauge recorded rainfall, leading to a total of 1664 profiles. The sample size underpinning the average value of positive rainfall calculated for each profile varied widely, with most based on one or two positive rainfall measurements, and with a few based on more than 10 positive rainfall measurements. This can be clearly seen from the distributional information shown in Figure 29. Treating these profile averages as essentially comparable, and analysing them as "observed data", is therefore problematic. However, it is of interest to see whether such an analysis, i.e. one based on average positive rainfall for each profile, leads to conclusions about the impact of Atlant operation on rainfall enhancement that are similar to our previous gauge-day based conclusions.

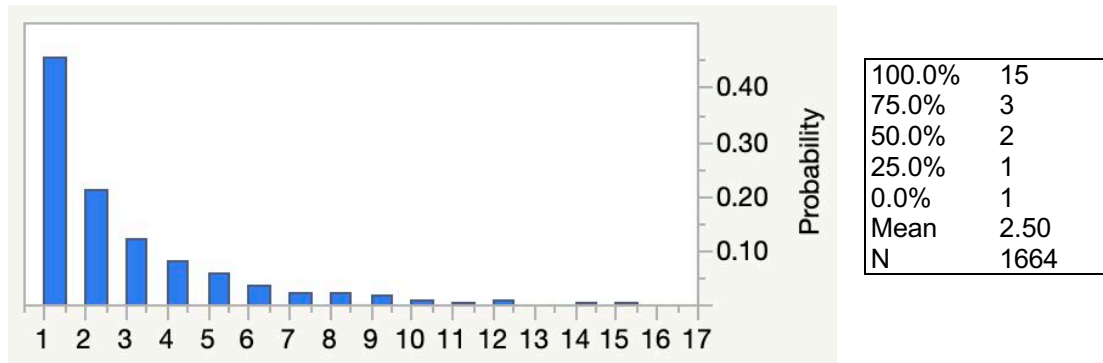


**Figure 29 Distribution of numbers of gauges recording rainfall in profiles where at least one gauge recorded rainfall. There were a total of 1664 profiles with positive average rainfall, averaging 2.5 gauge-day observations of positive rainfall for each profile.**

Rainfall averages for each profile were designated as control or a target for a particular Atlant site on the day depending on whether the site was operational and also whether the average was based on measurements for gauges downwind of the site on the day (note that by construction averages were based on gauge-level data for gauges that could be downwind of more than one operational Atlants on the day). There were 916 target averages and 748 control averages. Table 22 below shows how the information provided by these averages decreases as the number of years of operation of an Atlant in the trial decreases.

**Table 22 Numbers of target classifications by Atlant for the 1664 profiles by year, 2013 - 2018.**

Year	No of profiles	H1	H2	H3	H4	H5	H6	H7	H8	H9	H10
2013	161	55	35	0	0	0	0	0	0	0	0
2014	286	34	49	31	29	0	0	0	0	0	0
2015	337	37	37	32	37	16	20	0	0	0	0
2016	354	36	27	37	23	23	11	13	39	0	0
2017	350	38	33	33	23	15	17	9	40	13	29
2018	176	9	15	5	21	14	1	12	7	1	25
<b>2013-18</b>	<b>1664</b>	<b>209</b>	<b>196</b>	<b>138</b>	<b>133</b>	<b>68</b>	<b>49</b>	<b>34</b>	<b>86</b>	<b>14</b>	<b>54</b>

Table 23 shows summary information for the distribution of average positive rainfall for each profile, classified by the target or control status of each average. A t-test for the difference in the target and control means has a t-value of 1.61, which is weak evidence ( $p = 0.11$ ) for a real difference.

In order to control for the impact of natural rainfall when comparing profile averages of positive rainfall, we fitted a regression model to these averages with a similar structure to the model used in Table 14 for the analysis of 2013 - 2018 downwind gauge-day values of LogRain. In this case, however, we use straightforward Ordinary Least

Squares to fit average positive rainfall (rather than to gauge-day values of LogRain) and the model involves year effects (with 2017 serving as baseline). Parameter estimates for the fitted regression model are displayed in Table 24. The fact that both H3 and H5 record significant positive enhancement effects even with this more simplistic modelling exercise provides further support for the analysis results reported in previous sections.

**Table 23 Summary data for the distribution of profile average positive rainfall, classified by target and control status.**

Status	Count	Mean	SE	10%	25%	Median	75%	90%
Control	748	<b>3.74</b>	0.20	0.20	0.50	<b>1.93</b>	4.88	9.43
Target	916	<b>4.19</b>	0.19	0.20	0.60	<b>2.29</b>	5.60	10.46

**Table 24 Model fit to the 2013 - 2018 positive rainfall average values from the 1664 profiles corresponding to downwind gauge-day observations all with the same Atlant exposure. Parameter estimates with absolute t-values of 2 or more are shown in red. Average expected rain covariate is defined as exponentiated value of average of fitted values from 2013 - 2018 gauge-day model for upwind LogRain.**

Term	Estimate	t value
Intercept	0.672	1.054
year= 2013	<b>2.010</b>	3.560
year=2014	<b>1.100</b>	2.365
year=2015	<b>1.177</b>	2.702
year=2016	<b>1.189</b>	2.740
year=2018	0.382	0.734
Average gauge.elev	-0.090	-0.124
Average expected rain	<b>1.616</b>	11.922
Target H1	0.532	1.228
Target H2	0.118	0.265
Target H3	<b>1.516</b>	3.022
Target H4	-0.249	-0.489
Target H5	<b>1.462</b>	2.104
Target H6	-1.059	-1.302
Target H7	0.957	0.991
Target H8	0.115	0.181
Target H9	0.621	0.415
Target H10	0.643	0.807

## 8 Exploratory Analysis of 2018 Atlant Salalah Trial

### 8.1 Trial instrumentation and Implementation in the Salalah Region

The Atlant trial in Oman was extended to the Salalah region in the south of Oman in 2018. This involved deployment of two further Atlants, H11 and H12, with 19 automatic rain gauges installed in the area surrounding the Atlant sites. Details on the locations of

both these Atlants, and the new rain gauges are in the appendices. The trial ran from July 1 to October 31, with the two Atlants operating on a predefined randomised crossover sequence with one Atlant turned on each day and the other turned off, and with wind direction and speed information obtained from the 4am radiosonde at Salalah Airport. These data were used to identify the steering wind direction each day, which, as with the Hajar Mountains trial, was defined as the speed-weighted average of the radiosonde wind directions at 500hPa and 700hPa. Figure 30 show the distribution of steering wind directions observed at Salalah, classified by principal sector. It is interesting to observe that this distribution is similar to that observed in the Hajar Mountains trial, with exposure to southerly winds being the exception, rather than the rule.

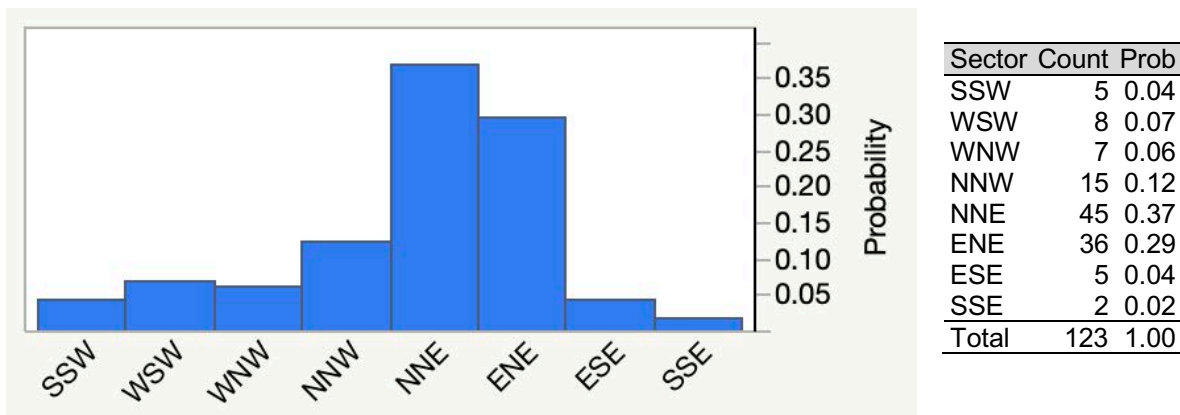


**Figure 30 Distribution of Salalah steering wind directions, classified by principal sector.**

Unfortunately, the Salalah radiosonde data did not provide any information on the usual key meteorological indices. However, daily Information on prevailing meteorological conditions were available from the nine AWS operated by DGMAN in the region. These had reasonably complete hourly data on the three major meteorological variables (dry air temperature, relative humidity and QFE air pressure) that had been found to be useful in rainfall modelling in the Hajar Mountains trial area. AWS data were also available on wind speed, but this did not prove as useful. Following the same approach as in the Hajar Mountains trial analysis, daily averages of the 10am to 8pm data for these AWS variables were summarised by their first and second principal components (wind speed, dry air temperature and relative humidity) and by their first principal component (QFE air pressure). Figure 31 shows the trends in the values of these derived DGMAN indices over the duration of the 2018 trial.

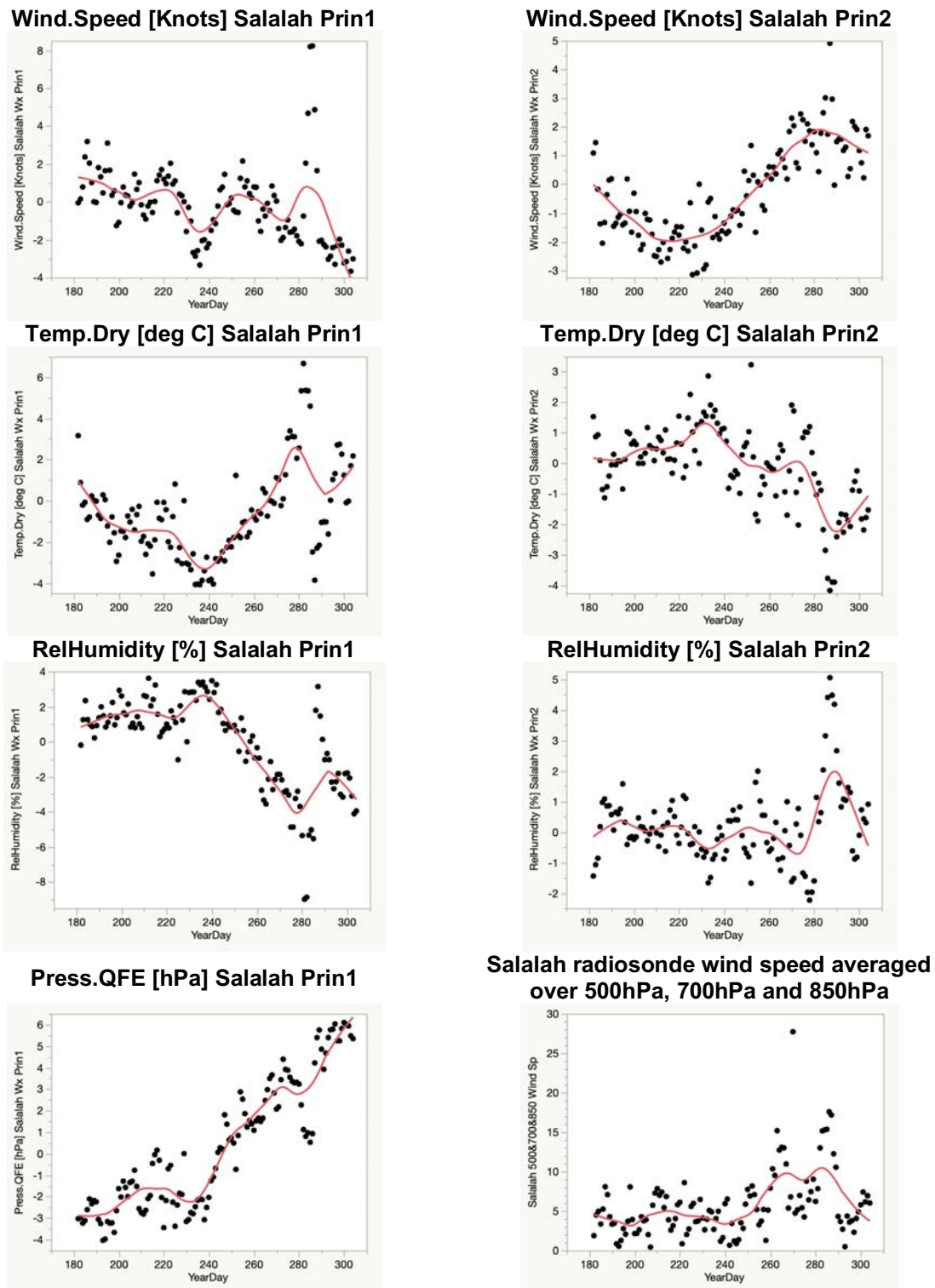


**Figure 31 Day to day variation in DGMAN meteorological summary variables and radiosonde wind speed. Red curve is a nonparametric trend. YearDay is day of year.**

## 8.2 Rainfall in the Salalah Trial Area 2018

Rainfall in the Salalah trial area was more frequent than in the Hajar Mountains trial area. Table 25 compares the relative frequencies of gauge-day rainfall events in the Hajar Mountains over 2013-18 with those observed in the Salalah trial area in 2018.

**Table 25 Counts and relative frequencies of gauge-day rainfall events in the Hajar Mountains 2013 - 2018 compared with Salalah 2018, cross-classified by whether the gauge-day observation was out of scope, upwind or downwind. The top number in each cell is the raw count, the second is the column percentage and the third is the row percentage.**

Gauge-day classification	Hajar Mountains 2013-2018			Salalah 2018		
	No rain recorded	Rain recorded	Total gauge-days	No rain recorded	Rain recorded	Total gauge-days
Out of Scope	44,592 39.41 92.90	3406 37.35 7.10	47,998 39.26 100.00	1253 66.05 79.61	321 72.95 20.39	1574 67.35 100.00
Upwind	29,440 26.02 95.01	1545 16.94 4.99	30,985 25.34 100.00	434 22.88 88.57	56 12.73 11.43	490 20.97 100.00
Downwind	39,108 34.57 90.37	4168 45.71 9.63	43,276 35.40 100.00	210 11.07 76.92	63 14.32 23.08	273 11.68 100.00
Total gauge-days	113,140 100.00 92.54	9,119 100.00 7.46	122,259 100.00 100.00	1,897 100.00 81.17	440 100.00 18.83	2,337 100.00 100.00

The Salalah trial area experiences significantly more rain than the Hajar Mountains, with approximately 19 per cent of the Salalah trial gauge-days recording rainfall compared with under 8 per cent of the Hajar Mountains trial gauge-days. However, most of this Salalah rainfall was out of scope, approximately 73 per cent compared with just over 37 per cent in the Hajar Mountains trial, with the major reduction being in the relative amount of downwind rain recorded, approximately 14 per cent in the Salalah trial compared with just under 46 per cent in the Hajar Mountains trial. That is, although rain fell in the Salalah trial area, the placement of rain gauges there was sub-optimal relative to the positioning of the Atlants and the prevailing steering wind directions. Some evidence for this is set out in Table 26, which shows the frequencies of gauge-days with positive rainfall according to different types, with target status for H11 and H12 distinguished. This indicates that H11 target events were nearly twice as likely to be observed compared with H12 target events. However, both frequencies were still very low compared to the frequency with which out of scope rainfall events were observed.



**Table 26 Upwind and downwind frequencies, Salalah 2018.**

Gauge-Day Type	No of gauge-days with rainfall > 0
Out of Scope	321
Upwind	56
Control	26
H11 Target	23
H12 Target	14

The timing and level of rainfall in the Salalah region in 2018 was also extremely variable. Figure 32 shows daily average positive rainfall recorded in the Salalah trial area over the period of the trial. Clearly, there was one extreme rainfall event during this time.

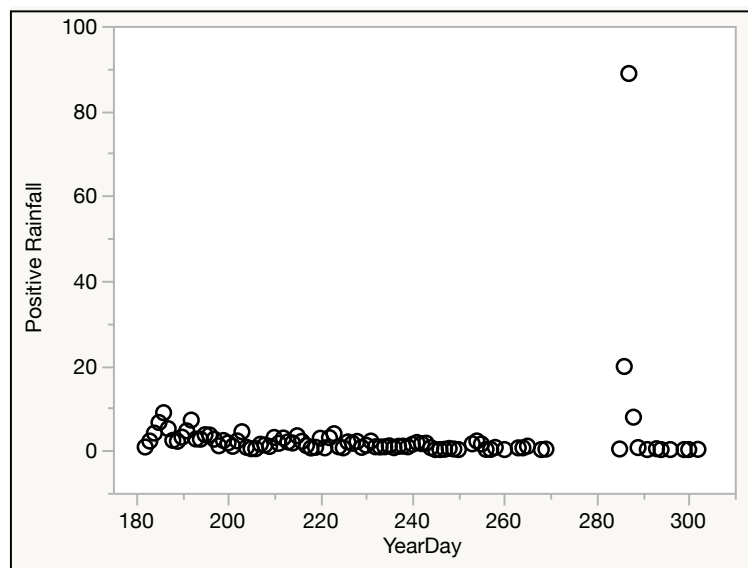


**Figure 32 Average positive daily rainfall (mm) in Salalah trial area, July 1 - Oct 31 2018. YearDay is day of year.**

This extreme rainfall event, which took place on Oct 14, was most likely monsoonal (since the steering wind was from the SSE sector) and had a significant impact on the trial data since it was mainly reflected in control gauge-day observations on the day. This can be seen in Figure 33 which shows the resulting distribution of positive rainfall values by type of gauge-day for Salalah 2018.

The left panel of Figure 33 shows that there were three very large (greater than 165mm) gauge-day rainfall readings, two associated with control gauge-days and one associated with an upwind gauge-day, and with all three recorded on Oct 14. There was also a large (greater than 50mm) target rainfall reading on the previous day. The right

panel of Figure 33 excludes these four gauge-day values in order to better see the differences in the distribution of positive rainfall between the different gauge-day types.

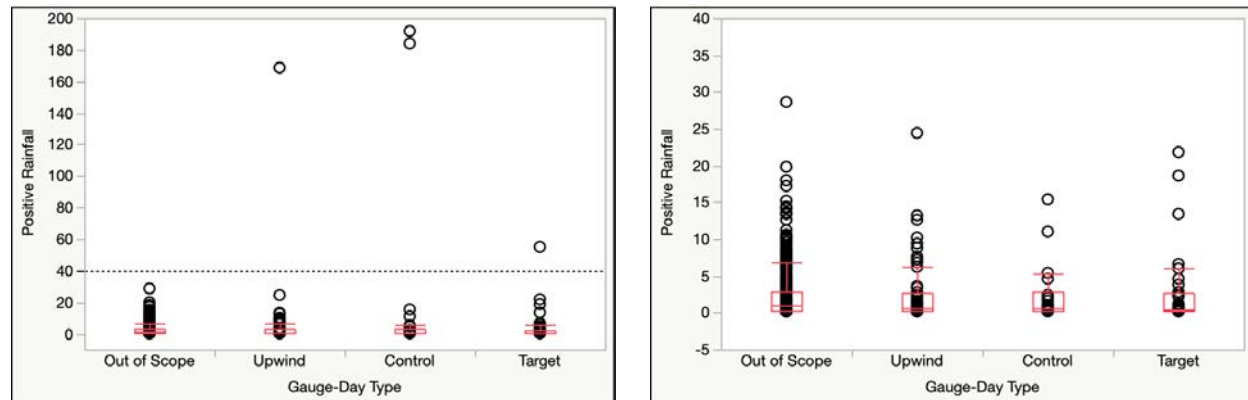


**Figure 33 Distribution of positive rainfall values recorded in Salah 2018, by type of gauge-day. Left panel shows all values. Right panel shows values restricted to less than 40mm.**

Table 27 shows average positive rainfall according to gauge-day type when all gauge-day observations are included and when these four extreme observations are excluded. The impact of excluding these outlying rainfall events on Oct 13 and 14 is clear, with average positive rainfall for control gauge-days dropping from 16.4mm to 2.1mm.

**Table 27 Number of rain events (gauge-days with positive rainfall) and average positive rainfall by type of gauge-day, Salah 2018.**

Gauge-Day Type	All gauge-days		Rainfall < 40mm	
	No of rain events	Average positive rainfall (mm)	No of rain events	Average positive rainfall (mm)
Out of Scope	321	2.5	321	2.5
Upwind	56	5.5	55	2.6
Control	26	16.4	24	2.1
Target	37	4.0	36	2.5

### 8.3 Attribution Analysis for Salah 2018

A crucial aspect of the randomised crossover design used in the 2018 Salah trial is daily spatial balance, in the sense that rainfall recorded at target gauges on a day can be compared with rainfall recorded at control gauges on the same day. However, because of the spatial arrangement of gauges, plus the fact that there were just 19 in total, this could not be achieved in Salah in 2018. In particular, of the 116 days of the trial when there were gauges downwind of either H11 or H12 or both, there was no rain measured on 66, with positive rainfall measured at just one downwind gauge on 42 of the remaining 50 days. That is, on most days when positive downwind rainfall was observed, it was either a control measurement or a target measurement. In effect,

because of distribution of gauges, the Salalah design ended up being highly imbalanced spatially.

To some extent, this imbalance can be controlled by the use of the DGMAN AWS meteorological summary variables displayed in Figure 31. However, these only vary from day to day, and so there is good reason to anticipate that subsequent regression modelling of the Salalah rainfall data will include a substantial amount of uncertainty due to lack of effective spatial controls. Justification for this caution is apparent in the non-significant bootstrap attribution results reported in Table 28. The permutation distributions generated for these attributions, which confirms this opinion, are shown immediately below, in Figure 34.

**Table 28 Attribution modelling results for Salalah 2018.**

Control Variable	All data		Rainfall > 40mm excluded	
	Est	t val	Est	t val
<b>Upwind model estimates</b>				
(Intercept)	1.339	1.930	1.572	2.341
gauge.elev	-2.664	-3.727	-2.775	-4.045
wind.sp	0.155	3.063	0.135	2.752
temp.dry.1	0.474	2.742	0.495	2.989
temp.dry.2	-0.356	-2.409	-0.289	-2.010
relh.1	0.660	4.083	0.622	4.000
No. gauge-days	56		55	
No. days	44		43	
<b>Downwind model estimates</b>				
(Intercept)	1.023	0.525	1.843	0.923
gauge.elev	-0.826	-0.464	-1.841	-0.982
expected rain	1.167	5.914	0.708	2.402
H11 target	0.009	0.019	-0.198	-0.435
H12 target	0.553	1.124	0.689	1.414
No. gauge-days	63		60	
No. days	50		48	
Actual downwind rainfall (mm)	572		141	
Natural rain*	538		108	
Attributed rain*	34		33	
%attribution (Std Error)*	6.3 (12.5)		35.2 (34.7)**	
median %attribution	3.9		31.9**	
% +ve attributions*	64.7		93.3	

\* These are bootstrap estimates, and should be treated with considerable caution given the highly unbalanced nature of the rainfall data obtained in the 2018 Salalah trial.

\*\* These estimates are after 87 (out of 10,000) bootstrap attribution estimates were discarded as extreme outliers. Note that the median bootstrap attribution of 31.9 per cent is insensitive to whether these outliers are discarded or not.

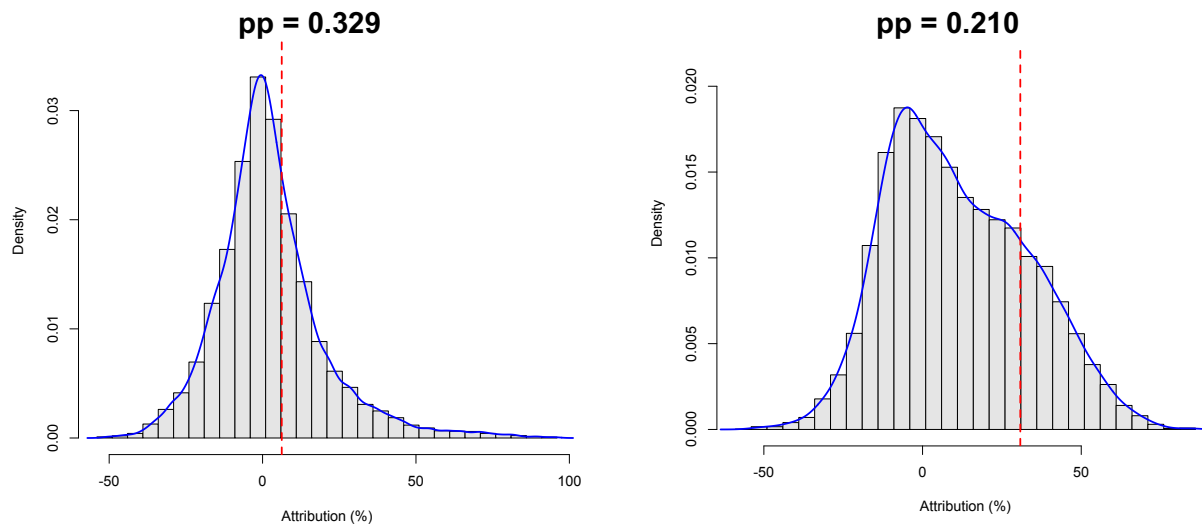


**Figure 34** Permutation distributions for estimated attribution, Salah 2018. Left panel uses all data, while right panel excludes four extreme gauge-day rainfall observations. Vertical red line is the attribution estimate. Permutation p-values (pp) are shown above each distribution. Neither is significant.

## 9 Summary and Conclusions

As far as we are aware, the 2013 - 2018 Hajar Mountains trial of the Atlant system was one of the best instrumented and most scientifically rigorous rainfall enhancement experiments carried out to date. Building on strict adherence to a randomised experimental design, and with sufficient instrumentation to ensure an effective sample size of positive rainfall events in an arid environment with enough power to drive a sophisticated evaluation methodology, the Hajar Mountains trial has conclusively demonstrated that operation of the Atlant system does lead to rainfall enhancement. Furthermore, this enhancement was consistent over the six years of the trial, which involved a variety of seasonal conditions ranging from favourable in the first half of the trial to unfavourable in the second half. In particular, by combining data from all six years, the analysis set out in this report indicates enhancement of between 15 and 18 per cent each year with an overall six-year enhancement of over 16 per cent and with negligible probability of there being no enhancement. Furthermore, a permutation analysis of the randomised operating schedules used 2013 - 2018 shows that there is virtually zero probability that the observed attribution could have happened by chance.

Having said this, it is also clear that these positive results were not observed at every Atlant. In particular, our analysis shows that rainfall enhancement was consistently most pronounced when H3, H5 and H7 were operating, while H4 and H6 were consistently poor performers. At this stage we do not have a definitive reason for why this discrepancy occurs, but we conjecture that local orographic conditions at these sites may imply that their "local" Atlant footprints are not well approximated by the rectangular model for the Atlant footprint that was used in our analysis. That is, where an Atlant is

positioned matters considerably as far as its effectiveness is concerned, and further research will be necessary to untangle the interaction of local orography with Atlant performance. Some support for this conclusion comes from the rather inconclusive results obtained in the 2018 Salalah trial, which in retrospect does not appear to have been adequately instrumented, and where local orographic effects, including placement of the Atlants, appear to not be optimal for identification of a rainfall enhancement effect. Certainly, if the Salalah trial is to continue then these issues will need to be given some thought.

The evaluation methodology used in this report was developed as part of the 2009 and 2010 Atlant trials in South Australia. Its key characteristic is that it is enhancement focussed, i.e., only data on rainfall events where positive rainfall has occurred, are used. The other aspect of this methodology, and crucial to it being enhancement focussed, is that it uses gauge-day data, which allows positive rainfall events at a gauge to be distinguished from zero rainfall events. Both aspects represent a substantial departure from more traditional rainfall enhancement evaluation methods which tend to focus on average rainfall in fixed target areas over longer periods of time and which therefore have considerable difficulty in isolating a small rainfall enhancement signal. In contrast, the gauge-day modelling approach has the capacity to isolate this signal provided sufficient gauges covering the target area are available. This was the case for the Hajar Mountains trial, but not necessarily for the Salalah trial.

The other crucial aspect of the gauge-day approach is that it requires specification of a model for the Atlant footprint, i.e., the area over which an Atlant effect can be expected to be measurable. The corridor-type model for the Atlant footprint was fixed prior to commencement of analysis of the 2013 trial data, based on consideration of local orographic features in the central part of the Hajar Mountains and involved assumptions about the direction of the prevailing winds. But this implies that the analysis reported here is then conditional on this footprint definition, and so care must be taken when attempting to extrapolate it to other environments.

A core requirement of the corridor-type model for the Atlant footprint is that it is oriented in the direction of the steering wind on the day. In particular, we claim that this direction is the same as the speed-weighted average of wind directions between 700hPa and 500hPa pressure levels. But this is an assumption, and furthermore one that is based on radiosonde measurements at Muscat airport, which is some distance from the Atlant sites in the Hajar Mountains. Consequently, it is of some interest to see whether this claim about the direction of the steering wind is consistent with the estimates of rainfall enhancement that we obtain. In Figure 35 we show how the estimated 2013-2018 attribution varies as we "tilt" the steering wind direction away from the 700hPa-500hPa speed-weighted average direction used in the analysis so far. This tilt is shown on the horizontal axis in Figure 35 and is in degrees, varying from  $-20^\circ$  (a  $20^\circ$  swing northwards up to  $0^\circ$  then turning southwards) to  $+20^\circ$  (a  $20^\circ$  swing southwards up to  $180^\circ$ , then turning northwards). It is clear from the estimated attributions displayed in Figure 35 that increased rainfall is most strongly associated with a tilt of  $0^\circ$ , i.e. the direction we have used in this report.

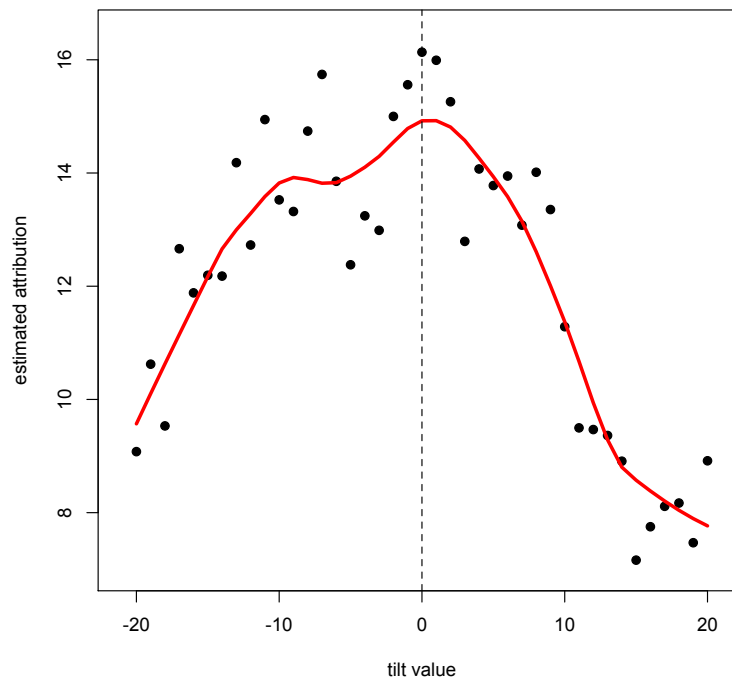


**Figure 35** Points are estimated attributions over 2013-2018 based on tilted daily steering wind directions. The red solid curve is a nonparametric trend estimate. The vertical dotted line shows the actual 2013-2018 attribution estimate.

The Atlant technology is low cost with minimal environmental impact, and on the basis of the results reported in the Hajar Mountains (15-18 per cent increased rainfall each year with a probability of a positive enhancement greater than 99 per cent) it appears to have the potential to significantly increase the availability of water resources in a region where these resources are under a high level of stress. But the climatic conditions that underpin summer rainfall in the Hajar Mountains of Oman are relatively unique. Ideally further experimentation using Atlant type (ground-based ionisation) methods in different environments is necessary.

## 10 References

- Al-Brashdi, HAS (2007) Forecasting Techniques for seedable storms over the Western Hajar mountains in the Sultanate of Oman. MSc thesis University of Pretoria.
- Al-Maskari J and Gadian A (2001) A study of orographic convection over the Hajar Mountains in northern Oman. Presented at International Symposium on Nowcasting and Very Short Range Forecasting (WSN05).
- Beare S, Chambers R, Peak S (2010) Statistical Modeling of Rainfall Enhancement. J. of Wea. Modif. 42, 13-32.

- Beare S, Chambers R, Peak S, Ring J (2011) Accounting for Spatiotemporal Variation of Rainfall Measurements when Evaluating Ground-Based Methods of Weather Modification. *J. of Wea. Modif.* 43, 44-63.
- Chambers R, Beare S, Peak S (2012) Using dynamically defined controls to evaluate the impact of an ionization technology. *J. of Wea. Modif.* 44, pp. 16-29.
- Chambers R and Chandra H (2013) A random effect block bootstrap for clustered data. *Journal of Computational and Graphical Statistics*, 22, 452-470.
- Charabi Y (2013) Projection of Future Changes in Rainfall and Temperature Patterns in Oman. *J. Earth Sci. Clim. Change*, 4:154.
- Harrison RG and Carslaw KS (2003) Ion-aerosol-cloud processes in the lower atmosphere, *Rev. Geophys.*, 41(3), 1012-1038.
- Kauffman P and Ruiz-Columbié A (2005) Artificial Atmospheric Ionization: A Potential Window for Weather Modification. 16th Conference on Planned and Inadvertent Weather Modification. *Am. Met. Soc.*
- Kaufman P and Ruiz-Columbié A (2009) Atmospheric DC Corona effect ionization as a potential tool for aerosol deposition: an experiment, *J. Wea. Mod.*, 41, 144-160.
- Khain A, Arkhipov V, Pinsky M, Feldman Y, YaRyabov (2004) Rain enhancement and fog elimination by seeding with charged droplets. Part I: Theory and numerical simulations. *J. Applied Meteorol.*, 43, 1513-1529.
- Moore CB, Vonnegut B, Rolan TD, Cobb JW, Holden DN, Hignight RT, McWilliams SM, Cadwell GW (1986) Abnormal polarity of thunderclouds grown from negatively charged air. *Science*, 233, 1413-1416.
- Tinsley BA, Rohrbaugh RP, Hei M, Beard KV (2000) Effects of Image Charges on the Scavenging of Aerosol particles by Cloud Droplets and on Droplet Charging and Possible Ice Nucleation Processes, *JAS*, 57, 2118- 2134.
- Tinsley BA, and Zhou L (2014) Comments on "Effect of Electric Charge on Collisions between Cloud Droplets". *J. Appl. Meteor. Climatol.* 53:5, 1317-1320.
- Vonnegut B, and Moore CB (1959) Preliminary attempts to influence convective electrification in cumulus clouds by introduction of space charge into the lower atmosphere, in *Recent advances in Atmospheric Electricity*, Pergamon Press, London, pp 317-322.
- Vonnegut B, Maynard K, Sykes WG, and Moore CB (1961) Technique for introducing low density space charge into the atmosphere, *J. Geophys. Res.*, 66(3), 823-830.
- Vonnegut B, Moore CB, Stout OE, Staggs DW, Bullock JW, Bradley WE (1962) Artificial modification of atmospheric space charge, *J. Geophys Res.*, 67, 1073-1083.

## Appendix A.1 – Instrumentation

### A.1 Atlant Installations with Operating Years

Atlant	Latitude (Decimal)	Longitude (Decimal)	Elevation (m)	2013	2014	2015	2016	2017	2018
H1	23.32246667	57.12330000	2670	x	x	x	x	x	x
H2	23.17633333	57.53166667	2157	x	x	x	x	x	x
H3	23.69440000	56.80110000	1621		x	x	x	x	x
H4	23.17320000	58.04420000	1395		x	x	x	x	x
H5	23.16423600	58.60931000	1876			x	x	x	x
H6	23.54725500	56.54952000	1466			x	x	x	x
H7	23.03750000	58.89194400	1574				x	x	x
H8	23.51541700	56.97934200	1501				x	x	x
H9	24.49743333	56.27663333	1200					x	x
H10	23.11778667	58.34160000	1675					x	x
H11	16.80636389	53.64171111	984						x
H12	16.72991111	53.11224722	1289						x



## A.2 DGMAN Automatic Weather Stations (AWS) with Contributing Years

AWS	Latitude (decimal)	Longitude (decimal)	Elevation (m)	2013	2014	2015	2016	2017	2018
<b>Hajar Mountains trial area</b>									
Adam Airport	22.50	57.37	328			x	x	x	x
Al Amerat	23.50	58.48	105	x	x	x	x	x	x
Al Mudhaibi	22.51	58.12	378	x	x	x			
Bahla	22.99	57.32	592	x	x	x	x	x	x
Bidiyah	22.46	58.85	316			x	x	x	x
Buraimi	24.23	55.92	372			x	x	x	x
Ibra	22.74	58.51	469			x	x	x	x
Ibri	23.20	56.43	323		x	x	x	x	x
Jabal Shams	23.24	57.27	2764	x	x				
Mahdha	24.54	56.05	560			x	x	x	x
Majis	24.47	56.64	2		x	x	x	x	
Muscat Airport	23.61	56.26	2	x		x	x	x	x
Nizwa	22.86	57.55	462	x	x	x	x	x	x
Qumaira	23.93	56.20	633			x	x	x	x
Qurayyat	23.22	58.90	18					x	x
Rustaq	23.40	57.43	322		x	x	x	x	x
Saiq	23.07	57.67	1995	x	x	x	x	x	x
Samail	23.31	57.95	417	x	x	x	x	x	x
Sunaynah	23.72	55.91	257			x	x	x	x
Suwaiq	23.83	57.28	39	x	x		x	x	x
<b>Salalah trial area</b>									
Al Mazyunah	17.84	52.66	499						x
Dhalkut	16.71	53.25	22						x
Mirbat	16.99	54.69	9						x
Qairoon Hairiti	17.25	54.09	881						x
Sadah	17.05	55.07	20						x
Salalah AirPort	17.04	54.10	23						x
Salalah Port	16.93	54.01	25						x
Taqah	17.04	54.40	18						x
Thumrait	17.68	54.02	448						x

### A.3 TIE Rain Gauges Locations

Gauge ID	Latitude	Longitude	Elevation
1	22.7905	57.85393333	479
2	22.84041667	57.8799	540
3	22.87118333	57.76013333	495
5	22.8143	57.5914	445
6	22.90993333	57.59236667	508
7	22.93595	57.50846667	547
8	22.82906667	57.48546667	483
9	22.88541667	57.35626667	555
10	23.0269	57.3671	631
11	23.00066667	57.31008333	591
12	22.92211667	57.25565	540
13	22.94205	57.12701667	519
14	23.03008333	57.15721667	557
15	23.06598333	57.01848333	886
16	22.99316667	57.00695	607
17	22.9643	56.86095	559
18	23.0767	56.7584	542
19	23.11783333	56.7835	464
20	22.99511667	56.74363333	462
21	22.9595	57.9015	253
22	23.02603333	57.92741667	747
23	23.07695	57.81686667	677
24	22.97521667	57.77885	588
25	23.0241	57.69378333	2015
26	23.0892	57.67875	2023
27	23.10643333	57.53411667	2000
28	23.03963333	57.50585	603
29	23.0672	57.42678333	771
30	23.15676667	58.25585	1958
31	23.15261667	57.2963	1263
32	23.10181667	57.28525	655
33	23.108	57.20495	762
34	23.2292	57.19921667	1968
35	23.22735	57.04995	729
36	23.15026667	57.07833333	964
37	23.16625	56.91615	590
38	23.2751	56.95531667	464
39	23.30091667	56.83566667	587
40	23.23026667	56.81385	547
41	23.11428333	57.9264	897
42	23.25038333	57.98971667	448

43	23.27705	57.91983333	426
44	23.16615	57.85278333	564
45	23.17681667	57.65133333	915
46	23.29108333	57.69321667	517
47	23.32113333	57.60571667	405
48	23.19951667	57.55973333	729
49	23.26558333	57.4456	587
50	23.36283333	57.47665	398
51	23.39985	57.33798333	442
52	23.27431667	57.33466667	715
53	23.28351667	57.2635	1677
54	23.39326667	57.23501667	535
55	23.45328333	57.105	677
57	23.37656667	57.0154	961
58	23.4644	57.0309	897
59	23.49973333	56.86356667	708
60	23.38526667	56.8564	693
61	23.31795	58.02283333	352
62	23.41255	58.083	263
63	23.4541	57.88523333	236
64	23.3966	57.84565	304
65	23.3815	57.76328333	321
66	23.45325	57.81663333	228
67	23.49655	57.67183333	186
68	23.37623333	57.66453333	337
69	23.45768333	57.51601667	275
70	23.54116667	57.5224	174
71	23.55263333	57.45201667	195
72	23.44176667	57.39368333	340
73	23.48413333	57.28715	377
75	23.65056667	57.14568333	288
76	23.5688	57.18168333	405
77	23.529	57.0109	764
78	23.65141667	57.08898333	413
79	23.66926667	56.9236	413
80	23.5669	56.89798333	808
82	23.62076667	58.05003333	35
84	23.5437	57.9673	116
85	23.56455	57.83578333	118
86	23.65433333	57.85886667	31
87	23.69096667	57.7077	29
89	23.63318333	57.52853333	107
92	23.64005	57.38251667	145
94	23.753	57.33158333	71

<b>96</b>	23.70503333	57.19936667	167
<b>97</b>	23.71715	57.0996	243
<b>99</b>	23.83296667	56.96405	104
<b>100</b>	23.75793333	56.92568333	310
<b>101</b>	23.76551667	56.83961667	364
<b>103</b>	23.65495	56.79543333	850
<b>104</b>	23.77128333	56.62815	750
<b>105</b>	23.78348333	56.73318333	501
<b>106</b>	23.5488	56.77233333	691
<b>107</b>	23.68541667	56.55198333	727
<b>108</b>	23.4101	56.7396	525
<b>109</b>	23.55543333	56.53355	532
<b>110</b>	23.63585	56.63636667	714
<b>111</b>	23.37913333	58.13855	257
<b>112</b>	23.36283333	58.39515	360
<b>113</b>	23.23778333	58.1191	394
<b>114</b>	23.14635	58.31315	739
<b>115</b>	23.2613	58.21771667	486
<b>116</b>	23.02756667	58.0171	683
<b>117</b>	23.06911667	58.32026667	711
<b>118</b>	22.94276667	58.05643333	587
<b>119</b>	22.86338333	58.21401667	650
<b>120</b>	23.07078333	58.18416667	522
<b>121</b>	22.80153333	57.40861667	672
<b>122</b>	22.8742	57.17423333	698
<b>123</b>	22.74526667	57.24565	560
<b>124</b>	22.68801667	57.5695	508
<b>125</b>	22.77585	57.64893333	554
<b>126</b>	22.70733333	57.73465	543
<b>127</b>	22.74645	57.85066667	695
<b>128</b>	22.7033	58.02601667	518
<b>129</b>	22.99278333	58.6007	624
<b>130</b>	22.87183333	58.05576667	357
<b>131</b>	22.70041667	58.15693333	406
<b>132</b>	22.85043333	58.59606667	471
<b>133</b>	22.86436667	58.30776667	636
<b>134</b>	22.96781667	58.2398	534
<b>135</b>	22.74743333	58.2858	322
<b>136</b>	22.6666	58.253	333
<b>137</b>	22.72413333	58.40973333	316
<b>138</b>	22.80675	58.43965	671
<b>139</b>	22.97213333	58.44955	573
<b>140</b>	23.11751667	58.45363333	518
<b>141</b>	22.80798333	56.99153333	481

<b>142</b>	23.06801667	56.6241	753
<b>143</b>	23.21561667	56.66201667	400
<b>144</b>	23.35405	56.64546667	589
<b>145</b>	23.54943333	56.6622	396
<b>146</b>	23.91891667	56.55045	314
<b>147</b>	23.29193333	56.37348333	398
<b>148</b>	23.21816667	56.46545	296
<b>149</b>	24.06913333	56.55985	710
<b>150</b>	23.68706667	56.45405	671
<b>151</b>	23.86631667	56.40633333	573
<b>152</b>	23.9444	56.35355	320
<b>153</b>	23.77371667	56.207	481
<b>154</b>	23.75468333	56.39401667	753
<b>155</b>	23.66138333	56.21836667	400
<b>156</b>	23.63938333	56.38401667	589
<b>157</b>	23.54493333	56.3479	396
<b>158</b>	23.50378333	56.20198333	314
<b>159</b>	23.3476	56.51526667	398
<b>160</b>	23.39058333	56.29218333	296
<b>161</b>	24.07411667	56.41856667	710
<b>162</b>	24.08966667	56.2624	856
<b>163</b>	23.58866667	56.00343333	267
<b>164</b>	24.10058333	56.07456667	516
<b>165</b>	24.21011667	56.17711667	594
<b>166</b>	24.24501667	56.35495	352
<b>167</b>	23.78411667	56.0134	320
<b>168</b>	24.2245	55.95666667	411
<b>169</b>	23.78786667	55.87471667	261
<b>170</b>	23.935	55.82521667	285
<b>171</b>	24.0167	55.9591	373
<b>172</b>	23.8313	56.4688	905
<b>173</b>	23.93441667	56.20175	642
<b>174</b>	23.86398333	56.64383333	612
<b>175</b>	24.00091667	56.65635	333
<b>176</b>	23.30573333	58.48318333	330
<b>177</b>	23.27953333	58.39725	512
<b>178</b>	23.22173333	58.68331667	277
<b>179</b>	23.2679	58.633	298
<b>180</b>	23.26515	58.75718333	163
<b>181</b>	23.33895	58.58741667	211
<b>182</b>	23.08681667	58.56865	412
<b>183</b>	23.04473333	58.64965	337
<b>184</b>	22.99258333	58.77608333	325
<b>185</b>	23.13403333	58.53388333	451

<b>186</b>	23.90515	56.74936667	209
<b>187</b>	22.88926667	58.6659	558
<b>188</b>	22.76376667	58.6678	429
<b>189</b>	22.72708333	58.52333333	467
<b>190</b>	23.09233333	58.85635	139
<b>191</b>	23.217	58.3101	687
<b>192</b>	23.34671667	58.2266	352
<b>193</b>	22.92661667	58.89511667	695
<b>194</b>	22.70915	58.76951667	452
<b>195</b>	22.83636667	58.86326667	700
<b>196</b>	22.62678333	58.67003333	397
<b>197</b>	22.88875	59.00393333	1277
<b>198</b>	22.77068333	58.96036667	886
<b>199</b>	22.68076667	58.89528333	518
<b>200</b>	22.57131667	58.80908333	382
<b>201</b>	22.68376667	58.97805	585
<b>202</b>	22.4673	58.8917	305
<b>203</b>	22.53715	58.97118333	404
<b>204</b>	24.358983	56.351317	336
<b>205</b>	24.315867	56.069383	563
<b>206</b>	24.382667	55.939783	402
<b>207</b>	24.44245	55.9124	394
<b>208</b>	24.458917	56.274833	546
<b>209</b>	24.466967	56.0648	604
<b>210</b>	24.55155	55.956933	560
<b>211</b>	24.5513	56.144867	729
<b>212</b>	24.6376	56.070467	593
<b>213</b>	24.359017	56.356733	404
<b>214</b>	17.09925	54.4715	506
<b>215</b>	17.03675	54.61315	726
<b>216</b>	17.1925	54.6231	1161
<b>217</b>	17.15591667	54.3438	795
<b>218</b>	17.229333	54.3986	939
<b>219</b>	17.0877667	54.337333	148
<b>220</b>	17.1079833	54.2175333	75
<b>221</b>	17.05811667	54.0778667	50
<b>222</b>	17.28056667	54.1634	817
<b>223</b>	17.1858	54.11863333	535
<b>224</b>	16.75928333	53.2360333	1077
<b>225</b>	16.96061667	53.87608333	50
<b>226</b>	16.94695	53.24795	910
<b>227</b>	16.75013333	53.41726667	18
<b>229</b>	17.09161667	53.89175	1024
<b>230</b>	17.0558	53.1058	885

<b>231</b>	17.21711667	53.33788333	812
<b>232</b>	16.8564333	53.4023333	1030
<b>233</b>	16.81711667	53.5563667	1088



## Appendix B – Operating Schedules 2013 - 2018

### B.1 2013 Operating Schedule

In 2013, the two Atlant sites were operated in a randomised crossover schedule. Rather than randomly generating the schedules for Hajar 1 and Hajar 2 and then combining them, a schedule was constructed from the 170 1-day groups containing 85 days Hajar 1 on and Hajar off; and 85 days Hajar 2 on and Hajar 1 off. The advantage of this approach is that it ensures that each combination is scheduled for an equal number of days. The 170 1-day groups were then randomly sequenced giving an operating schedule commencing 15 May 13 and completing 31 October 2013.

1=On 0=Off

Month	Day	H1	H2
May	15	1	0
May	16	1	0
May	17	0	1
May	18	0	1
May	19	0	1
May	20	1	0
May	21	0	1
May	22	1	0
May	23	0	1
May	24	0	1
May	25	1	0
May	26	0	1
May	27	0	1
May	28	0	1
May	29	1	0
May	30	1	0
May	31	0	1
June	1	0	1
June	2	1	0
June	3	0	1
June	4	0	1
June	5	0	1
June	6	0	1
June	7	1	0
June	8	0	1



<b>June</b>	9	0	1
<b>June</b>	10	1	0
<b>June</b>	11	0	1
<b>June</b>	12	0	1
<b>June</b>	13	1	0
<b>June</b>	14	1	0
<b>June</b>	15	1	0
<b>June</b>	16	0	1
<b>June</b>	17	1	0
<b>June</b>	18	1	0
<b>June</b>	19	1	0
<b>June</b>	20	0	1
<b>June</b>	21	1	0
<b>June</b>	22	1	0
<b>June</b>	23	0	1
<b>June</b>	24	1	0
<b>June</b>	25	0	1
<b>June</b>	26	0	1
<b>June</b>	27	1	0
<b>June</b>	28	0	1
<b>June</b>	29	1	0
<b>June</b>	30	1	0
<b>July</b>	1	1	0
<b>July</b>	2	0	1
<b>July</b>	3	0	1
<b>July</b>	4	0	1
<b>July</b>	5	1	0
<b>July</b>	6	0	1
<b>July</b>	7	1	0
<b>July</b>	8	0	1
<b>July</b>	9	1	0
<b>July</b>	10	0	1
<b>July</b>	11	1	0
<b>July</b>	12	1	0
<b>July</b>	13	0	1
<b>July</b>	14	0	1
<b>July</b>	15	0	1
<b>July</b>	16	1	0
<b>July</b>	17	0	1

<b>July</b>	18	1	0
<b>July</b>	19	0	1
<b>July</b>	20	0	1
<b>July</b>	21	0	1
<b>July</b>	22	0	1
<b>July</b>	23	1	0
<b>July</b>	24	0	1
<b>July</b>	25	1	0
<b>July</b>	26	0	1
<b>July</b>	27	1	0
<b>July</b>	28	1	0
<b>July</b>	29	1	0
<b>July</b>	30	1	0
<b>July</b>	31	0	1
<b>August</b>	1	1	0
<b>August</b>	2	1	0
<b>August</b>	3	0	1
<b>August</b>	4	1	0
<b>August</b>	5	1	0
<b>August</b>	6	1	0
<b>August</b>	7	0	1
<b>August</b>	8	1	0
<b>August</b>	9	1	0
<b>August</b>	10	0	1
<b>August</b>	11	0	1
<b>August</b>	12	0	1
<b>August</b>	13	1	0
<b>August</b>	14	1	0
<b>August</b>	15	0	1
<b>August</b>	16	0	1
<b>August</b>	17	1	0
<b>August</b>	18	1	0
<b>August</b>	19	0	1
<b>August</b>	20	0	1
<b>August</b>	21	0	1
<b>August</b>	22	0	1
<b>August</b>	23	0	1
<b>August</b>	24	1	0
<b>August</b>	25	1	0

<b>August</b>	26	1	0
<b>August</b>	27	0	1
<b>August</b>	28	1	0
<b>August</b>	29	0	1
<b>August</b>	30	1	0
<b>August</b>	31	1	0
<b>September</b>	1	0	1
<b>September</b>	2	1	0
<b>September</b>	3	1	0
<b>September</b>	4	0	1
<b>September</b>	5	1	0
<b>September</b>	6	1	0
<b>September</b>	7	0	1
<b>September</b>	8	1	0
<b>September</b>	9	1	0
<b>September</b>	10	0	1
<b>September</b>	11	0	1
<b>September</b>	12	1	0
<b>September</b>	13	0	1
<b>September</b>	14	1	0
<b>September</b>	15	1	0
<b>September</b>	16	1	0
<b>September</b>	17	1	0
<b>September</b>	18	1	0
<b>September</b>	19	1	0
<b>September</b>	20	0	1
<b>September</b>	21	0	1
<b>September</b>	22	0	1
<b>September</b>	23	0	1
<b>September</b>	24	1	0
<b>September</b>	25	0	1
<b>September</b>	26	1	0
<b>September</b>	27	0	1
<b>September</b>	28	0	1
<b>September</b>	29	1	0
<b>September</b>	30	1	0
<b>October</b>	1	1	0
<b>October</b>	2	1	0
<b>October</b>	3	0	1

<b>October</b>	4	1	0
<b>October</b>	5	1	0
<b>October</b>	6	0	1
<b>October</b>	7	0	1
<b>October</b>	8	0	1
<b>October</b>	9	1	0
<b>October</b>	10	1	0
<b>October</b>	11	1	0
<b>October</b>	12	0	1
<b>October</b>	13	1	0
<b>October</b>	14	1	0
<b>October</b>	15	0	1
<b>October</b>	16	0	1
<b>October</b>	17	0	1
<b>October</b>	18	1	0
<b>October</b>	19	1	0
<b>October</b>	20	0	1
<b>October</b>	21	1	0
<b>October</b>	22	0	1
<b>October</b>	23	1	0
<b>October</b>	24	1	0
<b>October</b>	25	0	1
<b>October</b>	26	1	0
<b>October</b>	27	0	1
<b>October</b>	28	0	1
<b>October</b>	29	0	1
<b>October</b>	30	0	1
<b>October</b>	31	0	1

## B.2 2014 Operating Schedule

The 2014 trial employed a randomised crossover design (similar to the 2013 trial). The crossover design applied to the trial had two pairings of Atlant sites operate on a randomly predetermined rotation basis throughout the trial with no breaks. That is Hajar 1 (H1) and Hajar 4 (H4) formed one group and operated together, and Hajar 2 (H2) and Hajar 3 (H3) formed the second group and operated together.

Note: Cells highlighted in red indicate changes in planned operating schedule due to mechanical faults – described in comments column.

Month	Day	H3	H1	H2	H4	Notes where planned operation not achieved
June	1	Off	On	Off	On	
June	2	On	Off	On	Off	
June	3	Off	On	Off	On	
June	4	On	Off	On	Off	
June	5	Off	On	Off	On	
June	6	Off	On	Off	On	
June	7	On	Off	On	Off	
June	8	On	Off	On	Off	
June	9	On	Off	On	Off	
June	10	Off	On	Off	On	
June	11	Off	On	Off	On	
June	12	Off	On	Off	On	
June	13	On	Off	On	Off	
June	14	On	Off	On	Off	
June	15	On	Off	On	Off	
June	16	Off	On	Off	On	The switching was reversed on 16/17 Jun. That is, where it says Off, it should have been On, and where it says On, it should have been Off
June	17	On	Off	On	Off	
June	18	On	Off	On	Off	
June	19	On	Off	On	Off	
June	20	Off	On	Off	On	
June	21	On	Off	On	Off	
June	22	Off	On	Off	On	
June	23	Off	On	Off	On	
June	24	Off	On	Off	On	
June	25	Off	On	Off	On	
June	26	On	Off	On	Off	
June	27	Off	On	Off	On	

June	28	On	Off	On	Off	
June	29	Off	On	Off	On	
June	30	Off	On	Off	On	
July	1	Off	On	Off	On	
July	2	On	Off	On	Off	
July	3	On	Off	On	Off	
July	4	Off	On	Off	On	
July	5	On	Off	On	Off	
July	6	Off	On	Off	On	
July	7	Off	On	Off	On	
July	8	Off	On	Off	On	
July	9	On	Off	On	Off	
July	10	On	Off	On	Off	
July	11	On	Off	On	Off	
July	12	On	Off	On	Off	
July	13	Off	On	Off	On	
July	14	On	Off	On	Off	
July	15	Off	On	Off	On	
July	16	On	Off	On	Off	
July	17	Off	On	Off	On	
July	18	On	Off	On	Off	
July	19	On	Off	On	Off	
July	20	On	Off	On	Off	
July	21	On	Off	On	Off	
July	22	Off	On	Off	On	
July	23	On	Off	On	Off	
July	24	Off	On	Off	On	
July	25	Off	On	Off	On	
July	26	Off	On	Off	On	
July	27	On	Off	On	Off	
July	28	Off	On	Off	On	
July	29	On	Off	On	Off	
July	30	Off	On	Off	On	
July	31	Off	On	Off	On	
August	1	Off	On	Off	On	
August	2	On	Off	On	Off	
August	3	Off	On	Off	On	
August	4	Off	On	Off	On	
August	5	On	Off	On	Off	
August	6	Off	On	Off	On	
August	7	On	Off	On	Off	

August	8	On	Off	On	Off	
August	9	On	Off	On	Off	
August	10	Off	On	Off	On	
August	11	On	Off	On	Off	
August	12	On	Off	On	Off	
August	13	Off	On	Off	On	
August	14	Off	On	Off	On	
August	15	On	Off	On	Off	
August	16	Off	On	Off	On	
August	17	On	Off	On	Off	
August	18	On	Off	On	Off	
August	19	Off	On	Off	On	
August	20	Off	On	Off	Off	H4 was planned On, but actual operation was Off due to HVG cable failure
August	21	On	Off	On	Off	
August	22	Off	On	Off	Off	H4 was planned On, but actual operation was Off due to HVG cable failure
August	23	On	Off	On	Off	
August	24	Off	On	Off	Off	H4 was planned On, but actual operation was Off due to HVG cable failure
August	25	On	Off	On	Off	
August	26	On	Off	On	Off	
August	27	On	Off	On	Off	
August	28	On	Off	On	Off	
August	29	Off	On	Off	Off	H4 was planned On, but actual operation was Off due to HVG cable failure
August	30	Off	On	Off	Off	H4 was planned On, but actual operation was Off due to HVG cable failure
August	31	On	Off	On	Off	
September	1	Off	On	Off	Off	H4 was planned On, but actual operation was Off due to HVG cable failure
September	2	Off	On	Off	Off	H4 was planned On, but actual operation was Off due to HVG cable failure
September	3	Off	On	Off	Off	H4 was planned On, but actual operation was Off due to HVG cable failure
September	4	On	Off	On	Off	

September	5	Off	On	Off	Off	H4 was planned On, but actual operation was Off due to HVG cable failure
September	6	On	Off	On	Off	
September	7	Off	On	Off	Off	H4 was planned On, but actual operation was Off due to HVG cable failure
September	8	Off	On	Off	On	
September	9	On	Off	On	Off	
September	10	Off	On	Off	On	
September	11	On	Off	On	Off	
September	12	Off	On	Off	On	
September	13	On	Off	On	Off	
September	14	Off	On	Off	On	
September	15	On	Off	On	Off	
September	16	Off	On	Off	On	
September	17	On	Off	On	Off	
September	18	On	Off	On	Off	
September	19	Off	On	Off	On	
September	20	On	Off	On	Off	
September	21	On	Off	On	Off	
September	22	Off	On	Off	On	
September	23	Off	On	Off	On	
September	24	Off	On	Off	On	
September	25	On	Off	On	Off	
September	26	On	Off	On	Off	
September	27	On	Off	On	Off	
September	28	Off	On	Off	On	
September	29	On	Off	On	Off	
September	30	On	Off	On	Off	
October	1	On	Off	On	Off	
October	2	Off	On	Off	On	
October	3	Off	On	Off	On	
October	4	Off	On	Off	On	
October	5	Off	On	Off	On	
October	6	On	Off	On	Off	
October	7	Off	On	Off	On	
October	8	On	Off	On	Off	
October	9	On	Off	On	Off	
October	10	Off	On	Off	On	
October	11	Off	On	Off	On	
October	12	On	Off	On	Off	



---

October	13	Off	On	Off	On	
October	14	On	Off	On	Off	
October	15	Off	On	Off	On	
October	16	Off	On	Off	On	
October	17	On	Off	On	Off	
October	18	On	Off	On	Off	

### B.3 2015 Operating Schedule

The 2015 trial employed a balanced randomised design. Given that there were 6 operational Atlants in 2015, and that the 30km corridor footprint model used for the analysis in 2013/2014 essentially isolates the Atlants from one another, there was no real reason to 'pair' Atlants (operational versus control) as was done in the past, particularly since there does not seem to be any reasonable way of spatially matching the Atlant locations.

The design aim was to have 3 Atlants operational every day (ensuring within day effects over the entire trial area were estimated with maximum precision), implying 20 different combinations of operating states on a day. A nominal trial period of 140 days was therefore used and this period was then segmented into 7 equal-sized blocks of 20 days each, with these 20 combinations randomly allocated to days within each block. Within each 20-day block, each Atlant is on for 10 days and off for 10 days. And within each day, three Atlants are on and three are off. The result was that each Atlant was planned to be on for 70 days and off for 70 days of the trial.

Note: Cells highlighted in red indicate changes in planned operating schedule due to mechanical faults – described in comments column.

1=On 0=Off

Month	Day	Block	H6	H3	H1	H2	H4	H5	Comments
June	14	1	0	1	0	1	1	0	
June	15	1	1	0	1	0	0	1	
June	16	1	1	0	0	1	0	1	
June	17	1	1	0	0	0	1	1	
June	18	1	0	1	0	0	1	1	
June	19	1	1	0	0	1	1	0	
June	20	1	0	1	1	0	0	1	
June	21	2	0	0	0	1	1	1	
June	22	2	1	1	0	0	1	0	
June	23	2	0	1	1	1	0	0	
June	24	2	0	0	1	1	1	0	
June	25	2	1	1	0	0	0	1	
June	26	2	1	0	1	0	1	0	
June	27	2	1	0	0	1	0	1	
June	28	2	1	0	0	1	1	0	
June	29	2	1	0	0	0	1	1	
June	30	2	0	1	0	1	0	1	
July	1	2	0	0	1	0	1	1	

July	2	2	1	1	1	0	0	0	
July	3	2	0	1	0	0	1	1	
July	4	2	0	0	1	1	0	1	
July	5	2	0	1	1	0	1	0	
July	6	2	1	0	1	1	0	0	
July	7	2	1	1	0	1	0	0	
July	8	2	0	1	1	0	0	1	
July	9	2	1	0	1	0	0	1	
July	10	2	0	1	0	1	1	0	
July	11	3	1	0	1	0	1	0	
July	12	3	0	1	0	0	1	1	
July	13	3	1	0	1	0	0	1	
July	14	3	1	0	0	1	0	1	
July	15	3	1	1	0	0	0	1	
July	16	3	1	0	0	1	1	0	
July	17	3	0	1	0	1	0	1	
July	18	3	0	1	0	1	1	0	
July	19	3	0	0	0	0	1	1	H1 issue with HV Cable
July	20	3	0	1	0	0	0	1	
July	21	3	0	0	0	1	0	0	H6 issue with Field wire
July	22	3	0	1	0	0	0	0	
July	23	3	0	0	0	0	1	0	H5 issue with communications
July	24	3	0	1	0	0	1	0	H1 issue with HV Cable
July	25	3	0	0	0	1	1	0	
July	26	3	0	1	0	0	1	0	
July	27	3	0	0	0	1	1	0	H1 HVG Cable / H5 communications
July	28	3	0	1	0	1	0	0	
July	29	3	0	0	0	1	0	0	
July	30	3	1	1	0	1	0	0	
July	31	4	1	0	0	1	0	0	
August	1	4	0	0	0	0	1	0	
August	2	4	1	0	0	0	1	0	
August	3	4	0	0	0	1	1	1	
August	4	4	1	0	0	1	0	0	

August	5	4	0	1	0	0	1	1	
August	6	4	0	1	1	0	1	0	
August	7	4	1	1	0	0	0	1	
August	8	4	1	0	1	0	1	0	
August	9	4	0	1	0	1	1	0	
August	10	4	0	1	0	1	0	1	
August	11	4	1	0	0	1	1	0	
August	12	4	1	0	1	0	0	1	
August	13	4	0	0	1	1	1	0	
August	14	4	1	1	0	0	1	0	
August	15	4	1	1	0	1	0	0	
August	16	4	1	1	1	0	0	0	
August	17	4	0	1	1	0	0	1	
August	18	4	0	1	1	1	0	0	
August	19	4	0	0	1	1	0	1	
August	20	5	1	0	0	1	0	1	
August	21	5	0	1	0	1	1	0	
August	22	5	1	0	0	0	1	1	
August	23	5	0	0	1	1	0	1	
August	24	5	1	0	1	0	0	1	
August	25	5	1	0	0	1	1	0	
August	26	5	0	1	0	0	1	1	
August	27	5	0	1	0	1	0	1	
August	28	5	1	0	1	0	1	0	
August	29	5	1	0	1	1	0	0	
August	30	5	0	1	1	0	0	1	
August	31	5	1	1	0	0	0	1	
September	1	5	1	1	1	0	0	0	
September	2	5	0	0	1	0	1	1	
September	3	5	1	1	0	1	0	0	
September	4	5	0	1	1	1	0	0	
September	5	5	0	0	1	1	1	0	
September	6	5	1	1	0	0	1	0	
September	7	5	0	0	0	1	1	1	
September	8	5	0	1	1	0	1	0	
September	9	6	0	1	1	1	0	0	
September	10	6	0	1	0	1	1	0	
September	11	6	0	0	0	1	1	1	
September	12	6	1	0	0	0	1	1	

September	13	6	0	0	1	1	0	1	
September	14	6	0	1	1	0	1	0	
September	15	6	1	1	1	0	0	0	
September	16	6	1	0	0	1	1	0	
September	17	6	0	1	0	0	1	1	
September	18	6	1	0	1	0	1	0	
September	19	6	0	1	1	0	0	1	
September	20	6	0	0	1	0	1	1	
September	21	6	1	0	0	1	0	1	
September	22	6	1	1	0	0	0	1	
September	23	6	1	1	0	0	1	0	
September	24	6	0	0	1	1	1	0	
September	25	6	1	1	0	1	0	0	
September	26	6	1	0	1	1	0	0	
September	27	6	1	0	1	0	0	1	
September	28	6	0	1	0	1	0	1	
September	29	7	0	0	1	1	1	0	
September	30	7	0	0	0	1	1	1	
October	1	7	1	1	0	1	0	0	
October	2	7	1	0	0	0	1	1	
October	3	7	1	0	1	0	1	0	
October	4	7	1	0	0	1	0	1	
October	5	7	1	0	1	0	0	1	
October	6	7	0	1	0	1	1	0	
October	7	7	0	1	1	1	0	0	
October	8	7	0	1	0	0	1	1	
October	9	7	1	1	0	0	0	1	
October	10	7	0	1	0	1	0	1	
October	11	7	1	0	0	1	1	0	
October	12	7	0	1	1	0	0	1	
October	13	7	0	1	1	0	1	0	
October	14	7	1	1	0	0	1	0	
October	15	7	0	0	1	1	0	1	
October	16	7	1	0	1	1	0	0	
October	17	7	0	0	1	0	1	1	
October	18	7	1	1	1	0	0	0	

## B.4 2016 Operating Schedule

Constraints on the 2016 trial design were:

1. Size: There were 8 Atlants available in 2016, with 4 operating each day.
2. Maximum Crossover: No Atlant was allowed to operate for more than two days in a row.
3. Maximum Spatial Coverage: No more than two contiguous Atlants could be operated on a day.

Given these constraints, the basic approach was to randomly choose a design that met all three constraints, while simultaneously minimizing the average number of times (over all 8 Atlants) that an Atlant was operated two days in a row.

The design assumed H1 - H6 were operated June 1 to June 30 and H1 - H8 were operated July 1 to October 31. The design was constructed by merging an optimum randomised 6 site design for the 30 days (June 1 - June 30) with an optimum randomised 8 site design for the 123 days (July 1 - October 31).

The optimum 6 site design was obtained by noting that there are 14 ways of choosing 3 out of 6 sites to be operational each day so that no more than two "contiguous" sites have the same operating status. This leads to 28 configurations when each one of these 14 is immediately followed by its "opposite" configuration (i.e. where we replace on (1) by off (0) and vice versa. A Monte Carlo search was then used to find an ordering of the 14 initial configurations so that when expanded to 28 in this way, the average number of pairs of days when a site had the same operating status was minimised. This design was then expanded to 30 days by selecting one day at random and placing a copy of its operating sequences at the "top" of the design (June 1), and the inverse of this set of operating sequences at the "bottom" of the design (June 30).

From July 1 H7 and H8 became operational. With 8 sites, a design has 34 different configurations where 4 sites are active each day, and no more than two contiguous sites have the same operating state. That is, there are 68 configurations when each such configuration is paired with its opposite. The optimum randomized design based on this set of configurations is then identified after a Monte Carlo search that aims to minimise the number of days on average a site has the same operating status two days in a row. For this design there are 12 days on average when a site will have the same operating state two days in a row. This design was then expanded to 123 days by repeating days 1 - 55. The final 2016 operating schedule was defined by combining these two designs.

Note: Cells highlighted in red indicate days when H7 and H8 could not be operated due to structural issues with the new Atlant design. These issues were corrected, and H7 and H8 were then operated according to the predefined 2016 operating schedule.

1=On 0=Off

Month	Day	H6	H3	H8	H1	H2	H4	H5	H7
June	1	0	1		0	0	1	1	
June	2	1	1		0	1	0	0	
June	3	0	0		1	0	1	1	
June	4	0	1		0	1	1	0	
June	5	1	0		1	0	0	1	
June	6	0	1		0	0	1	1	
June	7	1	0		1	1	0	0	
June	8	0	1		1	0	1	0	
June	9	1	0		0	1	0	1	
June	10	1	1		0	0	1	0	
June	11	0	0		1	1	0	1	
June	12	1	0		1	0	1	0	
June	13	0	1		0	1	0	1	
June	14	1	0		0	1	1	0	
June	15	0	1		1	0	0	1	
June	16	1	0		0	1	0	1	
June	17	0	1		1	0	1	0	
June	18	1	0		1	1	0	0	
June	19	0	1		0	0	1	1	
June	20	1	0		1	0	0	1	
June	21	0	1		0	1	1	0	
June	22	0	1		1	0	0	1	
June	23	1	0		0	1	1	0	
June	24	0	1		0	1	0	1	
June	25	1	0		1	0	1	0	
June	26	0	0		1	1	0	1	
June	27	1	1		0	0	1	0	
June	28	0	0		1	0	1	1	
June	29	1	1		0	1	0	0	
June	30	1	0		1	1	0	0	
July	1	1	1		1	0	1	0	
July	2	0	0		0	1	0	1	
July	3	0	1		1	0	1	0	
July	4	1	0		0	1	0	1	
July	5	0	1		1	0	1	1	
July	6	1	0		0	1	0	0	
July	7	0	1		0	0	1	1	
July	8	1	0		1	1	0	0	
July	9	0	1		0	1	0	1	

July	10	1	0		1	0	1	0	
July	11	0	1		0	1	1	0	
July	12	1	0		1	0	0	1	
July	13	0	1		0	1	0	1	
July	14	1	0		1	0	1	0	
July	15	0	1		1	1	0	0	
July	16	1	0		0	0	1	1	
July	17	1	0		0	0	1	0	
July	18	0	1		1	1	0	1	
July	19	1	0		0	1	0	0	
July	20	0	1		1	0	1	1	
July	21	1	0		1	1	0	0	
July	22	0	1		0	0	1	1	
July	23	1	1		0	1	0	0	
July	24	0	0		1	0	1	1	
July	25	0	1		1	1	0	1	
July	26	1	0		0	0	1	0	
July	27	0	0		1	0	1	1	
July	28	1	1		0	1	0	0	
July	29	0	0	1	1	0	1	0	
July	30	1	1	0	0	1	0	1	
July	31	0	1	1	0	0	1	0	
August	1	1	0	0	1	1	0	1	
August	2	0	1	1	0	1	0	0	
August	3	1	0	0	1	0	1	1	
August	4	1	0	1	0	1	1	0	
August	5	0	1	0	1	0	0	1	
August	6	0	1	0	1	0	0	1	1
August	7	1	0	1	0	1	1	0	0
August	8	1	0	1	1	0	0	1	0
August	9	0	1	0	0	1	1	0	1
August	10	1	0	0	1	1	0	1	0
August	11	0	1	1	0	0	1	0	1
August	12	1	1	0	1	0	0	1	0
August	13	0	0	1	0	1	1	0	1
August	14	1	0	0	1	0	1	1	0
August	15	0	1	1	0	1	0	0	1
August	16	1	0	1	0	0	1	1	0
August	17	0	1	0	1	1	0	0	1
August	18	1	0	1	0	1	0	1	0
August	19	0	1	0	1	0	1	0	1



August	20	0	0	1	1	0	0	1	1
August	21	1	1	0	0	1	1	0	0
August	22	0	0	1	0	1	0	1	1
August	23	1	1	0	1	0	1	0	0
August	24	1	1	0	0	1	1	0	0
August	25	0	0	1	1	0	0	1	1
August	26	1	1	0	0	1	0	1	0
August	27	0	0	1	1	0	1	0	1
August	28	0	1	0	0	1	1	0	1
August	29	1	0	1	1	0	0	1	0
August	30	0	0	1	0	1	1	0	1
August	31	1	1	0	1	0	0	1	0
September	1	1	0	1	1	0	1	0	0
September	2	0	1	0	0	1	0	1	1
September	3	1	0	0	1	0	1	0	1
September	4	0	1	1	0	1	0	1	0
September	5	1	0	0	1	0	0	1	1
September	6	0	1	1	0	1	1	0	0
September	7	1	1	0	1	0	1	0	0
September	8	0	0	1	0	1	0	1	1
September	9	0	1	0	1	0	1	0	1
September	10	1	0	1	0	1	0	1	0
September	11	0	1	0	1	0	1	1	0
September	12	1	0	1	0	1	0	0	1
September	13	0	1	1	0	0	1	1	0
September	14	1	0	0	1	1	0	0	1
September	15	0	1	1	0	1	0	1	0
September	16	1	0	0	1	0	1	0	1
September	17	0	1	1	0	1	1	0	0
September	18	1	0	0	1	0	0	1	1
September	19	0	1	0	0	1	0	1	1
September	20	1	0	1	1	0	1	0	0
September	21	0	1	0	1	1	0	0	1
September	22	1	0	1	0	0	1	1	0
September	23	1	0	1	0	0	1	0	1
September	24	0	1	0	1	1	0	1	0
September	25	1	0	1	0	1	0	0	1
September	26	0	1	0	1	0	1	1	0
September	27	1	0	0	1	1	0	0	1
September	28	0	1	1	0	0	1	1	0
September	29	1	1	0	0	1	0	0	1

September	30	0	0	1	1	0	1	1	0
October	1	0	1	0	1	1	0	1	0
October	2	1	0	1	0	0	1	0	1
October	3	0	0	1	1	0	1	1	0
October	4	1	1	0	0	1	0	0	1
October	5	0	0	1	1	0	1	0	1
October	6	1	1	0	0	1	0	1	0
October	7	0	1	1	0	0	1	0	1
October	8	1	0	0	1	1	0	1	0
October	9	0	1	1	0	1	0	0	1
October	10	1	0	0	1	0	1	1	0
October	11	1	0	1	0	1	1	0	0
October	12	0	1	0	1	0	0	1	1
October	13	0	1	0	1	0	0	1	1
October	14	1	0	1	0	1	1	0	0
October	15	1	0	1	1	0	0	1	0
October	16	0	1	0	0	1	1	0	1
October	17	1	0	0	1	1	0	1	0
October	18	0	1	1	0	0	1	0	1
October	19	1	1	0	1	0	0	1	0
October	20	0	0	1	0	1	1	0	1
October	21	1	0	0	1	0	1	1	0
October	22	0	1	1	0	1	0	0	1
October	23	1	0	1	0	0	1	1	0
October	24	0	1	0	1	1	0	0	1
October	25	1	0	1	0	1	0	1	0
October	26	0	1	0	1	0	1	0	1
October	27	0	0	1	1	0	0	1	1
October	28	1	1	0	0	1	1	0	0
October	29	0	0	1	0	1	0	1	1
October	30	1	1	0	1	0	1	0	0
October	31	1	1	0	0	1	1	0	0

## B.5 2017 Operating Schedule

The 2017 trial was conducted using a double-blind procedure. Prior to the commencement of the 2017 trial, six potential operating schedules were defined (all based on the same design principles as used in the 2016 design) and passed on to the Trading and Investment Establishment (TIE) of Oman, who were responsible for the physical conduct of the trial on behalf of the Oman Government. One of these schedules was then selected by TIE and used in the trial. The knowledge of which schedule had been used was kept from Australian Rain Technologies (ART) and the National Institute for Applied Statistics Research Australia (NIASRA). On completion of the trial, the data obtained from it were evaluated by NIASRA under the assumption that each of the six potential schedules had been the actual schedule used, and using identical statistical methodology. These preliminary results were passed to TIE who then provided the information on which schedule had been actually used. The subsequent analysis by NIASRA focused on this actual schedule. This use of a double blind reflects a continuous effort develop the best possible approach to limit sources of bias in estimating the level and confidence associated with potential rainfall enhancement. The actual schedule used is shown below.

1=On 0=Off

Month	Day	H9	H6	H3	H8	H1	H2	H4	H10	H5	H7
June	1		1	1	1	0	0	0		0	1
June	2		0	0	0	1	1	1		1	0
June	3		0	1	1	0	0	1		1	0
June	4		1	0	0	1	1	0		0	1
June	5		1	1	1	0	0	0		1	0
June	6		0	0	0	1	1	1		0	1
June	7		1	0	0	1	0	1		0	1
June	8		0	1	1	0	1	0		1	0
June	9		0	0	1	1	0	1		0	1
June	10		1	1	0	0	1	0		1	0
June	11		1	0	1	1	0	0		0	1
June	12		0	1	0	0	1	1		1	0
June	13		0	0	1	1	0	1		1	0
June	14		1	1	0	0	1	0		0	1
June	15		1	0	1	1	0	0		1	0
June	16		0	1	0	0	1	1		0	1
June	17		0	1	0	0	1	1		0	1
June	18		1	0	1	1	0	0		1	0
June	19		1	1	0	0	1	0		0	1
June	20		0	0	1	1	0	1		1	0
June	21		0	1	0	0	1	1		1	0
June	22		1	0	1	1	0	0		0	1
June	23		1	1	0	0	1	0		1	0
June	24		0	0	1	1	0	1		0	1
June	25		0	1	1	0	1	0		1	0
June	26		1	0	0	1	0	1		0	1
June	27		0	0	0	1	1	1		0	1
June	28		1	1	1	0	0	0		1	0
June	29		1	0	0	1	1	0		0	1

June	30		0	1	1	0	0	1		1	0
July	1		0	0	0	1	1	1		1	0
July	2		1	1	1	0	0	0		0	1
July	3		1	0	0	1	1	0		1	0
July	4		0	1	1	0	0	1		0	1
July	5		0	0	1	1	1	0		1	0
July	6		1	1	0	0	0	1		0	1
July	7		1	0	0	1	1	1		0	0
July	8		0	1	1	0	0	0		1	1
July	9		0	0	1	1	1	1		0	0
July	10	1	0	1	1	0	1	1	0	0	0
July	11	0	1	0	0	1	0	0	1	1	1
July	12	1	0	1	0	0	1	1	0	1	0
July	13	0	1	0	1	1	0	0	1	0	1
July	14	1	1	1	0	0	1	1	0	0	0
July	15	0	0	0	1	1	0	0	1	1	1
July	16	1	0	1	1	0	1	0	0	1	0
July	17	0	1	0	0	1	0	1	1	0	1
July	18	1	1	1	1	0	1	0	0	0	0
July	19	0	0	0	0	1	0	1	1	1	1
July	20	1	0	0	0	1	1	1	0	1	0
July	21	0	1	1	1	0	0	0	1	0	1
July	22	1	1	0	0	1	1	1	0	0	0
July	23	0	0	1	1	0	0	0	1	1	1
July	24	1	0	0	1	1	1	0	0	1	0
July	25	0	1	1	0	0	0	1	1	0	1
July	26	1	1	0	1	1	1	0	0	0	0
July	27	0	0	1	0	0	0	1	1	1	1
July	28	1	1	0	0	1	1	0	0	1	0
July	29	0	0	1	1	0	0	1	1	0	1
July	30	1	1	0	1	0	1	1	0	0	0
July	31	0	0	1	0	1	0	0	1	1	1
Aug	1	1	1	0	0	0	1	1	0	1	0
Aug	2	0	0	1	1	1	0	0	1	0	1
Aug	3	1	0	1	1	1	0	0	0	1	0
Aug	4	0	1	0	0	0	1	1	1	0	1
Aug	5	1	1	1	1	1	0	0	0	0	0
Aug	6	0	0	0	0	0	1	1	1	1	1
Aug	7	1	1	1	0	1	0	0	0	1	0
Aug	8	0	0	0	1	0	1	1	1	0	1
Aug	9	1	1	1	1	0	0	1	0	0	0
Aug	10	0	0	0	0	1	1	0	1	1	1
Aug	11	1	1	1	0	0	0	1	0	1	0
Aug	12	0	0	0	1	1	1	0	1	0	1
Aug	13	0	0	0	0	1	1	1	1	1	0
Aug	14	1	1	1	1	0	0	0	0	0	1
Aug	15	0	1	0	0	1	1	1	1	0	0
Aug	16	1	0	1	1	0	0	0	0	1	1
Aug	17	0	0	0	1	1	1	0	1	1	0
Aug	18	1	1	1	0	0	0	1	0	0	1
Aug	19	0	1	0	1	1	1	0	1	0	0
Aug	20	1	0	1	0	0	0	1	0	1	1
Aug	21	0	1	0	0	1	1	0	1	1	0

Aug	22	1	0	1	1	0	0	1	0	0	1
Aug	23	0	1	0	1	0	1	1	1	0	0
Aug	24	1	0	1	0	1	0	0	0	1	1
Aug	25	0	1	0	0	0	1	1	1	1	0
Aug	26	1	0	1	1	1	0	0	0	0	1
Aug	27	0	0	1	1	1	0	0	1	1	0
Aug	28	1	1	0	0	0	1	1	0	0	1
Aug	29	0	1	1	1	1	0	0	1	0	0
Aug	30	1	0	0	0	0	1	1	0	1	1
Aug	31	0	1	1	0	1	0	0	1	1	0
Sep	1	1	0	0	1	0	1	1	0	0	1
Sep	2	0	1	1	1	0	0	1	1	0	0
Sep	3	1	0	0	0	1	1	0	0	1	1
Sep	4	0	1	1	0	0	0	1	1	1	0
Sep	5	1	0	0	1	1	1	0	0	0	1
Sep	6	0	1	0	0	1	0	1	1	1	0
Sep	7	1	0	1	1	0	1	0	0	0	1
Sep	8	1	0	1	1	0	1	0	0	0	1
Sep	9	0	1	0	0	1	0	1	1	1	0
Sep	10	1	0	0	1	1	1	0	0	0	1
Sep	11	0	1	1	0	0	0	1	1	1	0
Sep	12	1	0	0	0	1	1	0	0	1	1
Sep	13	0	1	1	1	0	0	1	1	0	0
Sep	14	1	0	0	1	0	1	1	0	0	1
Sep	15	0	1	1	0	1	0	0	1	1	0
Sep	16	1	0	0	0	0	1	1	0	1	1
Sep	17	0	1	1	1	1	0	0	1	0	0
Sep	18	1	1	0	0	0	1	1	0	0	1
Sep	19	0	0	1	1	1	0	0	1	1	0
Sep	20	1	0	1	1	1	0	0	0	0	1
Sep	21	0	1	0	0	0	1	1	1	1	0
Sep	22	1	0	1	0	1	0	0	0	1	1
Sep	23	0	1	0	1	0	1	1	1	0	0
Sep	24	1	0	1	1	0	0	1	0	0	1
Sep	25	0	1	0	0	1	1	0	1	1	0
Sep	26	1	0	1	0	0	0	1	0	1	1
Sep	27	0	1	0	1	1	1	0	1	0	0
Sep	28	1	1	1	0	0	0	1	0	0	1
Sep	29	0	0	0	1	1	1	0	1	1	0
Sep	30	1	0	1	1	0	0	0	0	1	1
Oct	1	0	1	0	0	1	1	1	1	0	0
Oct	2	1	1	1	1	0	0	0	0	0	1
Oct	3	0	0	0	0	1	1	1	1	1	0
Oct	4	0	0	0	1	1	1	0	1	0	1
Oct	5	1	1	1	0	0	0	1	0	1	0
Oct	6	0	0	0	0	1	1	0	1	1	1
Oct	7	1	1	1	1	0	0	1	0	0	0
Oct	8	0	0	0	1	0	1	1	1	0	1
Oct	9	1	1	1	0	1	0	0	0	1	0
Oct	10	0	0	0	0	0	1	1	1	1	1
Oct	11	1	1	1	1	1	0	0	0	0	0
Oct	12	0	1	0	0	0	1	1	1	0	1
Oct	13	1	0	1	1	1	0	0	0	1	0

<b>Oct</b>	<b>14</b>	0	0	1	1	1	0	0	1	0	1
<b>Oct</b>	<b>15</b>	1	1	0	0	0	1	1	0	1	0
<b>Oct</b>	<b>16</b>	0	0	1	0	1	0	0	1	1	1
<b>Oct</b>	<b>17</b>	1	1	0	1	0	1	1	0	0	0
<b>Oct</b>	<b>18</b>	0	0	1	1	0	0	1	1	0	1
<b>Oct</b>	<b>19</b>	1	1	0	0	1	1	0	0	1	0
<b>Oct</b>	<b>20</b>	0	0	1	0	0	0	1	1	1	1
<b>Oct</b>	<b>21</b>	1	1	0	1	1	1	0	0	0	0
<b>Oct</b>	<b>22</b>	0	1	1	0	0	0	1	1	0	1
<b>Oct</b>	<b>23</b>	1	0	0	1	1	1	0	0	1	0
<b>Oct</b>	<b>24</b>	0	0	1	1	0	0	0	1	1	1
<b>Oct</b>	<b>25</b>	1	1	0	0	1	1	1	0	0	0
<b>Oct</b>	<b>26</b>	0	1	1	1	0	0	0	1	0	1
<b>Oct</b>	<b>27</b>	1	0	0	0	1	1	1	0	1	0
<b>Oct</b>	<b>28</b>	0	0	0	0	1	0	1	1	1	1
<b>Oct</b>	<b>29</b>	1	1	1	1	0	1	0	0	0	0
<b>Oct</b>	<b>30</b>	0	1	0	0	1	0	1	1	0	1
<b>Oct</b>	<b>31</b>	1	0	1	1	0	1	0	0	1	0

## B.6 2018 Operating Schedule

Because the two 2018 trial areas were in different parts of Oman and were subject to different meteorological and orographic conditions, the northern and southern trials were designed independently. As in 2017, a double-blind approach was taken, with ten different operating schedules produced for both H1 - H10 (using the same design approach as employed in 2017) and H11-H12 (using a more standard randomised crossover design). However, because of extensive missing radiosonde data for 2018, no separate 2018 analysis was carried out, and so only one of these ten alternative designs (the one actually used) was considered in our combined analysis. The following tables therefore show the actual operating schedules used in 2018, covering the 123 days July 1 - October 31 for the northern trial area (Hajar Mountains) H1 - H10, and the southern trial area (Salalah) H11 - H12.

Note: Cells highlighted in red indicate days when radiosonde data were not available and so even though the Atlants were operated as shown, rainfall measurements on these days could not be allocated to being downwind or upwind (or neither) of the Atalnt sites on these days.

### H1 – H10 Operating Sequence 1=On 0=Off

Month	Day	H9	H6	H3	H8	H1	H2	H4	H10	H5	H7
July	1	1	0	0	1	1	0	1	0	1	0
July	2	0	1	1	0	0	1	0	1	0	1
July	3	1	1	0	1	1	0	1	0	0	0
July	4	0	0	1	0	0	1	0	1	1	1
July	5	1	0	0	0	1	0	1	1	1	0
July	6	0	1	1	1	0	1	0	0	0	1
July	7	1	1	0	0	1	0	1	1	0	0
July	8	0	0	1	1	0	1	0	0	1	1
July	9	1	1	0	0	1	0	1	0	1	0
July	10	0	0	1	1	0	1	0	1	0	1
July	11	0	0	1	1	1	0	0	1	0	1
July	12	1	1	0	0	0	1	1	0	1	0
July	13	0	0	1	1	1	0	0	0	1	1
July	14	1	1	0	0	0	1	1	1	0	0
July	15	0	1	1	1	1	0	0	0	0	1
July	16	1	0	0	0	0	1	1	1	1	0
July	17	0	0	1	0	1	0	0	1	1	1
July	18	1	1	0	1	0	1	1	0	0	0
July	19	0	1	1	0	1	0	0	1	0	1
July	20	1	0	0	1	0	1	1	0	1	0
July	21	0	0	1	1	1	0	1	0	1	0
July	22	1	1	0	0	0	1	0	1	0	1
July	23	0	1	1	1	1	0	1	0	0	0

July	24	1	0	0	0	0	1	0	1	1	1
July	25	0	0	1	0	1	0	1	1	1	0
July	26	1	1	0	1	0	1	0	0	0	1
July	27	0	1	1	0	1	0	1	1	0	0
July	28	1	0	0	1	0	1	0	0	1	1
July	29	0	1	1	0	1	0	1	0	1	0
July	30	1	0	0	1	0	1	0	1	0	1
July	31	0	1	1	1	1	0	0	1	0	0
August	1	1	0	0	0	0	1	1	0	1	1
August	2	0	1	1	1	1	0	0	0	1	0
August	3	1	0	0	0	0	1	1	1	0	1
August	4	0	0	0	0	1	0	1	1	1	1
August	5	1	1	1	1	0	1	0	0	0	0
August	6	0	1	0	0	1	0	1	1	0	1
August	7	1	0	1	1	0	1	0	0	1	0
August	8	0	1	0	0	1	0	1	0	1	1
August	9	1	0	1	1	0	1	0	1	0	0
August	10	0	1	0	1	1	0	0	1	0	1
August	11	1	0	1	0	0	1	1	0	1	0
August	12	0	1	0	1	1	0	0	0	1	1
August	13	1	0	1	0	0	1	1	1	0	0
August	14	1	0	1	1	0	0	1	0	1	0
August	15	0	1	0	0	1	1	0	1	0	1
August	16	1	1	1	1	0	0	1	0	0	0
August	17	0	0	0	0	1	1	0	1	1	1
August	18	1	0	1	0	0	0	1	1	1	0
August	19	0	1	0	1	1	1	0	0	0	1
August	20	1	1	1	0	0	0	1	1	0	0
August	21	0	0	0	1	1	1	0	0	1	1
August	22	1	1	1	0	0	0	1	0	1	0
August	23	0	0	0	1	1	1	0	1	0	1
August	24	1	1	1	1	0	0	0	1	0	0
August	25	0	0	0	0	1	1	1	0	1	1
August	26	1	1	1	1	0	0	0	0	1	0
August	27	0	0	0	0	1	1	1	1	0	1
August	28	1	0	0	0	0	0	1	1	1	1
August	29	0	1	1	1	1	1	0	0	0	0
August	30	1	1	0	0	0	0	1	1	0	1
August	31	0	0	1	1	1	1	0	0	1	0
September	1	1	1	0	0	0	0	1	0	1	1
September	2	0	0	1	1	1	1	0	1	0	0
September	3	1	1	0	1	0	0	0	1	0	1
September	4	0	0	1	0	1	1	1	0	1	0
September	5	1	1	0	1	0	0	0	0	1	1



September	6	0	0	1	0	1	1	1	1	0	0
September	7	1	1	0	1	0	0	1	0	1	0
September	8	0	0	1	0	1	1	0	1	0	1
September	9	0	0	1	0	1	1	0	1	0	1
September	10	1	1	0	1	0	0	1	0	1	0
September	11	0	0	1	0	1	1	1	1	0	0
September	12	1	1	0	1	0	0	0	0	1	1
September	13	0	0	1	0	1	1	1	0	1	0
September	14	1	1	0	1	0	0	0	1	0	1
September	15	0	0	1	1	1	1	0	1	0	0
September	16	1	1	0	0	0	0	1	0	1	1
September	17	0	0	1	1	1	1	0	0	1	0
September	18	1	1	0	0	0	0	1	1	0	1
September	19	0	1	1	1	1	1	0	0	0	0
September	20	1	0	0	0	0	0	1	1	1	1
September	21	0	0	0	0	1	1	1	1	0	1
September	22	1	1	1	1	0	0	0	0	1	0
September	23	0	0	0	0	1	1	1	0	1	1
September	24	1	1	1	1	0	0	0	1	0	0
September	25	0	0	0	1	1	1	0	1	0	1
September	26	1	1	1	0	0	0	1	0	1	0
September	27	0	0	0	1	1	1	0	0	1	1
September	28	1	1	1	0	0	0	1	1	0	0
September	29	0	1	0	1	1	1	0	0	0	1
September	30	1	0	1	0	0	0	1	1	1	0
October	1	0	0	0	0	1	1	0	1	1	1
October	2	1	1	1	1	0	0	1	0	0	0
October	3	0	1	0	0	1	1	0	1	0	1
October	4	1	0	1	1	0	0	1	0	1	0
October	5	1	0	1	0	0	1	1	1	0	0
October	6	0	1	0	1	1	0	0	0	1	1
October	7	1	0	1	0	0	1	1	0	1	0
October	8	0	1	0	1	1	0	0	1	0	1
October	9	1	0	1	1	0	1	0	1	0	0
October	10	0	1	0	0	1	0	1	0	1	1
October	11	1	0	1	1	0	1	0	0	1	0
October	12	0	1	0	0	1	0	1	1	0	1
October	13	1	1	1	1	0	1	0	0	0	0
October	14	0	0	0	0	1	0	1	1	1	1
October	15	1	0	0	0	0	1	1	1	0	1
October	16	0	1	1	1	1	0	0	0	1	0
October	17	1	0	0	0	0	1	1	0	1	1
October	18	0	1	1	1	1	0	0	1	0	0
October	19	1	0	0	1	0	1	0	1	0	1

October	20	0	1	1	0	1	0	1	0	1	0
October	21	1	0	0	1	0	1	0	0	1	1
October	22	0	1	1	0	1	0	1	1	0	0
October	23	1	1	0	1	0	1	0	0	0	1
October	24	0	0	1	0	1	0	1	1	1	0
October	25	1	0	0	0	0	1	0	1	1	1
October	26	0	1	1	1	1	0	1	0	0	0
October	27	1	1	0	0	0	1	0	1	0	1
October	28	0	0	1	1	1	0	1	0	1	0
October	29	1	0	0	1	0	1	1	0	1	0
October	30	0	1	1	0	1	0	0	1	0	1
October	31	1	1	0	1	0	1	1	0	0	0

### H11 – H12 Operating Sequence

1=On 0=Off

Month	Day	H11	H12
July	1	1	0
July	2	0	1
July	3	1	0
July	4	0	1
July	5	0	1
July	6	1	0
July	7	0	1
July	8	1	0
July	9	0	1
July	10	1	0
July	11	1	0
July	12	0	1
July	13	1	0
July	14	0	1
July	15	1	0
July	16	0	1
July	17	0	1
July	18	1	0
July	19	0	1
July	20	1	0
July	21	1	0
July	22	0	1
July	23	1	0
July	24	0	1
July	25	0	1
July	26	1	0

July	27	0	1
July	28	1	0
July	29	0	1
July	30	1	0
July	31	1	0
August	1	0	1
August	2	1	0
August	3	0	1
August	4	0	1
August	5	1	0
August	6	0	1
August	7	1	0
August	8	0	1
August	9	1	0
August	10	1	0
August	11	0	1
August	12	1	0
August	13	0	1
August	14	1	0
August	15	0	1
August	16	1	0
August	17	0	1
August	18	0	1
August	19	1	0
August	20	0	1
August	21	1	0
August	22	0	1
August	23	1	0
August	24	1	0
August	25	0	1
August	26	1	0
August	27	0	1
August	28	0	1
August	29	1	0
August	30	0	1
August	31	1	0
September	1	0	1
September	2	1	0
September	3	1	0
September	4	0	1
September	5	1	0
September	6	0	1
September	7	1	0

September	8	0	1
September	9	0	1
September	10	1	0
September	11	0	1
September	12	1	0
September	13	0	1
September	14	1	0
September	15	1	0
September	16	0	1
September	17	1	0
September	18	0	1
September	19	1	0
September	20	0	1
September	21	0	1
September	22	1	0
September	23	0	1
September	24	1	0
September	25	1	0
September	26	0	1
September	27	1	0
September	28	0	1
September	29	1	0
September	30	0	1
October	1	0	1
October	2	1	0
October	3	0	1
October	4	1	0
October	5	0	1
October	6	1	0
October	7	0	1
October	8	1	0
October	9	1	0
October	10	0	1
October	11	1	0
October	12	0	1
October	13	1	0
October	14	0	1
October	15	0	1
October	16	1	0
October	17	0	1
October	18	1	0
October	19	1	0
October	20	0	1

---

<b>October</b>	21	1	0
<b>October</b>	22	0	1
<b>October</b>	23	1	0
<b>October</b>	24	0	1
<b>October</b>	25	0	1
<b>October</b>	26	1	0
<b>October</b>	27	0	1
<b>October</b>	28	1	0
<b>October</b>	29	1	0
<b>October</b>	30	0	1
<b>October</b>	31	1	0